

Heinrich Pette Institute
Leibniz Institute for Experimental Virology

**Identification of novel antivirals targeting the
human cytomegalovirus alkaline nuclease
pUL98**

Dissertation

submitted to the

Department of Chemistry

Faculty of Mathematics, Informatics and Natural Sciences

University of Hamburg

In fulfillment of the requirements

for the degree of

Doctor of Natural Sciences (Dr. rer. nat.)

by

Theodore I. Potgieter

born in Sasolburg (South Africa)

Hamburg 2019

Vorsitzender der Prüfungskommission: Prof. Dr. Wolfram Brune

Erstgutachter: Prof. Dr. Wolfram Brune

Zweitgutachter: Prof. Dr. Nicole Fischer

Datum der Disputation: 15. November 2019

First reviewer: Prof. Dr. Wolfram Brune

Second reviewer: Prof. Dr. Nicole Fischer

This study was conducted between November 2016 and September 2019 at the Heinrich Pette Institute - Leibniz Institute for Experimental Virology under the supervision of Prof. Dr. Wolfram Brune and Prof. Dr. Thomas Dobner.

List of Publications

This work was presented in part at the following conferences:

Date	Conference	Type of presentation
November 2016	Annual meeting of the German Center for Disease Research (DZIF) Cologne, Germany	Poster
March 2017	27th annual meeting of the Society for Virology e.V. (GfV) Marburg, Germany	Poster
September 2017	Annual meeting of the German Center for Disease Research (DZIF) Hamburg, Germany	Poster
March 2018	28th annual meeting of the Society for Virology e.V. (GfV) Würzburg, Germany	Poster
October 2018	13. Mini-herpesvirus Workshop, Hamburg Hamburg, Germany	Oral Presentation
November 2018	HPI Scientific Retreat Hamburg, Germany	Oral Presentation
December 2018	Annual meeting of the German Center for Disease Research (DZIF) Heidelberg, Germany	Poster

Table of Contents

1	Zusammenfassung.....	1
2	Abstract.....	3
3	Introduction.....	5
3.1	The herpesviruses.....	5
3.1.1	Alpha-herpesviruses.....	6
3.1.2	Gamma-herpesvirus.....	6
3.1.3	Beta-herpesviruses.....	6
3.1.3.1	Cytomegaloviruses.....	7
3.2	Human Cytomegalovirus.....	7
3.3	Prevalence of HCMV.....	8
3.4	Clinical Impact of HCMV.....	9
3.4.1	Congenital HCMV infection.....	9
3.4.2	HCMV disease in the immunosuppressed.....	10
3.4.2.1	HCMV and Solid-Organ Transplants.....	10
3.4.2.2	HCMV and Hematopoietic Stem Cell Transplants.....	11
3.5	Lytic replicative lifecycle of HCMV.....	11
3.5.1	The Immediate-Early Phase.....	13
3.5.2	The Early phase of replication.....	13
3.5.2.1	The viral alkaline nucleases.....	15
3.5.2.2	UL12 in HSV-1.....	16
3.5.2.3	The KSHV SOX protein.....	16
3.5.2.4	The HCMV pUL98.....	18
3.5.3	The Late Phase of replication.....	19
3.5.3.1	The Terminase Complex.....	20
3.5.4	The importance of the viral lifecycle.....	22
3.6	Current therapies used for HCMV infection.....	22
3.6.1	Therapies targeting viral DNA replication.....	22
3.6.1.1	Ganciclovir/Valganciclovir and Acyclovir.....	23

3.6.1.2	Cidofovir and Brincidofovir.....	24
3.6.1.3	Foscarnet.....	26
3.6.1.4	Fomivirsen.....	26
3.6.2	Inhibitors of the pUL97 viral kinase.....	27
3.6.2.1	Maribavir.....	27
3.6.3	Inhibitors of the terminase complex.....	28
	The terminase complex as an antiviral target.....	28
3.6.3.1	Letemovir.....	29
3.6.4	Other inhibitors of the viral terminase complex.....	30
3.6.4.1	Benzoimidine ribonucleosides.....	30
3.6.4.2	Tomeglovir.....	31
3.7	The need for new antiviral compounds.....	32
3.7.1	The viral alkaline nuclease as an antiviral target.....	32
3.7.1.1	Compounds targeting the HCMV alkaline nuclease.....	33
3.8	Characterization of Novel Antiviral Compounds.....	33
4	Rationale for this work.....	34
5	Results.....	35
5.1	Target Validation of UL98.....	35
5.2	Development of an alkaline nuclease activity assay suitable for high-throughput screening.....	38
5.2.1	Designing an expression system for tagged pUL98.....	38
5.2.2	Inducing expression of pUL98.....	39
5.2.3	Purification of the pUL98 protein.....	40
5.2.4	Activity of pUL98.....	42
5.2.5	Contaminating bands are unlikely to show DNase activity.....	43
5.2.5.1	The contaminating bands are not the result of protein degradation.....	44
5.2.6	Generation of additional pUL98 proteins.....	47
5.2.7	The double-purified pUL98 shows activity.....	48
5.2.7.1	Double-Tagged Full-Length pUL98 shows no extraneous bands.....	49
5.2.8	Conceptualizing a high-throughput screening system of pUL98 inhibitors.....	51

5.2.9	Proof-of-Concept of High-throughput fluorescence-based assay	52
5.2.10	Substrates Used in Fluorescence Assay	53
5.2.11	Determining the optimal incubation time of the high-throughput screen.....	54
5.2.12	pUL98 shows strong activity at 200 ng	55
5.3	Identifying inhibitors of pUL98	56
5.3.1	High-throughput screen of a small-molecular compound library.....	56
5.3.2	Validation of the identified compounds.....	58
5.3.3	Inhibitors require further screening	59
5.3.4	Toxicity of the 11 Identified Compounds.....	60
5.3.5	Plaque Reduction Assay screening of compounds reveals <i>in vivo</i> effectiveness	62
5.4	Characterization of Compound A	63
5.4.1	Compound A Impacts the Growth of HCMV TB40/E	63
5.4.2	The Inhibitory Activity of Compound A is comparable to Ganciclovir.....	64
	Compound A is effective against other herpesviruses.....	65
5.4.3	Compound A is a likely non-competitive inhibitor of pUL98.....	66
5.4.4	Inhibition of double-tagged protein rules out residual effects of background	
	bands	70
5.4.5	The Cytotoxicity of Compound A.	70
5.4.6	Quantifying structural derivatives of Compound A.....	71
5.4.6.1	Enzymatic activity of the 100 compounds.....	72
5.4.6.2	Toxicity analysis of the Compound A derivatives.....	73
5.4.6.3	Plaque reduction assay and SI calculation show a promising lead candidate.....	74
6	Discussion.....	77
6.1	UL98 alkaline nuclease activity is essential for HCMV growth.....	77
6.1.1	Timing of expression of pUL98 during the viral life cycle	78
6.2	Advantages of a potential pUL98 crystal structure.....	78
6.3	Improvement of the high-throughput screen.....	80

6.4	Identification and characterization of compounds inhibiting pUL98	81
6.5	Optimization of Compound A and future directions.....	83
6.6	Closing Remarks	84
7	Materials	87
7.1.1	Cells	87
7.1.2	Cell culture media and reagents.....	87
7.1.3	Methylcellulose overlay for plaque reductions.....	88
7.1.4	Bacteria	88
7.1.5	Bacterial growth media.....	88
7.1.6	Antibiotics.....	88
7.1.7	Viruses	89
7.1.8	Viruses generated in this work.....	89
7.1.9	Plasmids	89
7.1.10	Plasmids generated in this work	89
7.1.11	Primers	90
7.1.12	Enzymes.....	92
7.1.13	Reagents for small-scale plasmid and BAC extraction (“Mini-prep”).....	92
7.1.14	Protease Inhibitors	93
7.1.15	Reagents for protein purification	93
7.1.16	Reagents for agarose gel electrophoresis.....	94
7.1.17	Reagents for SDS-PAGE polyacrylamide gel electrophoresis	94
7.1.18	Primary Antibodies	95
7.1.19	Secondary Antibodies	95
7.1.20	Fluorescently-Tagged DNA Substrates	95
7.1.21	Compounds	96
7.1.22	Reagents for fluorescence-based protein activity assay (“Enzymatic assay”)...	96
7.1.23	Commercial kits	96

7.1.24	Other materials used	96
8	Methods.....	97
8.1	Molecular biology methods.....	97
8.1.1	Primer synthesis	97
8.1.2	Polymerase Chain Reaction (PCR).....	97
8.1.2.1	Reaction conditions and setup.....	97
8.1.3	Fusion PCR	98
8.1.4	DNA restriction digestion	98
8.1.5	Agarose gel electrophoresis	98
8.1.6	Purification of DNA.....	98
8.1.7	DNA ligation.....	98
8.1.8	Storage of bacterial stocks	99
8.1.9	Generation of electrocompetent <i>E. coli</i>	99
8.1.10	Bacterial Transformation	99
8.1.11	Cloning Procedure	99
8.1.12	Quikchange™ Cloning protocol	100
8.1.13	Creation of mutant virus strains using <i>en passant</i> mutagenesis	100
8.1.14	Isolation of Plasmid DNA (“Miniprep”).....	101
8.1.15	Isolation of plasmid and BAC DNA (“Midiprep”).....	102
8.1.16	DNA sequencing.....	102
8.1.17	Expression of UL98 Protein.....	102
8.2	Protein Biochemistry.....	102
8.2.1	His-tag purification of UL98 Protein.....	102
8.2.2	Strep-tag purification of double-tagged protein.....	103
8.2.3	Determination of protein concentration of purified protein.....	103
8.2.4	SDS polyacrylamide gel electrophoresis (Immunoblot).....	103
8.2.4.1	Preparation of samples	103
8.2.4.2	Gel preparation and electrophoreses.	104

8.2.4.3	Semi-dry blotting	104
8.2.4.4	Coomassie Staining.....	104
8.2.5	Quantification of activity of purified protein.....	104
8.2.6	Proof of concept of the enzymatic assay.....	105
8.2.7	Quantification of enzymatic nuclease activity of purified protein.....	105
8.2.8	Quantification of optimal substrate concentration.....	105
8.2.9	Substrate Synthesis	105
8.2.10	Compounds	106
8.2.11	Fluorescence-based enzymatic assay for testing inhibitors of purified protein 106	
8.2.12	Screening of the small molecular compound library	106
8.3	Cell biology and virology methods	106
8.3.1	Cell culture.....	106
8.3.1.1	Determining cell concentration.....	107
8.3.1.2	Freezing cells for storage.....	107
8.3.1.3	Thawing frozen cells.....	107
8.3.2	Transfection of viral BACs into mammalian cells	107
8.3.3	Culture of virus stock.....	108
8.3.4	Determination of HCMV TCID ₅₀	108
8.3.5	Cell viability assay.....	108
8.3.6	CMV plaque-reduction assay (PRA)	109
8.3.6.1	Determination of CMV plaque titer	109
8.3.6.2	CMV plaque-reduction assay.....	109
8.3.6.3	Determination of HSV-1 plaque titer.....	110
8.3.6.4	HSV-1 Plaque reduction assay.....	110
8.3.7	Viral growth kinetic of Compound A	110
8.4	Statistical Analysis and Figure Generation	111
9	References.....	113
10	Appendix.....	127

10.1	Toxicity of chemicals	127
10.2	Curriculum vitae	131
11	Acknowledgements.....	133
12	Eidesstattliche Versicherung.....	135

List of Abbreviations Used

ACV	Acyclovir
AD	(Compound) A Derivative
AIDS	Acquired Immunodeficiency Syndrome
AN	alkaline nuclease
BAC	bacterial artificial chromosome
BCV	Brincidofovir
	1H- β -D-ribofuranosyl-2- bromo-5,6- dichlorobenzimidazole
BDCRB	
bp	base pairs
CC ₅₀	Cytotoxic Concentration (50%)
cDNA	Complementary DNA
CDV	Cidofovir
CMV	cytomegalovirus
CTL	C-terminal deletion
Da	Dalton
dpt	Days post transfection
dsDNA	double-stranded DNA
DTS	double-tagged (Strep)
E	Early
EBV	Epstein-Barr virus
FOS	Foscarnet
GCV	Ganciclovir
HCMV	human cytomegalovirus
HHV	human herpesvirus
HSCT	hematopoietic stem-cell transplant
HSV-1	herpes simplex virus 1
HSV-2	herpes simplex virus 2
IC ₅₀	Inhibitory concentration (50%)
IE	Immediate-Early
IPTG	isopropyl β -D-1-thiogalactopyranoside
kDa	kilo Daltons (1000 Daltons)
KSHV	Kaposi's sarcoma-associated herpesvirus
L	Late
MBV	maribavir
MCMV	murine cytomegalovirus
MOI	multiplicity of infection
ND10	nuclear domain 10
Pep	pepstatin
PRA	plaque reduction assay
Ro5	(Lipinski's) Rule of Five
SC	supercoiled

SES	socioeconomic status
SI	selectivity index
SOT	solid-organ transplant
ssDNA	single-stranded DNA
TCID ₅₀	Tissue culture infectious dose (50%)
TRS	terminal repeat short
UL	unique long
US	unique short
vDNA	viral DNA
VGCV	Valganciclovir
VZV	varicella-zoster virus
wt	wild-type

1 Zusammenfassung

Das humane Cytomegalovirus (HCMV) ist eine der Hauptursachen für angeborene Schäden bei Neugeborenen und verursacht schwere Erkrankungen bei immunsupprimierten Patienten. Ein Impfstoff gegen das HCMV ist bisher nicht verfügbar und die derzeitigen Behandlungen von HCMV-infizierten Patienten konzentrieren sich weitgehend auf die Beeinträchtigung der viralen DNA-Replikation oder der Verpackung des viralen Genoms. Jedoch sind diese Therapieansätze häufig mit starken Nebenwirkungen belastet und es kommt mitunter zu Resistenzen der viralen Stämme gegen diese Behandlungen, was auf die Notwendigkeit neuer viraler therapeutischer Ziele hinweist.

Die virale alkalische Nuklease, ein in allen Herpesvirus-Unterfamilien konserviertes Enzym, gilt als potenzielles Ziel. Bei HCMV wird dies durch das UL98-Gen kodiert. Mehrere HCMV-UL98-Mutanten konnten erzeugt werden, die die Virusreplikation nachweislich beeinflussten. Dies deutet darauf hin, dass das UL98 für das Viruswachstum essentiell ist und ein geeignetes Ziel für eine antivirale Therapie darstellt. Um diese Hypothese im Detail zu überprüfen, wurde das UL98-Gen in das pET28b(+)/BL21(DE3)-Expressionssystem geklont und gereinigt. Zudem wurde ein Fluoreszenztest entwickelt, welcher ein DNA-Oligonukleotidsubstrat, gekoppelt mit einem Fluorophor und Quencher, verwendet, um eine Quantifizierung der pUL98-Aktivität zu ermöglichen. Der Abbau des Substrates durch die virale Nuklease resultiert in der Trennung vom Fluorophor und Quencher, wodurch es zu einer Erhöhung der Fluoreszenz kommt, die durch einen ELISA-Reader nachgewiesen werden kann. Als Inhibierungskontrolle des Assays diente ein bereits bekannter Inhibitor, namentlich Atanyl Blue PRL (Acid Blue 129), der die Nukleaseaktivität von pUL98 konzentrationsabhängig reduzieren kann. Mit diesem System wurden 27.690 Substanzen in der *Small Compound Library* der Medizinischen Hochschule Hannover (MHH) untersucht. Dies führte zur Identifizierung mehrerer Substanzen, die die Nukleaseaktivität von pUL98 stark hemmten. Die potentiellen Inhibitoren wurden nachfolgend verifiziert, charakterisiert und auf Zelltoxizität überprüft. Zudem wurde die mögliche Hemmung der Substanzen auf die virale Replikation in Plaque-Reduktionstests analysiert. Zwei Substanzen konnten als vielversprechend eingestuft werden: *Compound A* und *Compound D*. Während *Compound D* nur gegen HCMV getestet wurde, konnte mit *Compound A* eine Reduktion der viralen Replikation gegen das HCMV, HSV-1 und MCMV gezeigt werden. Anschließend wurden mehrere Strukturderivate von *Compound A* *in vitro* untersucht, um die Wirksamkeit gegen

HCMV-Infektionen zu verbessern und die Toxizität zu minimieren. Ein solches Derivat, AD-51, zeigte eine deutlich verbesserte Wirksamkeit im Vergleich zu *Compound A* und demonstriert die Anforderungen an eine gute vorläufige Leitsubstanz für eine zukünftige HCMV Therapie.

Diese Studie soll als Sprungbrett für die Entwicklung einer neuen Klasse von Virostatika gegen Herpesviren dienen, die nicht auf die virale Replikation oder die Verpackungswege abzielen.

2 Abstract

Human cytomegalovirus (HCMV) is a leading cause of congenital sequelae in neonates and causes serious disease in immunocompromised patients. A vaccine against HCMV is not available, and current treatment of HCMV largely focuses on interfering with viral DNA replication or viral genome packaging; however, side effects are common and viral strains resistant to these treatments have been reported, indicating a need for new viral therapeutic targets. The viral alkaline nuclease, an enzyme conserved in all herpesvirus subfamilies, is considered a potential target. In HCMV, this is encoded by the UL98 gene. Several HCMV-UL98 mutants which impact the activity of the alkaline nuclease were generated and shown to severely impair viral replication. This suggests that UL98 is essential for viral growth and is a suitable target for antiviral treatment. To test this hypothesis UL98 was cloned in the pET28b(+)/BL21(DE3) expression system and purified in order to design a fluorescence assay that makes use of a DNA oligonucleotide substrate coupled to a fluorophore and a quencher. Upon degradation by the viral nuclease, fluorophore and quencher are separated resulting in an increase in detectable fluorescence, allowing for the quantification of pUL98 activity. As a proof of principle of the fluorescence assay pUL98 nuclease activity was reduced in this system by a known inhibitor, Atanyl Blue PRL (Acid Blue 129), in a dose-dependent manner.

The system was then used to screen 27,690 compounds in the Small Compound Library at the Medizinische Hochschule Hannover. This led to the identification of several compounds which strongly inhibited the purified UL98 activity. The inhibitory activities of the identified compounds were verified, further characterized and were tested for cell toxicity, while inhibition of viral replication was screened by plaque reduction assay. Two compounds show promise as potential inhibitors of HCMV replication: Compound A and Compound D. While compound D was only tested against HCMV, compound A was tested against HCMV, HSV-1 and MCMV and showed reduction of viral growth. Several structural derivatives of Compound A were then investigated in order to improve its efficacy against HCMV infection *in vitro* as well as reduce its toxicity. One such derivative, AD-51, showed greatly improved efficacy compared to Compound A and demonstrates the requirements of a good preliminary lead compound for HCMV treatment.

This study aims to serve as a stepping stone for the creation of a new class of antivirals against the herpesviruses that do not target the viral replication or packaging pathways.

3 Introduction

3.1 The herpesviruses

The Herpesviridae are a family of double-stranded (ds) DNA viruses. Their linear dsDNA genome is packaged within a protein capsid, together termed the nucleocapsid. The nucleocapsid is surrounded by a proteinaceous matrix containing several viral proteins termed the tegument. The nucleocapsid and tegument layer is enveloped in a lipid bilayer studded with viral receptors such as the glycoprotein complexes I and III which recognize cellular surface receptors and facilitate viral entry into the host cell (Figure 1). The herpesviruses are subdivided into three subfamilies (alpha- beta-, and gamma-herpesviruses) each showing a large variety in their host specificity, with some herpesviruses showing tropism only for a restricted range of cell types while others are capable of infecting a broad range of host cells (1,2).

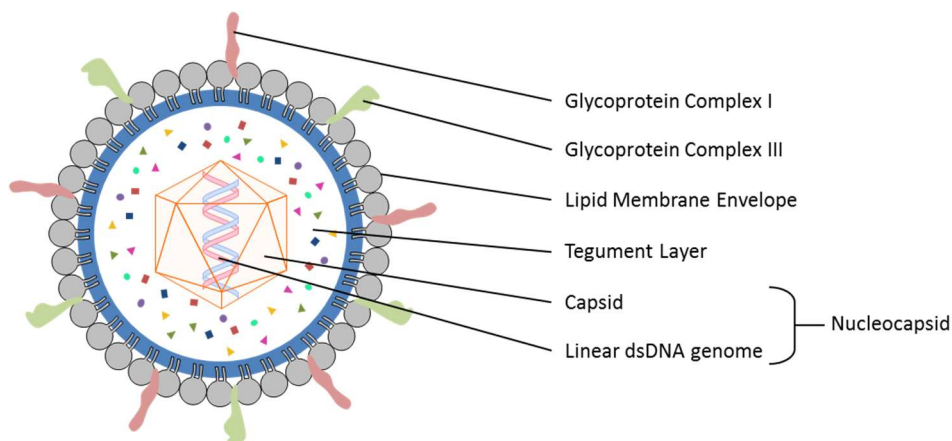


Figure 1. Schematic diagram of the overall structure of herpesviruses.

Herpesviruses switch between two dominant phases in their life cycle, termed the latent phase and the lytic phase. In the latent phase, viral genetic material is silently introduced as an episome into the host cell nucleus. The few viral genes expressed serve mainly to maintain latency and forming the basis of a lifelong infection (1). In contrast, during the lytic phase, the virus actively replicates within the host cell and expresses a number of viral genes.

3.1.1 Alpha-herpesviruses

Three human alpha-herpesviruses exist, the herpes simplex viruses types 1 and 2 (HSV-1 & HSV-2) and Varicella Zoster Virus (VZV) (3,4). In a natural setting human alpha-herpesviruses replicate in epithelial cells and establish latency in neuronal cells (2). Reactivation of viral replication in neuronal cells re-infects epithelial cells, with HSV-1 causing labial herpes, HSV-2 causing genital herpes, and VZV causing chickenpox (3,4). In rare cases, HSV-1 and -2 can also replicate in the central nervous system CNS and cause herpes simplex encephalitis (4).

3.1.2 Gamma-herpesvirus

Only two human gamma-herpesviruses are known, the Kaposi's sarcoma-associated herpesvirus (KSHV) and Epstein - Barr virus (EBV). Unlike the alpha-herpesviruses, EBV mainly targets endothelial cells but becomes latent in B cells (5). EBV is the cause of infectious mononucleosis and rare lymphoproliferative diseases, but can cause lymphomas in immunocompromised hosts through transformation of latently infected cells (5–7).

KSHV, like EBV, shows cell tropism predominantly for lymphocytes (8). KSHV usually persists as a latent infection in the host and very rarely causes disease in the immunocompetent host. However, in the immunocompromised host, it may transform latently infected lymphocytes. This is causative of three oncogenic diseases, Kaposi's sarcoma, HHV-8-associated Multicentric Castleman's Disease, and Primary Effusion Lymphoma (6–8).

3.1.3 Beta-herpesviruses

The betaherpesviral subfamily contains four human herpesviruses, the human herpesviruses 6A, 6B and 7 (HHV-6A, -6B, and -7, together referred to as the Roseoloviruses), and the human cytomegalovirus (HCMV) (9,10). Both HHV-6A/B and HHV-7 show tropism for CD4+ T lymphocytes; HHV-7 exclusively infects CD4+ T lymphocytes while HHV-6A/B is able to infect a larger variety of host cells but preferentially infects the lymphocytes (10). Both viruses cause roseola disease in infants, and HHV-7 has been additionally indicated to cause drug hypersensitivity syndrome and encephalopathy in infected individuals (10).

3.1.3.1 Cytomegaloviruses

The cytomegaloviruses (CMVs) derive their name from the enlarged cytoplasm displayed by infectious cells in histopathology, first described in 1881 by Dr. Hugo Ribbert in a report on sections taken from a kidney of a stillborn displaying nephritis (11). These enlarged cells were first thought to be invading protozoa before a viral etiology was proposed and confirmed in the 1950s by visualizing viral particles (12–14). Murine cytomegalovirus (MCMV) was the first cytomegalovirus successfully isolated from the salivary glands of mice and propagated in cell culture by Dr. Margaret Gladys Smith in 1954 (15). Shortly afterwards, human cytomegalovirus (HCMV) was isolated independently by Smith in 1956, Rowe et al. in 1956, and Weller et al. in 1957 (16–18).

3.2 Human Cytomegalovirus

The first complete genome sequence of HCMV was published in 1990 by Chee et al, who worked on the laboratory-attenuated AD169 strain (19). This and subsequent studies showed that the genome of HCMV consists of 235,000 base pairs encoding approximately 170 characterized ORFs; however, recent studies based on transcriptome analysis have forwarded a putative number of around 700 ORFs (20). While HCMV establishes latency in myeloid cells and is present in the salivary glands, as indeed all CMVs are, subsequent studies showed that the virus was capable of replicating in a broad variety of cells from retinal cells to fibroblasts, and HCMV particles have been found in virtually all body fluids (9). It is important to note that several strains of HCMV exist, with some strains being laboratory-attenuated and having lost viral factors present in clinical samples. For example, the strain AD169 has lost an entry complex known as the pentameric glycoprotein complex, removing the virus' ability to enter epithelial cells (21–23). Other strains, such as TB40/E, are laboratory-attenuated but have not lost viral genes coding for protein products important for *in vivo* infections and are considered to be representatives of clinical HCMV isolates (24–26). HCMV, like all CMVs, is highly species specific, as noted by Smith in 1956 when she stated in her paper on HCMV propagation that “Each virus or strain of the virus is probably species-specific, since all attempts to infect animals of one species with virus derived from another species have failed” (16). This species-specificity means that MCMV is used as an *in vitro* model of HCMV infection, as the general properties of MCMV infection and pathogenesis are similar to that of HCMV (27).

3.3 Prevalence of HCMV

HCMV is globally highly seroprevalent, i.e., detectable in circulating blood serum in high proportions of the global population. However, disparities in the percentage of HCMV positive individuals between countries can be seen. A metaanalysis focusing on studies of CMV prevalence in global populations on women of reproductive age carried out by Cannon, Schmid, and Hyde found that global seroprevalence tends to be at its lowest in the developed world, such as continental Europe's prevalence of 40-50%, while the highest rates tend to be found in developing countries such as those in sub-Saharan Africa and Latin America, where prevalence is over 90% (see Figure 2) (28).

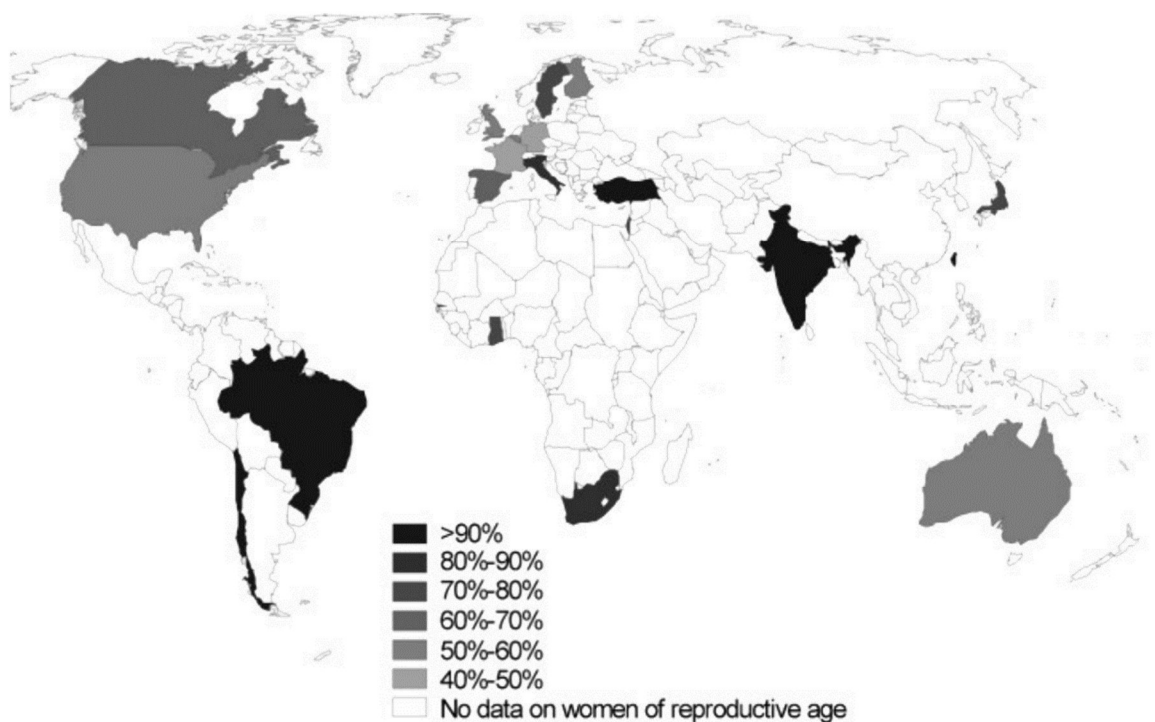


Figure 2. Global seroprevalence of HCMV presented as a percentage of women of reproductive age by country. Darker gradients indicate higher percentages, white indicates no data. Adapted from (28).

Geographic location is not the only indicator of HCMV prevalence. Several other socioeconomic factors also play a role; for example, the incidence of HCMV increases in older individuals, with several studies indicating a prevalence of 60% in individuals older than 50, because the risk of exposure increases over time (summarized in 27). Both sexes are thought to be equally susceptible to HCMV exposure, especially in the developed world, but studies focusing on Africa found that males tended to have higher rates of seroprevalence

(28). Finally, studies focusing on socioeconomic status (SES, measured by income, educational attainment and other markers) show a trend of individuals with lower SES exhibiting higher rates of seroprevalence (28,29). These trends all indicate that the rate of HCMV seroprevalence seems to be related to the transmission pathways of the virus, i.e. breastfeeding, childcare and related social customs, and sexual activity (28,30). Countries in the developed world tend to have better sanitation and less overcrowding, which may lead to a reduced incidence of HCMV. However, it must be noted that the seroprevalence of HCMV in several developed countries, such as Sweden, Taiwan, Japan, and Australia, are higher than those of their geographic neighbors, and even then the “lowest” rates in countries such as Germany are above 40% (28,31).

3.4 Clinical Impact of HCMV

The elevated rates of HCMV seroprevalence is due to the fact that primary infection with HCMV in healthy individuals usually has no symptoms, or at most presents with mild flu-like symptoms (9). Reactivation of the virus in these individuals is also asymptomatic and is efficiently cleared by the immune system, meaning that infected individuals seldom realize that they have been infected (9,32). This is in stark contrast to immunocompromised individuals, such as organ transplant recipients and patients with Acquired Immunodeficiency Syndrome (AIDS), or those with immature immune systems such as neonates, each of which show severe disease in HCMV infection (9).

3.4.1 Congenital HCMV infection

Congenital CMV infection can arise in two major ways, both of which are related to the seropositivity of the pregnant woman. Firstly, it can arise when a seronegative woman undergoes primary seroconversion during pregnancy. Second, it can arise when a seropositive mother undergoes reactivation of the virus, with the second scenario being around 75% more common than the first in studies focusing on the United States (32). Ten percent of congenital infections are symptomatic at birth, and in rare cases can lead to death. Sequelae arise in 50% of these symptomatic cases and may be severe. The remaining 90% of congenital infections are asymptomatic at birth, but in around 10% of these cases sequelae may still arise later in the infected infant’s life (32–35). The most common of these is sensineural hearing loss, but cerebral palsy, cognitive impairment, or vision loss can also occur (32). While the general population is largely unaware of the disease, congenital HCMV is the largest infectious cause of sensory or cognitive impairment, showing a higher prevalence in developed countries such

as the US than many other cases of congenital impairment, such as Down's syndrome or *spina bifida*, as seen in Figure 3.

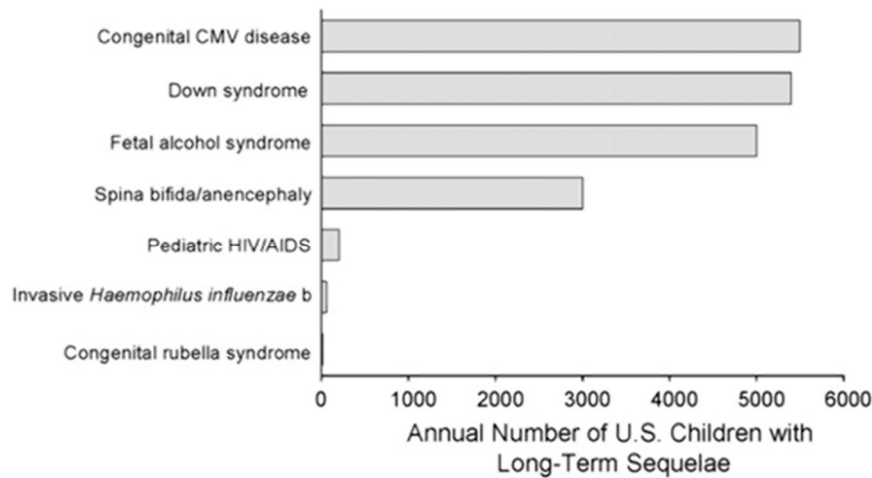


Figure 3. Prevalence of long-term sequelae caused by congenital disease in live births in the United States of America. Adapted from (32).

3.4.2 HCMV disease in the immunosuppressed

HCMV disease arising in the immunosuppressed constitutes the other major clinical impact of lytic HCMV replication and can be further divided into disease experienced by recipients of solid-organ transplants (SOT) or hematopoietic stem cell transplants (HSCT).

3.4.2.1 HCMV and Solid-Organ Transplants

SOT recipients suffer a risk of HCMV disease when they are seronegative and receive seropositive organs (36). In SOT recipients, HCMV reactivation can lead to the classical “HCMV syndrome” defined as detection of HCMV in the blood accompanied by fever, fatigue or malaise, neutropenia or leukopenia, a reduction in cell platelet counts and/or the elevation of hepatic aminotransferases, leading to retinitis, hepatitis, gastrointestinal disease, CNS disease, myocarditis, end organ disease, allograft loss and death (37). HCMV syndrome is also tentatively linked not only to acute allograft failure but also long-term rejection, especially in cardiac and renal grafts (36,38–40). Treatment of HCMV in SOT patients is either done preemptively or prophylactically, with the former consisting of monitoring HCMV levels until detected at a certain threshold followed by treatment, and the latter focusing on a course of antivirals given regardless of whether HCMV is detected in the patient (36,41). Arguments for and against both of these methods exist: prophylaxis tends

toward more favorable outcomes than preemptive therapies despite the adverse effects caused by current antiviral therapies as well as the risk of selecting for resistant viral mutants, with several clinical studies being focused on emerging resistance (summarized in 35).

3.4.2.2 HCMV and Hematopoietic Stem Cell Transplants

In HSCT patients, the reactivation of HCMV can be as high as 40-50%, but unlike the HCMV syndrome seen in SOT patients, reactivation in HSCT patients depends on their HCMV status and manifests as an asymptomatic shedding of the virus (36). Despite being asymptomatic, this shedding may lead to eventual end organ failure and death, meaning that HSCT patients exhibiting virus shedding are monitored in case they progress to a disease stage (36). HSCT patients are generally not prophylactically treated with commonly-used anti-HCMV drugs, with the exception of the recently-discovered letermovir, because the drugs cause myelosuppression (42).

3.5 Lytic replicative lifecycle of HCMV

In order to understand the current state of antiviral treatment and the viral mechanisms they target, it is necessary to present the lytic phase of the viral lifecycle of HCMV. Indeed, during the latent phase, viral genes are not expressed and cannot be targeted by drugs. The lytic phase consists of a very tightly temporally-regulated cascade of viral gene expression after entry of the virus into a host cell. These genes are divided into three defined consecutive groups termed the immediate-early (IE) genes, the early (E) genes and the late (L) genes. Each of these temporally separated groups is responsible for different aspects of the viral lifecycle (an overview is given in figure 4)(43).

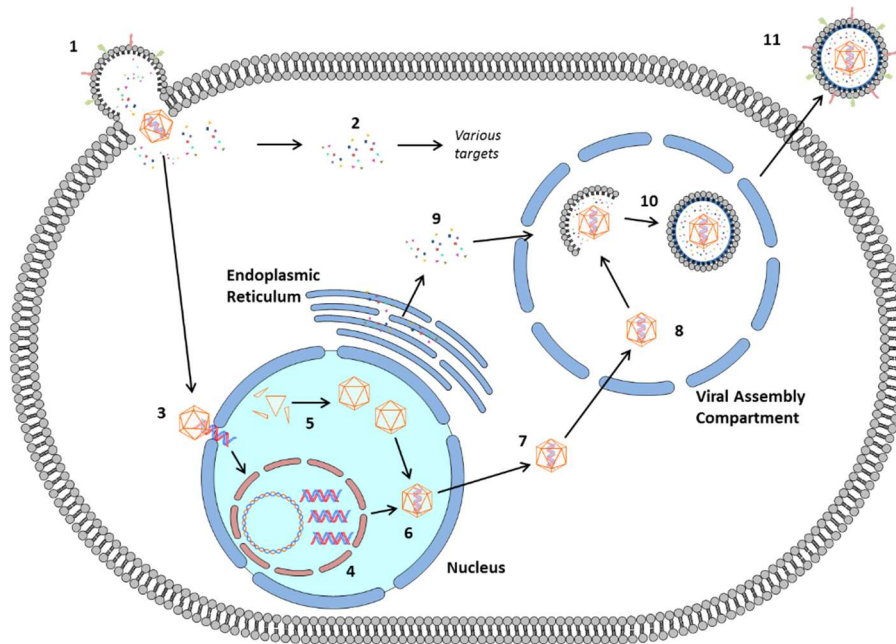


Figure 4. Simple overview of the lytic phase of the HCMV viral lifecycle. 1) The HCMV particle enters the host cell by fusing with the membrane or via endocytosis (not shown) and releases the nucleocapsid and viral tegument, beginning the Immediate-Early (IE) phase of infection. Released tegument proteins (2) interact with various host factors in order to suppress the innate immune response and attenuate the host cell for viral replication. The nucleocapsid (3) is transported to the host nucleus via microtubules and the viral dsDNA genome is injected through a nuclear pore. The Early (E) phase of replication begins when the dsDNA genome is circularized and viral genome replication begins in viral replication compartments (VRCs) (4). Capsids are assembled within the nucleus (5) and viral DNA is packaged within viral capsids by the terminase complex (6), beginning the Late (L) phase of viral replication. Assembled nucleocapsids then bud out of the nucleus (7) and are transported to the Viral Assembly Compartment (8), where they are packaged with newly-synthesized tegument proteins and enveloped (9 & 10). Viral particles then bud out of the host cell membrane, gaining the receptor complexes as mature viral particles (11).

Viral entry into the host cell is mediated by one of two viral complexes. The trimeric complex, consisting of the viral glycoproteins gH, gL and gO, facilitates viral entry into fibroblasts, while viral entry into epithelial cells is facilitated by the pentameric complex consisting of gH, gL, pUL128, pUL130 and pUL131 (44–46). Upon entry into the host cell, the virus releases both the capsid and the contents of the viral tegument into the cytoplasm. Some viral tegument proteins, such as pp71 (the product of UL82), immediately begin to suppress the host antiviral response (47,48). The capsid then migrates via the host microtubules to the nucleus, where it enters through docking of the viral capsid to the nuclear pore complex (48,49). Once the viral genome has entered the nucleus it is circularized and the Immediate-Early phase begins.

3.5.1 The Immediate-Early Phase

Several factors are expressed during the Immediate-Early (IE) phase, some of which act to begin transcription of viral DNA (vDNA) and others that modulate the host's innate immune response in order to generate a conducive environment for further replication. Of these factors, the most important is IE2, which encodes several isoforms due to differential splicing of the UL122-123 gene region (43,50,51). These completely indispensable isoforms are present throughout the entire viral lytic cycle and act as major transactivators of HCMV genes involved in viral replication (51–54).

Other proteins expressed during the IE phase, such as IE1, act to antagonize intrinsic antiviral defenses. Like IE2, IE1 is a group of gene products expressed by the differential splicing of the UL122-123 region (50,51). While it is also a transactivator of certain HCMV genes it also impairs the host innate immune defense by disrupting PML nuclear bodies (PML-NBs) (51,55–57). The host apoptotic response is also controlled by the IE proteins vMIA (encoded by UL37ex1) and vICA (encoded by UL36), which act to sequester the apoptotic cellular protein *Bax* and prevent procaspase-8 cleavage, respectively (58,59). Host PKR activation, which can potentially shut down translation in infected cells, is also inhibited by the tegument proteins IRS1/TRS1 during this phase (51,60).

Finally, IE2 products interact with the tegument protein pp71 and other IE factors at the *oriLyt* site to begin viral DNA (vDNA) replication, leading to the Early phase of the virus lifecycle (61).

3.5.2 The Early phase of replication

Genes expressed during the Early (E) phase of the viral lytic lifecycle are largely involved in the synthesis of vDNA in a cellular environment that has been primed during the IE phase (43). HCMV DNA replication occurs in a similar manner to that of other herpesviruses in that it proceeds in a biphasic manner which begins with a theta-type mechanism before progressing to a rolling circle mechanism (62).

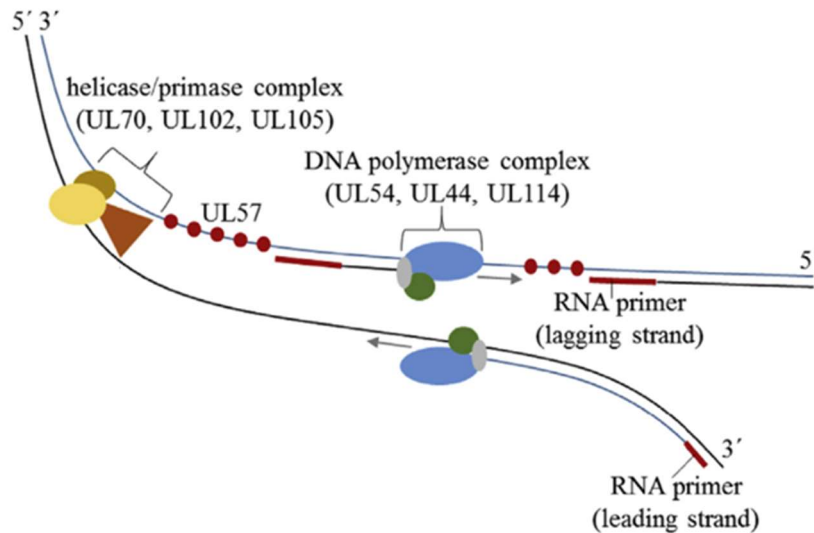


Figure 5. Graphical summary of HCMV replication. Potential activities of antiviral therapies are given in red. Adapted from (36).

Initiation of vDNA replication requires the interaction of pp71 and IE2 with the viral *oriLyt* (61). The viral replication compartment (VRC) is then formed with IE2 and E1 acting to recruit component proteins (43,63,64). These include amongst other factors the six core replication proteins, namely the viral helicase/primase complex consisting of pUL70, pUL102 and pUL105, the DNA polymerase pUL54 and the associated factor pUL44 as well as the single stranded DNA binding protein pUL57 (figure 5) (57). vDNA is first unwound by the helicase/primase complex, following which the single strands are bound by pUL57, thought to prevent reannealing of the separate strands and to be involved in repair and recombination of synthesized vDNA (43,57,64–66). The viral DNA polymerase then forms a complex with the processivity factor pUL44, which may prevent dissociation of the pUL54 polymerase from the viral template (67,68). Indeed, Sinigalia et al. showed that pUL44 mutants reduced DNA synthesis by causing the improper binding of pUL44 to the template DNA while not impairing its interaction with pUL54 (68).

The exact composition of the VRCs is little understood, and several factors other than the core six replication proteins are thought to be involved in vDNA replication. This is underlined by the fact that in addition to forming a protein complex with the viral polymerase, pUL44 also interacts with several other proteins, such as pUL84, and recruits them to the VRCs (57,69). One such protein is the uracil DNA glycosylase pUL114, which removes uracil erroneously incorporated into vDNA. pUL114 is involved in base-excision

repair and is indirectly recruited by pUL44 to associate with the catalytic domain of pUL54 to form the final polymerase complex (70,71). While vDNA replication can still occur in the absence of pUL114 it is severely diminished compared to wild-type replication, indicating that the presence of the protein is required for efficient vDNA replication (43,72). Following the formation of this polymerase complex, vDNA replication then takes place at the replication forks in the periphery of the VRCs, with nascent synthesized vDNA being localized to the center (57,73).

3.5.2.1 The viral alkaline nucleases

The family of viral alkaline nucleases (ANs) is a conserved group of herpesviral endo- and/or exonucleases that play various roles at later stages of the Early phase of vDNA replication (termed Early-Late or E-L), depending on the virus. While all herpesviruses encode for an AN their nucleotide sequences tend to be divergent. This is in contrast to their protein structures which contain conserved domains called I-VII (74) (Figure 6) The herpesviral nucleases also show sequence similarity with the λ -phage exonucleases, with which five of the seven conserved domains are shared, suggesting an avenue of insight to the function of the nucleases (74,75).

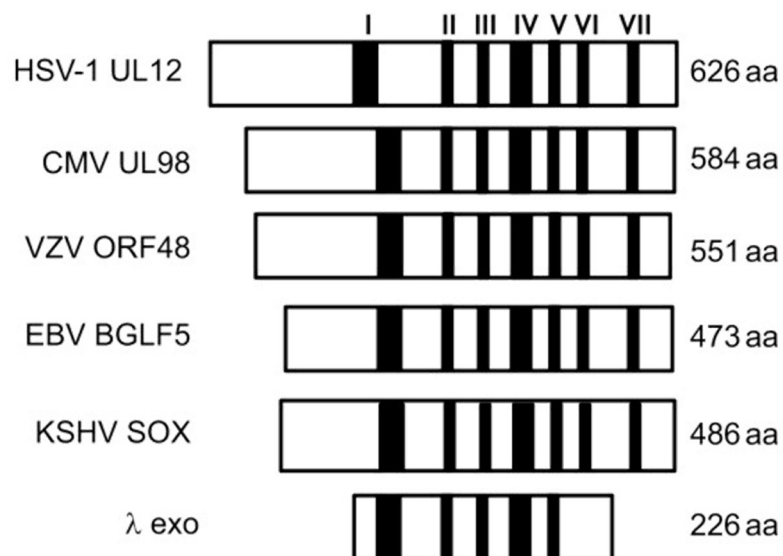


Figure 6. Overview of alkaline nuclease protein structure homologs between Herpes Simplex-1 (HSV-1, UL12), (human) cytomegalovirus (HCMV, UL98), Varicella Zoster Virus (VZV, ORF48), Epstein-Barr virus (EBV, BGLF5), Kaposi's sarcoma-associated herpesvirus (KSHV, SOX), and the λ -phage nuclease (Exo). The seven conserved domains are labelled I-VII. Adapted from (74).

The ANs have only recently begun to be investigated in depth, with focus being mostly on the alpha-herpesvirus Herpes Simplex-1 (HSV-1) AN encoded by UL12 and the shut-off and endonuclease (SOX) protein of the gamma-herpesvirus Kaposi's sarcoma-associated herpesvirus (KSHV, also known as Human herpesvirus 8, HHV-8).

3.5.2.2 UL12 in HSV-1

Like HCMV, the HSV-1 genome is replicated in a concatemeric form that is then recognized by its packaging machinery (reviewed in 76). However, unlike HCMV, the replicating genome of HSV-1 shows branched structures that are similar to those seen in recombination events (77,78). Replicating HSV-1 genomes do not migrate in a pulse-field gel, an assay of the amount of branching present in DNA, indicating that they are heavily branched and therefore most likely not replicating via a simple rolling-circle mechanism (74,77). Replicating HSV-1 genomes also contain a large amount of nicks and gaps, unlike the genomes of other DNA viruses, which in turn runs the risk of activating the antiviral aspects of the host DNA-Damage Response (DDR) (79). In order to prevent this HSV-1 expresses a single-stranded DNA binding protein encoded by the gene ICP8 as well as a 5'-3' exonuclease (Exo) encoded by UL12, which together are able to perform single-stranded annealing (80,81). HSV-1 AN-null mutants are known to be severely growth compromised; while the mutant is able to replicate its genome, the resulting product is prone to fragmentation and nuclear egress is severely impacted (82). Disruption of the exonuclease function of the AN by mutating a residue in the known catalytic triad resulted in similar growth patterns seen in the AN-null mutant, with cell-to-cell spread and viral dissemination severely impaired *in vitro*, indicating that the AN is indispensable for proper viral growth (74). Grady et al. were also able to show that loss of the exonuclease function of the AN resulted in improper packaging of the viral genome, with an increase in non-infectious A and B capsids instead of the fully-formed and infectious C capsid (74).

3.5.2.3 The KSHV SOX protein

The AN homolog within the gamma-herpesvirus KSHV is the protein encoded by the viral ORF37 gene, termed the SOX protein. Unlike the other herpesviral ANs, the SOX protein also carries out a host-shutoff function, which serves to prevent the host transcription on the mRNA level during lytic replication (83,84). This double-activity is also seen in the EBV BGLF5 protein. However, in other herpesviruses, the shutoff function is performed by additional proteins that are not homologous to the ANs (85,86).

The structure of SOX has been solved by Dahlroth in 2009, revealing that the SOX protein is active as a monomeric protein consisting of an N-terminal domain containing 10 α -helices and a C-terminal domain containing five-stranded β -sheets flanked by five α -helices. The C-terminal domain, termed the “core domain,” shows high similarity to other members of the PD-(D/E)XK nuclease superfamily (see Figure 7) (87). The overall protein structure was found to form a crevice containing highly conserved residues that bind to DNA. Because this crevice is relatively large, Dahlroth postulates that the AN must be able to bind to dsDNA *in vivo*, as opposed to binding only to ssDNA, which would be transiently generated in *in vitro* studies, precluding the determination of ssDNA/dsDNA binding by the protein. SOX shows structural similarity to the λ -phage Exo nuclease, even if it shows little sequence similarity, suggesting functional convergence with the phage exonuclease (87).

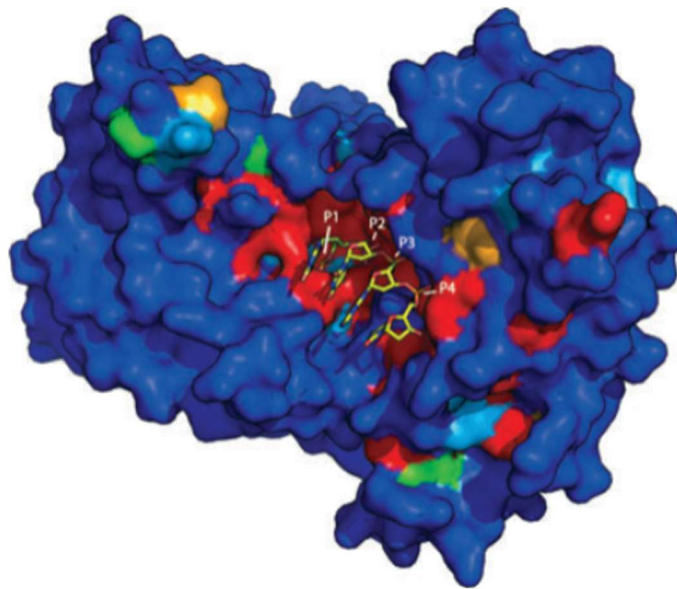


Figure 7. Structure of DNA bound to the KSHV SOX protein in the highly conserved crevice (center). Conserved residues are presented in red, with lesser conserved residues progressing in a color gradient to blue. The DNA molecule is presented as a ball-and-stick model. Adapted from (87).

Assays of the AN activity and the host-shutoff activity are separable by use of specific mutants, as identified by PCR mutational analysis (88). Mutating pSOX at T24I, A61T, P176S, V369I, D474N, and Y477* impairs the host-shutoff function without impacting the AN activity. By replacing a glutamine with a histidine at position 129, Uppal et al. were able to impair the nuclease activity of SOX while maintaining the shutoff function of the protein

(89). This mutant showed pulse-field gel migration results with a similar pattern of improperly processed vDNA as to that seen in HSV-1 mutants, indicating that the KSHV SOX is as essential to proper vDNA replication as UL12 is in HSV-1 (89).

3.5.2.4 The HCMV pUL98

Like the other herpesviruses, HCMV also encodes for an AN with the gene UL98. Like most ANs the pUL98 protein exhibits both 5'-3' and 3'-5' endo- and exonuclease activity, and are active predominantly at alkaline pH, low- to mid-salt concentrations and require a divalent cation such as Mg^{2+} (90,91). Unlike the other ANs discussed here, the exact role of pUL98 during lytic replication is still unknown. However, most ANs in other herpesviruses have been recently shown to impact the proper processing of viral genomic DNA into fully-assembled capsids. It is therefore reasonable that pUL98 would also have a similar role in the viral life cycle. It is known that pUL98 is essential for viral growth, with transposon disruption of the UL98 gene in two separate positions carried out by Yu et al., and genome-wide deletions carried out by Dunn et al., leading to no discernable virus growth (92,93).

Subsequent modeling and mutagenic work have been carried out on the virus. Kuchta et al. generated a structural prediction model of pUL98 based on the KSHV crystal structure, and predicted an active site containing the residues R164, S252, D254, E278, and K280, shown in Figure 8. (90).

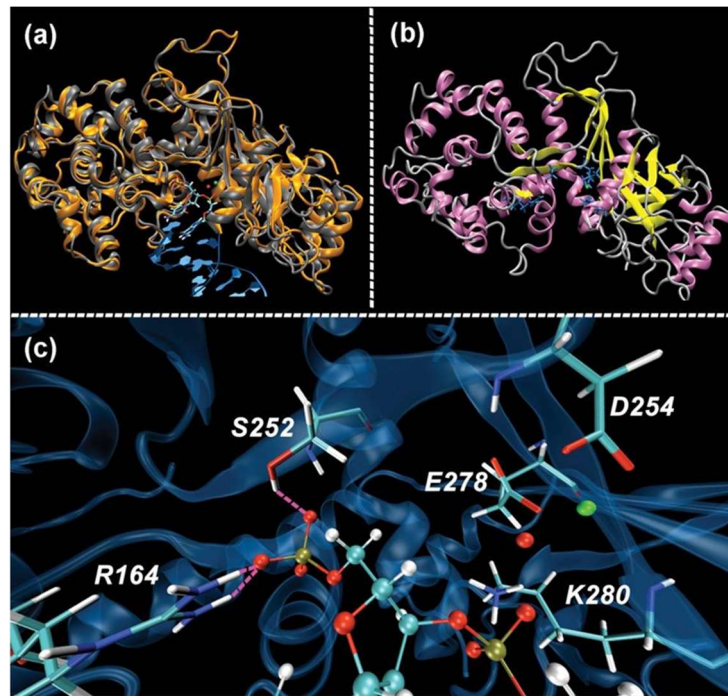


Figure 8. Predicted structure of pUL98. (a) Predicted structure of pUL98 (orange) overlaid on crystal structure of KSHV-SOX (grey). (b) Predicted structure of pUL98. α -helices in pink, β -sheets in yellow. (c) Predicted active site of pUL98 showing the positions of the active site residues R164, S252, D254, E278 and K280, with D254A and E278A thought to coordinate the Mg^{2+} ion and a water molecule. Adapted from (90).

Mutating residues of these putative active sites to alanine lead to a reduction in activity of purified pUL98, indicating their importance for proper protein function. Kuchta et al. were also able to demonstrate that replacing the UL98 gene with *E.coli* galK in a bacterial artificial chromosome containing the GFP-positive HCMV AD169 strain led to a lethal phenotype, while insertion of a UL98 gene from the Towne strain of HCMV partially restored activity. Additionally, introducing a stop codon/frameshift mutation in exon 5 of the UL98 gene of the AD169 strain led only to severely attenuated growth instead of a lethal phenotype (90). This still indicates that interference with the proper expression severely hampers viral dissemination *in vitro*, and the results of Kuchta agree with similar results seen by Grady et al. in that AN mutants generate singly-infected cells with no or slow viral dissemination (74).

3.5.3 The Late Phase of replication

Once the replication of genomic vDNA begins, the virus enters the Late phase of lytic replication. During this phase, the virus begins manufacturing new viral capsids within the nucleus, and the genomic vDNA is processed by a variety of viral proteins, such as members of the terminase complex (42, reviewed in 94).

3.5.3.1 The Terminase Complex

Once the rolling-circle phase of HCMV viral replication is reached, full length viral genomes must be processed into unit-length genomes and packaged into the newly-constructed capsids within the nucleus. Unlike other viruses, such as HIV, which construct their capsids around newly synthesized DNA, HCMV inserts unit-length DNA into completed capsids by processing the head-to-tail concatemers of the viral genome generated by the replicating rolling-circle with help of the viral terminase complex (figure 9) (95).

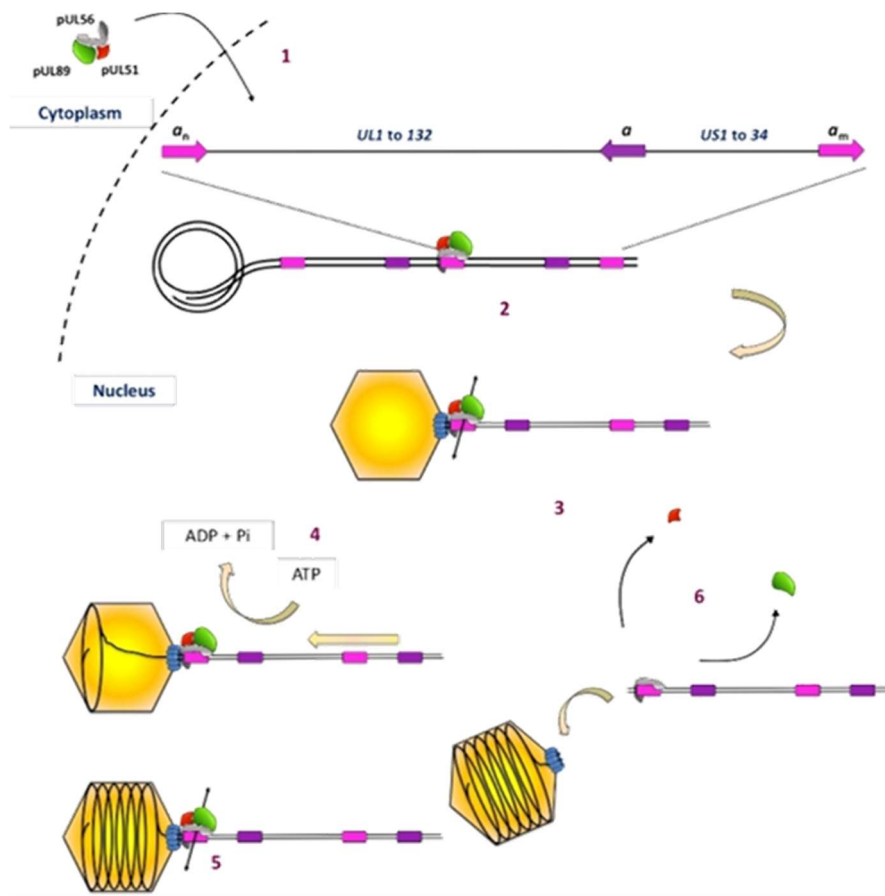


Figure 9. Mechanism of Action of the HCMV Terminase Complex. 1. The viral factors pUL56, pUL89 and pUL51 form the homo-oligomeric terminase complex and translocate within the host nucleus, where they 2. detect the AT-rich *pac* motif in the “a” region of the terminal ends and internal repeats of the concatemeric viral HCMV genome and 3. cleave the duplex and recruit a proviral capsid, positioning the complex at the unique portal vertex of the capsid. The complex then 4. uses ATP energy to translocate the viral genome into the procapsid, until it reaches 5. a second specific *pac* signaling motif and cleaves the duplex again, “measuring out” and packaging a unit length of the viral genome into the capsid. 6. The complex then subsequently dissociates from the DNA substrate for further recruitment to a *pac* packaging signal motif. Adapted from (94).

The viral terminase complex is composed of the viral factors pUL56, pUL89 and pUL51, which form a homo-oligomer that recognizes specific AT-rich regions of the concatemeric genome termed *cis-acting packaging signal* or *pac* motifs in the genome (highlighted in Figure 9) (96–99). Correct interplay between pUL56 and the other components of the terminase complex is essential for its successful formation: knockdown of one subunit generally diminishes the levels of the other subunits within the replication compartment (97,100). Following a preliminary site-specific cut made in the *pac* region, the complex then recruits a formed procapsid and positions the DNA to be translocated to a unique portal vertex, where pUL56 interacts with the portal protein pUL104, allowing for the correct translocation of vDNA into the capsid. The essential nature of this interaction was demonstrated by Krosky et al. and Dittmer et al., who found that interference with this interaction by use of the benzimidazole-D ribonucleosides BDCRB and the 2,5,6-trichloro-1-beta-D-ribofuranosyl benzimidazole TCRB completely prevented HCMV maturation (101,102). The complex then translocates the viral genome into the capsid until it recognizes a second site-specific *pac* region, where it cleaves the duplex a second time, in effect “measuring out” a unit length of the viral genome into the capsid (94,99). Following this final cut the components of the complex then detach and dissociate away from the replicating DNA for recycling into further virome packaging (103).

Other proteins are also thought to be involved in the function of the viral terminase complex, albeit indirectly. HCMV strains harboring pUL52 mutants generated by Borst et al. were found to result in uncleaved viral concatemers, even though the levels of the three terminase subunits were unchanged within the VRC, indicating that pUL52 may play an indirect role in the terminase complex activity (98). In the same vein, knockdown of pUL77 and pUL93, two viral proteins involved in the nuclear egress complex which interact with pUL50 and pUL53, resulted in the generation of only B-capsids. This form of capsid is present in the host nucleus and cytoplasm, and contains only scaffold protein, as opposed to non-infectious empty A capsid and the viral genome-containing C capsid. These results suggest that there may be an interaction between nuclear egress and vDNA packaging (104–107). However, the biological functions, specific structures, and localization of these proteins remain as of yet poorly defined.

Following vDNA packaging, the viral capsid then buds out of the host nucleus and into the cytosol, where it is subsequently trafficked into the viral assembly complex (AC). The AC consists of multiple viral proteins and the host endoplasmic reticulum (ER), Golgi apparatus,

and endoplasmic compartments (108). Here, the encapsulated viral particle buds into vesicles present in the AC, gaining their tegument and envelope in the process. After this final assembly, the virus-containing vesicle then fuses with host cell membrane, releasing the viral particle as well as several “dense bodies,” i.e., non-infectious particles containing large amounts of tegument proteins, but no capsid/genome (43,108).

3.5.4 The importance of the viral lifecycle

The tight regulation and complexity of the HCMV viral lifecycle therefore offers many possible antiviral targets. These range from theoretically disrupting the viral modulation of the host innate immune response and ideally leading to the safe apoptosis of an infected cell, to interference with vDNA synthesis, particle maturation, or even egress. However, this complexity also makes targeting any one pathway difficult, because there is functional redundancy within some of the viral lifecycle; out of the approximately 170 ORFs, only around 41-45 seem to be absolutely essential for viral replication in cell culture (92,93). The non-essential genes may play important roles *in vivo*, but a lack of adequate response in a cell-based system makes these genes difficult to develop as antiviral targets. As of this writing, several of the current therapies therefore target these essential genes, which can be broadly classified by their viral targets, as explored below.

3.6 Current therapies used for HCMV infection

3.6.1 Therapies targeting viral DNA replication

The relative complexity of the vDNA replication system along with the essential virus-specific factors involved means that the complex has long been seen as a potential target for antiviral therapies (as discussed in section 3.5.2). Several of the currently in-use therapies target this pathway in a variety of ways, along with several therapies currently in development. However, several drawbacks exist in using these major therapies. Firstly, and most seriously, the rise of CMV resistances to these therapies calls into question whether they will be effective in future therapeutic settings. Secondly, the major drugs all have relatively poor safety profiles, especially in regard to nephrotoxicity, and are often administered in long-term doses by invasive routes (109).

3.6.1.1 Ganciclovir/Valganciclovir and Acyclovir

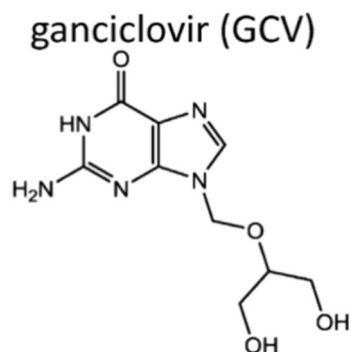


Figure 10. Molecular structure of ganciclovir (GCV). Adapted from (36).

One of the earliest approved drugs against HCMV disease is the acyclic deoxyguanosine analogue Ganciclovir (GCV) and its prodrug, Valganciclovir (VGCV) (Figure 10) (110,111). GCV is currently the most widely used treatment in HCMV infection and is known to be of benefit in immunocompromised hosts with HCMV disease, as well as congenitally infected infants (112,113). GCV is also used in the prophylaxis against potential HCMV disease in patients preparing for organ transplantation (114).

The mechanism of action of GCV relies on targeting the vDNA polymerase encoded by the gene UL54; however, GCV must first be phosphorylated to a triphosphate form for it to be active. First, GCV is phosphorylated to a monophosphate form by the viral kinase encoded by UL97. Then, it is phosphorylated to its final active form in an additional two steps by a variety of host kinases, for example dGMP kinase and guanylate kinase (110,115,116). Once in its active triphosphate form, the processed GCV acts a nucleoside analogue of the viral DNA polymerase, competitively inhibiting the elongation of vDNA after incorporation as well as chain termination (117). VGCV, the prodrug, releases GCV upon cleavage of a promoiety. VGCV shows higher oral bioavailability than GCV, which is administered intravenously (118–120).

As a nucleoside analogue (nucleosides are identical to nucleotides but do not contain a phosphate group), GCV/VGCV may be incorporated by the host cellular DNA polymerase, but shows much higher affinity for the viral DNA polymerase: it was reported to exhibit an inhibition constant of 1.7 μM for the viral DNA polymerase, versus 17 μM for the cellular polymerase (110). Additionally, GCV is in itself not highly cytotoxic in mammalian cells,

because it requires the presence of the pUL97 kinase for proper conversion to its active form, precluding activation in uninfected cells (111). However, because GCV is a substrate of both pUL97 and pUL54, GCV is susceptible to resistance mutations arising in either viral protein. As prophylaxis against HCMV in SOT tends to take the form of long timeframes with frequent administration of the drug, roughly 5-10% of SOT patients eventually develop resistant infections, usually mapping to the UL97 ORF encoding for the viral kinase (121,122). In addition, GCV/VGCV have common hematological side effects such as anemia, neutropenia and thrombocytopenia (111).

The compound Acyclovir (ACV) is a potent antiviral in HSV-I and VZV infections and works in a similar manner to that of GCV (36,123,124). While ACV can be converted to a triphosphate metabolite by pUL97, the resulting metabolite is a suboptimal substrate for the pUL54 DNA polymerase and shows only moderate effect against HCMV infection (125). While one study did show that the administration of valaciclovir (a promoiety comparable to VGCV) did prevent HCMV disease in renal transplant patients, the use of ACV to treat HCMV disease is regarded as being insufficient (126).

3.6.1.2 Cidofovir and Brincidofovir

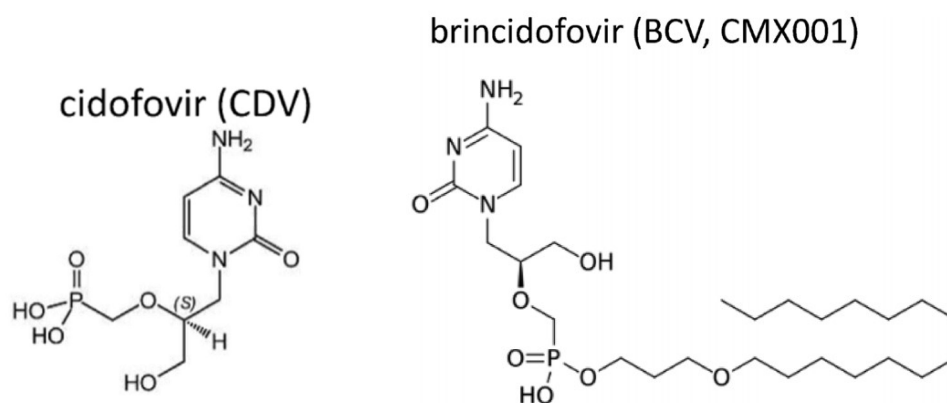


Figure 11. Molecular structure of cidofovir (CDV) and brincidofovir (BCV). Adapted from (36).

Cidofovir (CDV) (Figure 11) is an intravenously administered nucleoside analogue that acts in a very similar manner to GCV/VGCV. Unlike GCV, CDV is already in a monophosphate form and does not need prior processing by the viral pUL97 kinase. Instead, CDV requires only conversion to a diphosphoryl metabolite by host cellular kinases, such as pyruvate kinase and creatinine kinase, among others (127). Once processed, CDV acts as a competitor

for deoxycytidine triphosphate. Once incorporated into the replicating viral genome, it acts as a chain terminator, meaning that the addition of subsequent nucleotides is far less efficient, especially if two subsequent CDV residues are incorporated (128,129).

The independence of CDV from the pUL97 kinase means that CDV also carries a broad spectrum of activity against a variety of DNA viruses, such as other herpesviruses, polyomaviruses, adenoviruses, and others (summarized in 127). Due to this property, CDV has been used to treat HIV patients with HCMV retinitis, as Britt and Prichard point out that the broad-spectrum activity of the drug may be an asset in complex situations where co-infections are present; however, it is not orally bioavailable and demonstrated significant nephrotoxicity in human trials, hampering its clinical use (36,112,131). For this reason, CDV is mostly used as a secondary treatment against HCMV, especially when resistance to GCV is suspected, as CDV resistance maps exclusively to pUL54. HCMV resistance to CDV can therefore also lead to GCV resistance (121).

Brincidofovir (BCV, also known under CMX001) is an unapproved derivative of CDV belonging to a novel class of compounds termed the acyclic nucleoside phosphonates (131, summarized in 132). These compounds were generated following previous studies focusing on generating alkylglycerol phosphate or alkylpropyl phosphate esters of CDV and other antiviral drugs, a procedure which led to an increase in antiviral effectiveness of the altered compounds in animal models of HCMV (134,135). The addition of the lipid ester moiety greatly increased not only the antiviral activity of the drug when compared to CDV *in vitro*, but also its oral bioavailability compared to CDV in both MCMV animal models and HCMV trials. This is a large benefit, as CDV is predominantly administered intravenously in therapy (135–138). More importantly, the ester moiety significantly decreased its uptake in the kidney, reducing its nephrotoxicity (135). BCV also exhibits an increased broad-spectrum activity against other DNA viruses compared to CDV, enhancing the compound's potential as a broad antiviral for use in immunocompromised individuals with co-infection (130).

Resistance against BCV is expected to be the same as that of CDV, as upon the cleavage of the ester moiety from BCV yields high cytosolic amounts of CDV. Mutations generated *in vitro* conferring resistance to BCV generally caused resistance to both BCV and CDV, but maintained sensitivity to foscarnet (see below) and GCV (139). Unfortunately, while BCV did reduce HCMV levels in a phase II clinical trial for stem cell transplant patients as well as

in a phase III controlled clinical trial, it failed to meet its primary endpoints and is currently being reformulated as an intravenous therapy (36,140,141).

3.6.1.3 Foscarnet

foscarnet (FOS)

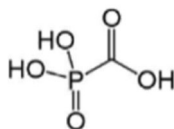


Figure 12. Molecular structure of foscarnet (FOS). Adapted from (36).

Like GCV and CDV, the pyrophosphate analogue Foscarnet (FOS) (Figure 12) acts on the viral DNA polymerase in order to hamper vDNA elongation. However, unlike GCV and CDV, FOS binds reversibly to the pyrophosphate binding site on the viral DNA polymerase. This binding interferes with the cleavage of pyrophosphate from the nucleoside triphosphate substrate, terminating DNA replication by preventing its incorporation into the nascent strand (142). This allosteric activity of FOS means that it does not require processing by cellular or viral factors in order to demonstrate efficacy. Like CDV, FOS also shows some activity against other herpesviruses, namely Herpes Simplex-1 and -2 (HSV-1 and -2), Epstein - Barr virus (EBV), and Varicella Zoster Virus (VZV). Also like CDV, FOS is of use in cases of co-infection (130).

FOS has been used in treatment in patients exhibiting AIDS with HCMV retinitis; however, FOS does cause renal toxicity, which limits the usefulness of the drug in clinical settings (143,144). However, as resistance to FOS involves a mechanism separate to resistance to GCV, cross-resistance is seldom seen between the drugs; nevertheless, a mutation in the viral DNA polymerase conferred a 6.3-fold increase in resistance to FOS as well as a 2.3-fold increase in resistance to GCV (121,145).

3.6.1.4 Fomivirsen

Another approved treatment of note is fomivirsen, an antisense phosphorothioate complement oligonucleotide of the viral mRNA encoding for IE2, which disrupts the HCMV lytic lifecycle by preventing IE2 translation (146,147). While this compound shows a long 55 h half-life *in vitro*, it is infrequently used in comparison to GCV, because it is largely limited to

the retina and shows poor systemic availability *in vivo* (148). Fomivirsen is no longer available from the manufacturer (109).

3.6.2 Inhibitors of the pUL97 viral kinase

The viral kinase encoded by the viral gene UL97 plays several roles in the replication of HCMV, and was first identified as the kinase responsible for the phosphorylation of the antiviral compounds GCV and ACV (116,125). Subsequent investigation has revealed that disruption of the kinase drastically reduced viral titers (149,150). This is because the viral kinase plays several roles within viral infection, including phosphorylation of host target proteins lamin a, lamin c, and p32 in the nuclear lamina; the phosphoryl inactivation of the retinoblastoma family; and the phosphorylation of the RNA polymerase II carboxyl-terminal domain. Interference of any of these functions can impact the viral lifecycle (151–153). This broad activity and necessity of pUL97 to the viral lifecycle makes the viral kinase an ideal target candidate for antiviral therapies.

3.6.2.1 Maribavir

maribavir (MBV)

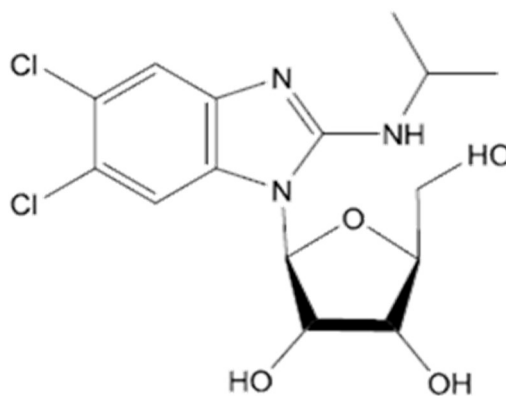


Figure 13. Molecular structure of the antiviral candidate compound maribavir. Adapted from (36).

The novel antiviral maribavir (Figure 13) was discovered by investigating chemical analogues of BDCRB, upon which it was discovered that the compound did not act on the terminase complex as expected. Instead, maribavir interacted in a novel way with the viral kinase (154). Indeed, after this discovery, the use of maribavir was an essential tool in elucidating the functions of pUL97 in infection.

Maribavir is well-tolerated in animal models and demonstrates favorable pharmacokinetic properties (155–157). It is a highly specific inhibitor of the pUL97 kinase, and due to these properties, was selected for further investigation into clinical trials. Unfortunately, maribavir failed to meet its clinical endpoint objectives in its first phase III trial (158). Further phase III trials focusing on comparing maribavir's efficacy with that of GCV are underway, and clinical development of the drug continues (36). However, it must be noted that while maribavir shows promise, it may not be of use in any combination therapy with currently accepted drugs relying on phosphorylation by pUL97 such as GCV/VGCV (159,160).

Resistance to maribavir is described as lying predominantly outside the pUL54 pathways, meaning that resistance to maribavir usually does not confer resistance to other commonly used antiviral drugs such as GCV/VGCV and CDV. There have been some rare functionally viable pUL97 *null* mutants that have arisen in a lab setting which confer resistance to maribavir as well as GCV/VGCV (161). Some mutations specific to maribavir resistance also map to the viral UL27 gene, which encodes for a viral protein responsible for degrading the host acetyltransferase Tip60 (162). It is not known whether interfering with the expression of UL27 is a viable alternative to the use of maribavir, as UL27 knockouts results in a half log reduction in viral titers *in vitro*, with no apparent effect on viral dissemination and replication in animal models (163).

3.6.3 Inhibitors of the terminase complex

The terminase complex as an antiviral target.

Current therapy for HCMV infection revolves around the major drugs GCV, CDV, and FOS, as described earlier in this work. These drugs have significant disadvantages, such as the development of resistances against them and severe side effects. The elucidation of the composition of the terminase complex, the discovery of its essential nature in the HCMV viral lifecycle, and the fact that the complex is unique in that there is no mammalian equivalent, immediately led to its investigation as a potential antiviral target. Indeed, Krosky et al. were speculating on the antiviral potential of BDCRB as early as 1998. However, even though the terminase complex presents a compelling antiviral target, only one therapy has been approved for use in HCMV treatment – the small molecule letermovir (164).

3.6.3.1 Letermovir

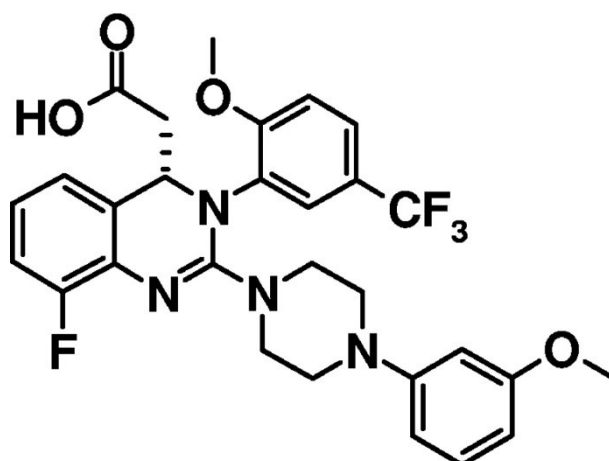


Figure 14. Molecular structure of the small molecular compound letermovir. Adapted from (165).

Approved by the US Food and Drug Administration (FDA) in 2017 as a novel antiviral therapy and prophylactic against HCMV in hematopoietic stem cell transplant patients, Letermovir is a potent inhibitor of the HCMV terminase complex, exhibiting an improved effect compared to GCV (Figure 14) (164). It is also far better tolerated than the current therapeutics used in treating HCMV, with negligible cytotoxicity *in vitro* (164). In phase II trials, the drug was not only well-tolerated by the study participants, but was able to prevent HCMV infection in hematopoietic stem cell transplant patients, while reducing clinically significant infection 24 weeks post organ graft (42,166).

Upon investigating the effect of treating HCMV with letermovir, Goldner et al. were able to demonstrate that there was a marked increase in uncleaved concatemeric HCMV genomes as well as an increase in the production of the non-infective scaffold-protein containing B capsids (167). However, to date, the exact mechanism of action of letermovir on the HCMV viral terminase complex is still unknown; although, data published from Lischka et al. indicate that letermovir may act upon the large terminase subunit pUL56 (165).

Studies focusing on HCMV gain-of-resistance to letermovir have been less optimistic (122,168). Several mutations in the pUL56 large terminase subunit have been identified after letermovir treatment, with Chou especially noting that the large terminase subunit encoded by UL56 rapidly accumulates several mutations that confer resistance to letermovir treatment without affecting viral growth rates (122). Other subunits of the viral terminase were also

shown to confer resistance to letermovir treatments after accumulating certain mutations: one study compared the mutation profiles in resistant HCMV strains and found similar patterns of resistance in both UL56 and UL89, both of which may confer cross-resistance or be independent of each other (169). In contrast to the strong resistance seen in large and/or small terminase units mutations in UL51 tend to confer only partial resistance to letermovir (170). Unfortunately, letermovir resistance has been reported in HSCT patients treated prophylactically with letermovir, with resistance mapped mostly to the UL56 region (171,172)

3.6.4 Other inhibitors of the viral terminase complex

While letermovir is the only approved drug targeting the viral terminase complex, several other drugs are currently under development.

3.6.4.1 Benzoimidine ribonucleosides

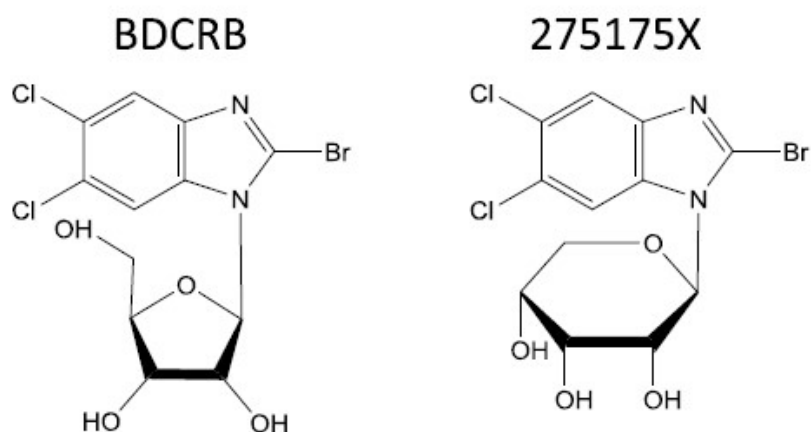


Figure 15. Molecular structure of the antiviral candidate compounds of the benzoimidine ribonucleosides BDCRB and 275175X. Adapted from (36).

The class of benzoimidine ribonucleosides (BRs) has long been known as inhibitors of the viral terminase pathway. The archetype of this class of small molecules is BDCRB, with studies carried out in 1995 and 1998 that demonstrated its potent antiviral effects both *in vitro* and *in vivo* (173,174). While members of the BR class of compounds are nucleoside analogues that do not target vDNA replication directly, like the analogues GCV or CDV, they interfere with the packaging of vDNA by acting on pUL56 and pUL89, causing cleavage sites to go unrecognized (101,175). Analogues BDCRB were additionally shown to interfere with the essential nature of the docking function between pUL56 and pUL104 (102).

However, for all its promise as an antiviral candidate, BDCRB was found to be rapidly degraded by 8-oxoguanine DNA glycosylase and N-methylpurine DNA glycosylase, leading to the termination of its investigation as an antiviral target (176). A stable variant of the compound, 275175X (2-Bromo-5,6-dichloro-1-(β -D-ribofuranosyl)-1H-benzimidazole) (Figure 15), has been recently generated, and also found to be effective against HCMV both *in vitro* and *in vivo*, via a similar mechanism to BDCRB (177–179). An in-depth study of resistance to this compound was additionally carried out and found to be characterized by resistance mutations within UL56 and UL89, similar to that of other terminase-targeting antiviral compounds (169). Although the antiviral effects of 275175X look promising, no clinical study or trial is underway as of the writing of this work (36).

3.6.4.2 Tomeglovir

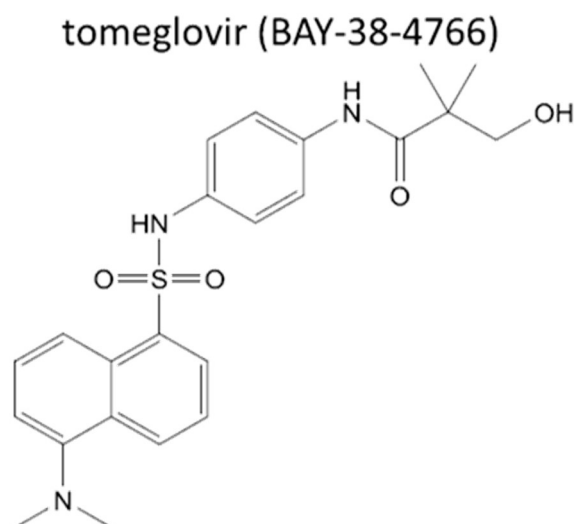


Figure 16. Molecular structure of the antiviral candidate compound Tomeglovir (BAY-38-4766). Adapted from (36).

Another promising antiviral candidate is the compound tomeglovir (also known by the codename BAY-38-4766) (Figure 16). This antiviral was the lead compound in a group of small molecular compounds investigated by Reefschlaeger et al. (180). Tomeglovir shows a very broad antiviral spectrum and is also effective against HCMV in an infected mice model, with further studies showing that the compound had good pharmacokinetic properties (36,181). Mapping of HCMV mutations caused by treatment with tomeglovir showed that they centered on the genes UL56 and UL89, confirming the compound's antiviral activity against the viral terminase pathway. More recent work indicated that some of these mutations

also confer cross-resistance to letermovir, while other mutations are unique to treatment with tomeglovir (169,182).

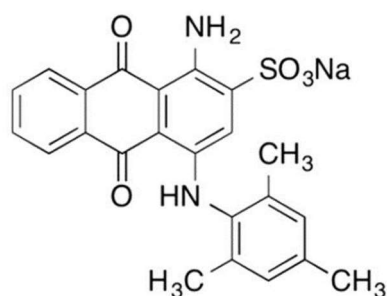
3.7 The need for new antiviral compounds

The rise in resistance to currently used drugs as well as their poor safety profiles call for the identification of novel antiviral targets as well as therapies against them. This is highlighted by Britt and Prichard (2018): they noted that until the recent approval of letermovir, most of the approved drugs have been approved in the late 1980s, a situation which has proven conducive for the emergence of resistance within the clinical setting. The complex balance of the HCMV viral lifecycle, while difficult to investigate, does provide for ample unique antiviral targets. This is especially the case for viral factors essential for the correct synthesis of the viral genome, as several of the pathways discussed show no homolog to host cellular factors. One such essential factor is the family of viral alkaline nucleases.

3.7.1 The viral alkaline nuclease as an antiviral target

Work focusing on the alkaline nucleases have highlighted their potential as an antiviral target. During their work on HSV-1's UL12, Grady et al. were able to show that treatment of infected cells with a variety of α -hydroxytropolones inhibited the AN's exonuclease function, leading to similar kinetics seen in their single-residue and AN-null mutants (74). Similarly, Uppal et al.'s generation of KSHV SOX protein with impaired AN activity showed improperly-processed DNA, as seen in the HSV-1 mutants, indicating a similar mechanism of function and the potential of KSHV SOX as an antiviral target (89). While, as of writing, comparable experiments in HCMV have not been carried out, it is known that pUL98 is essential for viral growth, with disruption of the UL98 gene in two separate studies carried out by Yu et al. and Dunn et al. leading to no discernable virus growth (92,93).

3.7.1.1 Compounds targeting the HCMV alkaline nuclease



Atanyl Blue PRL (Acid Blue 129)

Figure 17. Molecular structure of Atanyl Blue PRL (Acid Blue 129). Adapted from (183).

To date, only one compound has been shown to be active against pUL98. Using the knowledge that emodin, an anthraquinone molecule, inhibits the HSV-1 pUL12 AN, Alam et al. investigated various anthraquinone derivatives for their ability to inhibit pUL98 (183). Of the derivatives tested, they found that one anthraquinone, Atanyl Blue PRL (also known as acid blue 129, see Figure 17), was effective against pUL98 in human MRC-5 fibroblasts and showed low cytotoxicity. This finding is consistent with earlier work done on the anti-CMV properties of the compound (183). However, Atanyl Blue PRL shows a relatively high IC_{50} of 9.3 μ M, and no further information on development of this compound is available as of writing of this work.

3.8 Characterization of Novel Antiviral Compounds

In general, novel antiviral compounds need to be found that 1. exhibit a good inhibition of viral growth, often measured by the concentration at which a compound inhibits 50% of viral growth, called the IC_{50} , 2. exhibit low toxicity against host cells, often measured by the concentration at which they cause cytotoxicity in 50% of host cells, or CC_{50} , and 3. are selective for the viral target, quantified by the ratio of the $CC_{50} : IC_{50}$, also known as the Selectivity Index (SI) (a brief explanation of these concepts can be found in 183). Ideally, a novel antiviral will have a low IC_{50} , ideally in the low micromolar to nanomolar range; above 10 μ M, compounds begin to interfere with the Cytochrome P450 pathway, a common pathway used by cells to metabolize drugs (185). An ideal compound therefore has a high CC_{50} , low IC_{50} and a high SI, indicating a preliminary candidate antiviral demonstrating safety and selectivity for the viral target.

4 Rationale for this work

This work first aims to validate the viral AN pUL98 as a viable antiviral target. The severe side-effects of commonly used anti-CMV antivirals and the rise in resistance to these therapies underline the need for improved antivirals (36,169,171). pUL98 has been shown to be an essential protein for viral replication and dissemination and is not involved in the viral pathways targeted by currently used drugs, making pUL98 a candidate as a novel antiviral target. (90,92,93).

The second aim of this work is to develop a high-throughput screening system to identify novel inhibitors of the viral AN. Inhibitors identified in the high-throughput screen will then be verified and characterized for their activity in an infectious model. Inhibitors demonstrating good activity against pUL98 will also be tested for activity against other herpesviral ANs in order to identify any broad-spectrum activity.

In addition to this work, a crystal structure will be generated with the aim of solving the structure of pUL98. This will be done with the help of collaborators, and insights from this will then serve as a method to further design novel compounds inhibiting pUL98 based on the structure of the protein active site.

It is expected that the results of this study will expand current knowledge of pUL98 as an antiviral target and identify novel inhibitors of the CMV AN.

5 Results

5.1 Target Validation of UL98

Proteins and/or functions essential for viral growth are potentially suitable drug targets. In order to ascertain whether pUL98 was essential for viral growth, I modified the nucleotide sequence underlying the highly-conserved aspartic acid at position 254 (D254) and glutamic acid at position 278 (E278) within the catalytically active site predicted by Kuchta et al. (90). Moreover, modification of these residues should not affect the overlapping UL99 region.

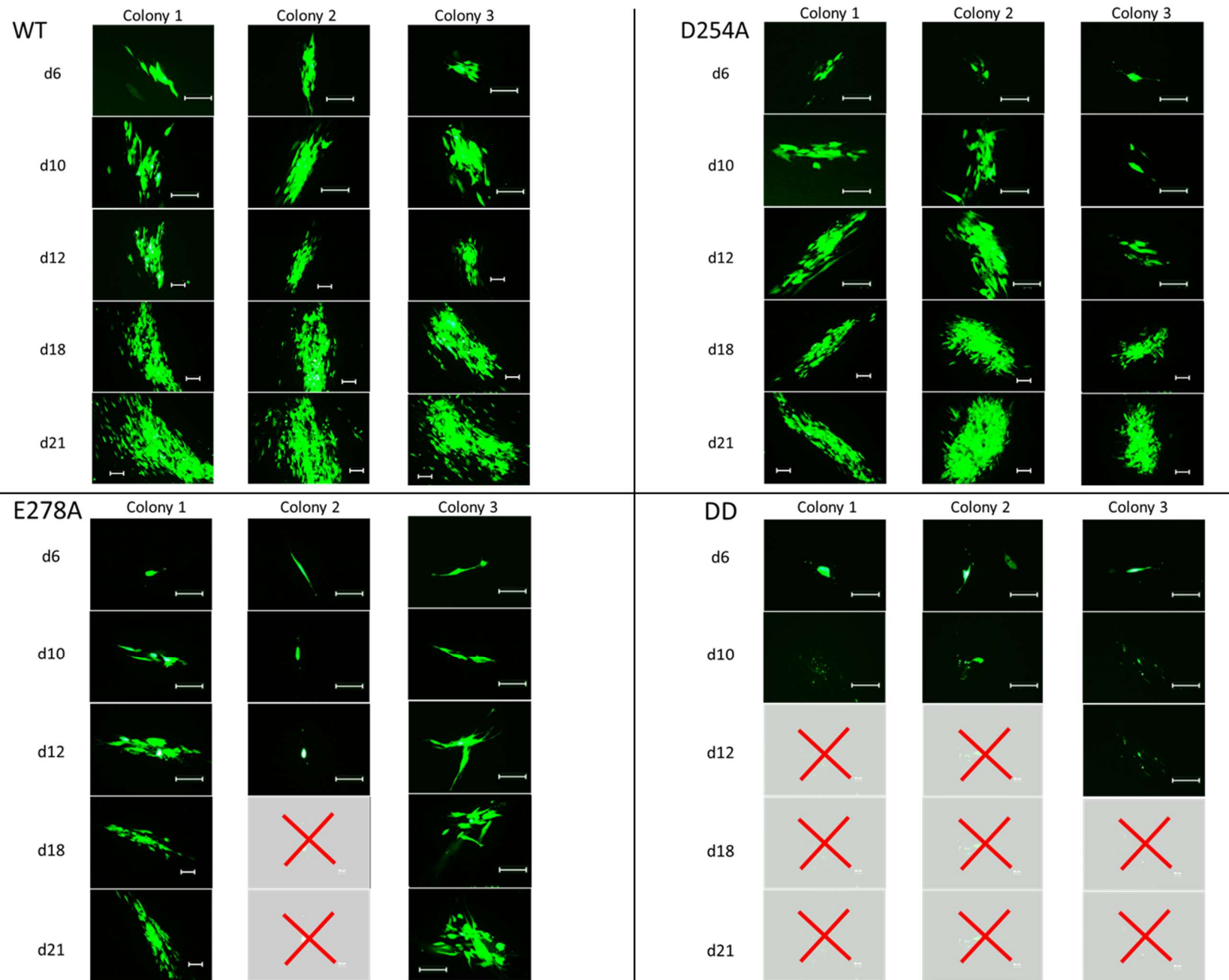
To do this, I introduced point mutations by *en passant* mutagenesis, as described in section 8.1.13. The target region was the UL98 region of a bacterial artificial chromosome (BAC) containing the HCMV strain TB40/E*wt*-GFP with an HA-tagged UL98 protein (referred to in this work as wt-GFP), a variant of the TB40/E strain which contains a green fluorescent protein (GFP) cassette driven by a simian-virus 40 (SV40) promoter (186). Using this method, I then generated three separate virus mutants based on the structural modeling carried out by Kuchta et al. (see section 3.5.2.4): namely, the mutant D254A, in which an adenosine is changed to cytosine at nucleotide position 177191, changing the protein sequence at position 254 from an aspartic acid to an alanine; the mutant E278A, in which an adenosine is changed to a cytosine at nucleotide position 177263, changing the protein sequence at position 278 from a glutamic acid to an alanine; and DD, a mutant containing both the above changes, changing the protein sequence to alanines at positions 254 and 278. Base substitutions were verified by commercial Sanger sequencing (Figure 18 overleaf). The verified wt-GFP and the three mutant BACs were then transfected into MRC-5 cells in order to reconstitute the virus.

As GFP is expressed by the HCMV construct, only infected cells will fluoresce green. This allowed me to follow the reconstitution and growth of the virus by observing the spread of fluorescence after transfecting the BACs over a period of 21 days. All modifications of the active site of pUL98 lead to attenuation of viral growth compared to the wt-GFP over the 21 days (Figure 19). While viral growth was seen in the D254A mutant, it showed a much more attenuated growth than the *wt* virus, forming only small foci which slowly expand compared to the faster and more widespread growth of the *wt* virus, which formed visible plaques at 18 days post transfection. This attenuated growth was also observed in the other single-residue active-site mutant E278A. In contrast, the DD mutant virus was lethal as no growth was seen,



Figure 18. Results of Sanger sequencing of A) D254A, B) E278A, and C) DD. The wt-GFP nucleotide and protein sequence is compared to that of the mutants, with differences in nucleotides highlighted in red. A) Changing an adenosine to cytosine in the D254A mutant at nucleotide position 17719 expressed an alanine instead of an aspartic acid at protein position 254. B) Changing an adenosine to a cytosine in the E278A mutant at nucleotide position 177263 expressed an alanine instead of a glutamic acid at protein position 278, C) Introducing both alterations from A and B to the wt-GFP genome generated the double DD mutant containing both D254A and E278A. No other nucleotide alterations caused by the en passant mutagenesis method are found in these sequences (“scarless mutagenesis”).

Figure 19 (overleaf). Timecourse of MRC-5 cells transfected with BACs containing wt-GFP (WT), D254A mutant, E278A mutant, or DD mutant. Pictures of fluorescence of three colonies per condition were taken at 6, 10, 12, 18 and 21 days post transfection (dpt). wt-GFP virus reconstitution occurred rapidly, with GFP foci spreading to a general spread by day 21. The D254A mutant showed slower virus spread compared to wt-GFP by 21 dpt, with smaller foci and no general spread. A slower spread is seen in the E278A mutant, with only very small foci seen at 21 dpt. The DD mutant showed a lethal phenotype, with virus not spreading from single cells after transfection and cells apoptosing by day 10 and subsequent loss of the virus at later timepoints, represented by a crossed-out gray field. Scale bar is equal to 200 μm .



as only a few green cells were visible and did not propagate or expand before their death at day 10 post transfection. These results are consistent with previous research on the essentiality of pUL98 for viral growth, such as seen by Yu et al and Dunn et al. (92,93). This indicates and confirms that interfering with only the active site of pUL98 leads to significantly attenuated growth or is lethal to the virus. The importance of the catalytic site of pUL98 for viral growth suggests that the alkaline nuclease is a valid antiviral target of HCMV *in vitro*.

5.2 Development of an alkaline nuclease activity assay suitable for high-throughput screening

5.2.1 Designing an expression system for tagged pUL98

As I wished to design a high-throughput screening system for pUL98, it was necessary for me to clone, express, and purify pUL98 in an appropriate expression system. To this end, I then cloned the AD169 UL98 region into the multiple cloning site of the pET28b+ plasmid backbone. This plasmid uses the T7 promoter allowing for the expression of the cloned protein upon addition of isopropyl β -D-1-thiogalactopyranoside (IPTG) in the *E.coli* strain BL21(DE3). I PCR amplified the AD169 UL98 region with a forward primer containing a recognition site for the restriction enzyme *Bam*HI and a reverse primer containing the site for *Not*I. Following amplification, both the UL98 sequence and the pET28b(+) vector were digested with *Bam*HI and *Not*I, and the UL98-containing insert was cloned from position 202-167, resulting in a 7,107 base pair plasmid containing the UL98 region in-frame with an internal 6x-His tag in the reverse 3' -5' strand, which I termed 6x-His-pUL98 (Figure 20).

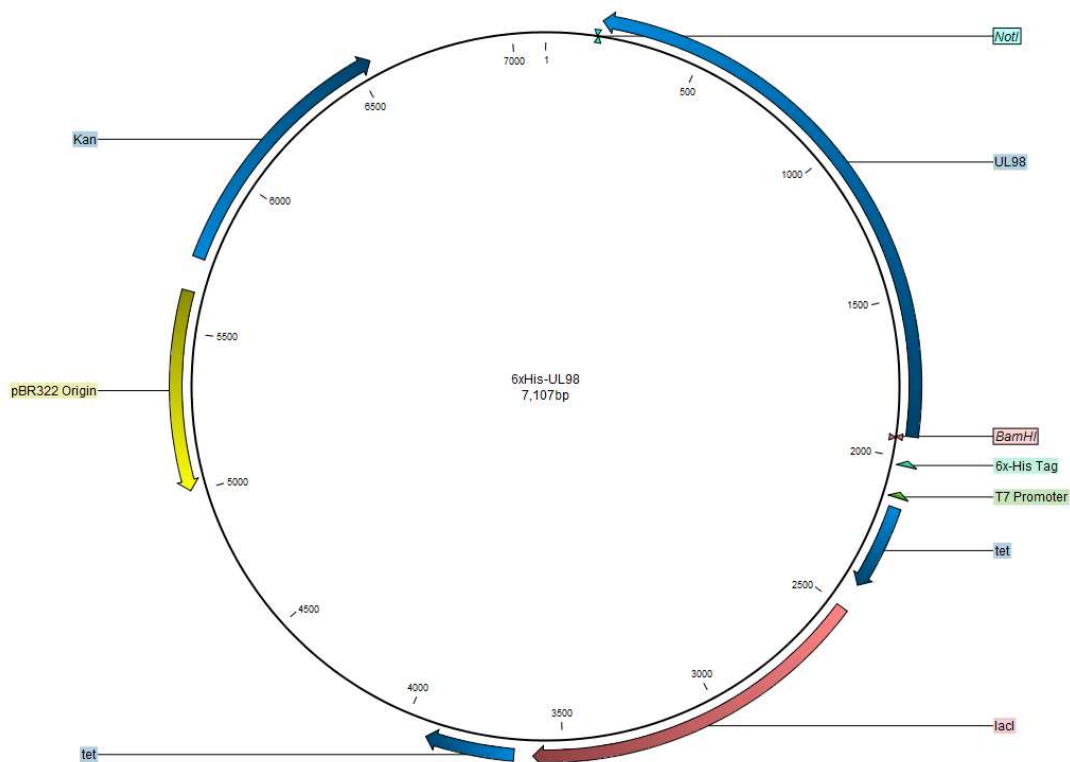


Figure 20. Plasmid map of 6x-His-pUL98. Shown is the UL98 sequence derived from the HCMV AD169 strain inserted into the pET28b (+) expression plasmid. Also shown is the Kanamycin resistance cassette Kan, the 6x-His sequence attached to the UL98 sequence by a linker of 75 base pairs, the T7 promoter and lacI expression system and the pBR322 replication origin.

5.2.2 Inducing expression of pUL98

The expression of the protein was done using the pET28b (+)-BL21(DE3) system. In this system, the *E. coli* strain BL21(DE3) was induced to express the protein by adding IPTG and allowing the bacteria to grow at a reduced temperature in order to prevent the formation of inclusion bodies for a set time. Because the final concentration of IPTG, temperature, and induction time differ for each system, these factors must be optimized for each procedure. To that end, three combinations of IPTG concentrations, induction temperatures and induction times were tested. These were named Method 1 to 3 and are detailed in Table 1. Methods 2 (90) and 3 (183) were sourced from previous work done on expression of pUL98 in the pET28b(+) system, while Method 1 was designed upon advice from Dr. Shankar Kumar, an expert in the use of the system.

Method Number	Conditions
1	0.5 mM IPTG, 30 °C for 4 hours
2	1 mM IPTG, 22 °C for 3 hours
3	1 mM IPTG, 25 °C for 3 hours

Table 1. Table describing three methods for the induction of 6x-His-pUL98 in the pET28b (+) system. Methods describe varying amounts of IPTG to BL21(DE3) bacteria upon growth to $OD_{560} = 0.6$ as well as varying lengths and temperatures of induction.

After inducing expression of protein using the different methods, the protein was purified according to the protocol given in section 8.2.1 of this thesis. The purified protein was then visualized by immunoblot staining with mouse α -6x-His antibody, because no antibody against pUL98 is commercially available. While all methods showed expression of the 6x-His-tagged pUL98, method 3 yielded the highest amount, as evidenced by the dense band of pUL98 in Lane 3 at 65 kDa (Figure 21).

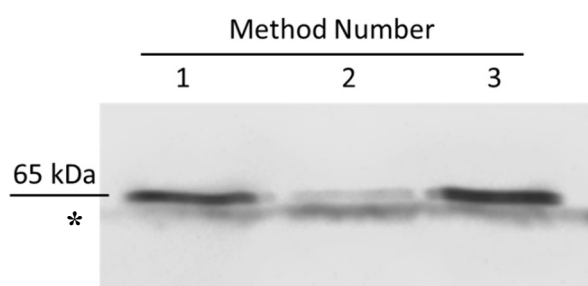


Figure 21. Immunoblot staining with mouse antibody recognizing the 6x-His-tagged pUL98 generated by the three tested induction methods 1-3. Method 3 showed the highest amount of protein expressed by the pET28b(+) system compared to the other two systems. Gel percentage: 12 % acrylamide, visualized using ECL substrate in a Fusion camera system, exposure for 1 min 30 secs. *: artifact of protein transfer from SDS-PAGE gel to nitrocellulose membrane.

5.2.3 Purification of the pUL98 protein

Once the condition for the induction of pUL98 in bacteria was optimized, I extracted pUL98 and checked the purity of the batches. For this I used two methods; first, I ran a sample of the batch on a polyacrylamide gel and visualized total protein present in the batch by staining with the protein binding Coomassie dye. A second sample of the protein batch was then separately immunoblotted and stained with the α -6x-His antibody used in section 5.2.2, which determines whether any other His-containing proteins were carried forward during the purification.

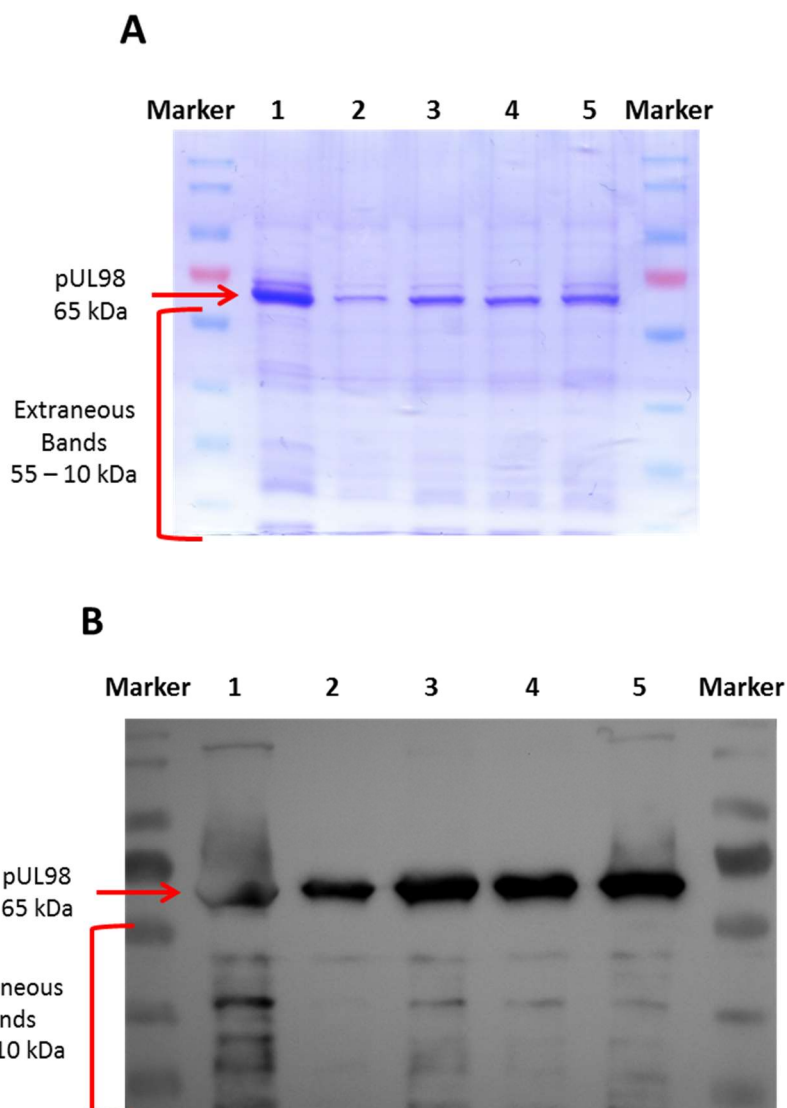


Figure 22. Example Coomassie dye total protein stain (A) and immunoblot (B) of five separate 6x-His-pUL98 batches (lanes 1-5). In A the total protein can be seen by the Coomassie stain, where the extraneous bands are faintly visible from 55-20 kDa (red bracket). This is more clearly seen in the immunoblot in B, where the membrane is stained with α -6x-His antibody which highlights the 6x-His-tag containing pUL98 at 65 kDa (red arrow). Several extraneous bands can be seen from 55-20 kDa (red bracket), indicating that these extraneous bands contain 6x-His and were co-purified with the pUL98.

The Coomassie stain in Figure 22A shows the total amount of protein present in batches 1-5. A strong band was seen at 65 kDa in each batch which is likely pUL98 as it corresponds to the predicted 65 kDa size. In addition, extraneous bands are visible in each batch from 55-10 kDa. The same pattern could be seen in the 6x-His stained immunoblot in Figure 22B, indicating that the bands at 65 kDa were likely to be pUL98, while the additional bands contain His and were probably co-purified with the pUL98 and were unlikely to be artifacts arising during the immunostaining procedure.

I therefore decided to test whether these extraneous bands would interfere with the activity of the purified pUL98 or exhibit DNase activity of their own, as this would severely impact any tests based on the purified protein.

5.2.4 Activity of pUL98

As purified pUL98 was intended for further downstream use, it is important to determine whether the protein was functionally active. This is necessary because purification of the protein from an expression system does not guarantee that the protein will be folded appropriately or retains function outside of the host environment.

As it is known that pUL98 shows no sequence or endo/exonuclease preference a simple assay to confirm functional activity was devised. In this assay purified protein was incubated in Nuclease buffer for 12 hrs in the presence of a plasmid. It was expected that the purified protein would nick or digest the plasmid DNA if it retained activity. As plasmid DNA is circular and present in different conformations in solution, any digestion of the plasmid would lead firstly to less plasmid, and secondly to more open and/or linear forms as the plasmid structure was degraded.

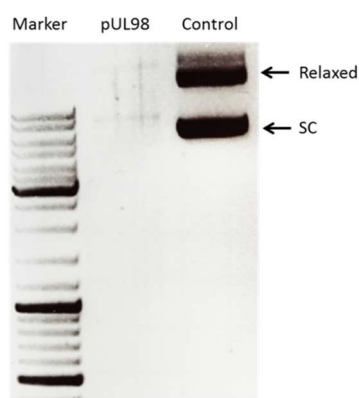


Figure 23. Activity assay of NiNTA-purified 6x-His-pUL98. 250 ng pcDNA3 (plasmid cDNA) is added to either purified 1 µg 6x-His-pUL98 in Nuclease buffer (pUL98 lane) or Nuclease buffer only (Control lane) and incubated for 12 hrs. at 37 °C. pcDNA3 is almost entirely degraded in the pUL98 well while the control shows the expected supercoiled (SC) and relaxed bands, indicating that the protein purified by the NiNTA-6x-His procedure is functionally active.

Purified 6x-His-pUL98 protein (pUL98 lane) was able to fully degrade the plasmid DNA after 12 hours, with little or no relaxed (i.e. plasmids that are nicked and not coiled) or supercoiled (SC) plasmid bands detected in the pUL98 lane compared to the pcDNA control (Control) (Figure 23). There was also no linear band visible in the pUL98 lane, which is expected when the plasmid is digested, probably due to the fact that it also had been degraded. This result

shows that purified batch of 6x-His-pUL98 still maintained nuclease activity, even after purification.

5.2.5 Contaminating bands are unlikely to show DNase activity

The DNase activity seen in Figure 23 may be due in part to the extraneous bands observable in the gel in Figure 22 possibly containing contaminating nucleases, as has been posited by Kuchta et al. in their work on purified pUL98 (90). It was therefore important to investigate any possible potential residual DNase activity in the purified protein batch as a whole.

To this end I introduced a single base substitution (nucleotides A to C at position 5936) using the QuikChange™ (Agilent Technologies) method which caused an aspartic acid to alanine substitution at position 254 of the protein (D254A). This mutation was chosen as it severely attenuates viral growth as seen in the experiments in Figure 19 and therefore should attenuate the DNase activity of the purified protein.

The 6x-His-D254A-pUL98 protein was then purified using the NiNTA-His method, and the purified protein was then subjected to an activity assay. In this assay, a pcDNA plasmid was degraded by either the 6x-His-pUL98 protein or the 6x-His-D254A mutant in nuclease buffer. The assay is run at 37 °C for 6 hrs because this time point is before the digestion runs to completion, allowing for better visualization of differences of activity between the two proteins.

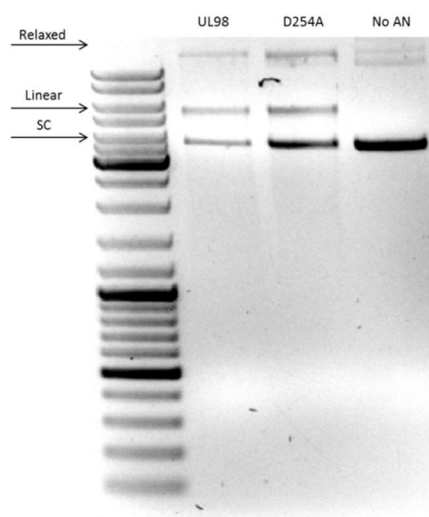


Figure 24. 250 ng pcDNA3 was added to 1 µg of either 6x-His-pUL98 protein (UL98) or 6x-His-D254A-pUL98 protein in 20 µl nuclease buffer or nuclease buffer only (Empty Control) and incubated for 6 hrs. at 37 °C. The resulting products were then run on a 1% Agarose gel in TAE buffer. D254A-UL98 protein showed a reduced nuclease activity compared to that of the fully-functional 6x-His-pUL98 as seen by the increased amount of supercoiled (SC), linear, and relaxed bands compared to the fully-functional 6x-His-pUL98 protein.

The results in Figure 24 show that the undigested plasmid in the Empty Control showed only the Supercoiled (SC) and relaxed band but not the linear band. The linear band appeared in the 6x-His-pUL98 (lane UL98) meaning that the plasmid was degraded by the protein sample. The D254A-UL98 protein (lane D254A) also showed a linear band, but the plasmid bands were denser than in the UL98 lane, indicating that less digestion of the plasmid was taking place.

The result is in agreement with the results seen in Figure 19, where the D254A mutant virus showed attenuated growth and not complete death, reflecting that some residual activity of the mutant protein was kept. While this reduced activity cannot completely rule out DNase activity of the contaminating band, it does mean that such activity is unlikely.

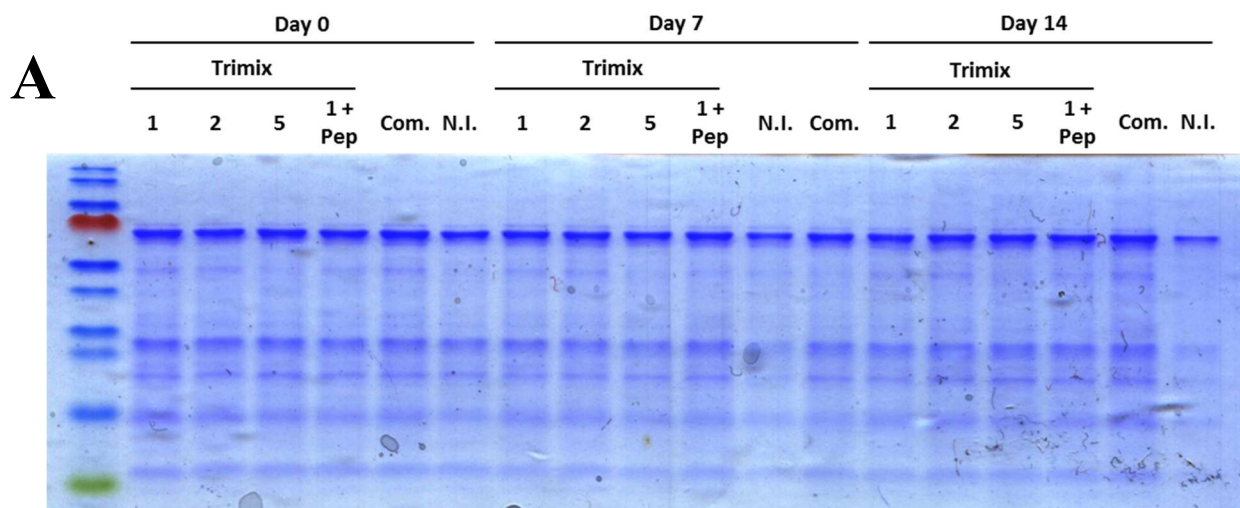
5.2.5.1 The contaminating bands are not the result of protein degradation

My goal was to generate protein pure enough for the generation of crystals for structure resolution, so I decided to investigate whether the extraneous bands present in the purified protein was due to degradation of the purified 6x-His-pUL98 protein. Even though the lysis buffer contained protease inhibitors, I could not rule out the possibility that the inhibitors used were not active against potential proteases co-purified with the pUL98. I therefore developed an assay where six separate batches of 6x-His-pUL98 were purified in the presence of different protease inhibitors at diverse concentrations, as detailed in Table 2:

Condition Name	Proteases Used
1x Trimix	200 μ M Pefabloc SC, 5 μ g/ml Leupeptin, 5 μ g/ml Aprotinin
2x Trimix	400 μ M Pefabloc SC, 10 μ g/ml Leupeptin, 10 μ g/ml Aprotinin
5x Trimix	1 mM Pefabloc SC, 20 μ g/ml Leupeptin, 20 μ g/ml Aprotinin
1x + Pep	200 μ M Pefabloc SC, 5 μ g/ml Leupeptin, 5 μ g/ml Aprotinin, 1 μ g/ml Pepstatin
Complete (Com.)	1x commercial protease inhibitor tablet, EDTA-free
N.I.	No Inhibitor

Table 2. Conditions used to purify six separate batches of 6x-His-pUL98, detailing type and concentration of protease inhibitors used.

Once purified, the batches were then kept at 4 °C for 14 days, with protein samples taken at day 0, day 7 and day 14 which were snap-frozen using dry ice and stored at -80 °C. Samples were then run on a 12% polyacrylamide gel, and total protein was visualized by Coomassie staining. The pUL98 bands of each condition at 65 kDa were then quantified with densitometry against their day 0 sample *in silico* and summarized in table B in Figure 25. If proteases were present and were uninhibited, a higher degradation of the protein should have been observed over time, with an expected loss of the protein band at 65 kDa and an increase in intensity of the bands below 65 kDa.



B

Treatment	Day	Percentage relative to Day 0
1x Trimix	0	100.0%
	7	97.0%
	14	97.0%
2x Trimix	0	100.0%
	7	96.4%
	14	100.0%
5x Trimix	0	100.0%
	7	100.0%
	14	100.0%
1x + Pep	0	100.0%
	7	90.0%
	14	100.0%
Complete	0	100.0%
	7	92.1%
	14	100.0%
N.I.	0	100.0%
	7	89.1%
	14	56.4%

Figure 25. (A) Coomassie-stained polyacrylamide gel of 6x-His-pUL98 extracted using various protease inhibitor conditions at three timepoints, demonstrating the impure batches at 55-30 kDa. The conditions used are detailed in Table 2. The full-length pUL98 band used for densitometry quantification in B at 65 kDa is indicated. 12% Polyacrylamide gel, 5 μ g protein loaded per well. **(B)** Results of densitometry analysis carried out on the indicated band in A. Results of Day 7 and 14 are given as a percentage of Day 0. With the exception of the No Inhibitor (N.I.) batch all protease inhibitors preserved the protein with only small variations detected.

Substantial degradation occurred in the absence of any protease inhibitors (N.I.), with the 65 kDa pUL98 band at day 14 being only 56.4% of the original day 0 band. However, the lower bands at 55-10 kDa also decreased during this time, indicating that these bands were unlikely

to represent products of degradation, as they would have been expected to increase in intensity. In contrast, the densities of both the pUL98 band and the lower bands were stable at all time points in the presence of the Trimix inhibitor, regardless of the concentration used. This stability was also seen in the presence of the Trimix + Pep and the Complete inhibitors. Small variations in these bands could be seen, such as in the 1x + Pep condition, which showed a drop to 90% at day 7; however, the day 14 sample showed a relative amount of 100% to the 1x + Pep at day 0, indicating that the reduced protein at day 7 was more likely due to a loading error than to protease activity.

The degradation of the N.I. condition over time showed that proteases are co-purified with the protein, but the addition of protease inhibitors during the lysis step of protein extraction prevented their activity regardless of the inhibitors or the concentrations that were used. Moreover, there was no increase in the lower bands in the N.I while the bands were stable in the protease-inhibited conditions, indicating that the contaminating bands were not likely to be the product of protein degradation in the purified batch, and the extracted protein was stable enough for crystallization efforts.

5.2.6 Generation of additional pUL98 proteins

Because the contaminating bands were not degradation products but did contain His residues, I suspected that they could be histidine-rich bacterial proteins that were co-purified with pUL98. In order to exclude these, I added a further 4 histidine residues by plasmid cloning to the N-terminal 6x-His tag in the 6x-His-pUL98 pET28b(+), which may have improved the binding affinity of the tagged protein to the NiNTA beads and decreased the probability of co-purifying the histidine-rich proteins. I also decided to introduce a second tag at the C-terminus of the pUL98 protein, which would guarantee that only full-length expressed pUL98 would be purified from NiNTA-purified batches. I decided to use the Strep-II Tag™ system (Iba Lifesciences, Germany) based on the binding affinity of streptavidin to biotin because the system uses a very small tag consisting of 10 amino acids, minimizing any potential misfolding or loss-of-function of purified pUL98. The system additionally functions very well at pH 8.0, which is the working pH used to purify pUL98.

In order to generate a double-tagged pUL98, I introduced the 10 amino acid StrepTag-II via cloning to position 6939 to the 10x-His-tagged pUL98, a construct which I then termed Double-Tagged (Strep)-UL98, or DTS-UL98, given as construct B in Figure 26.

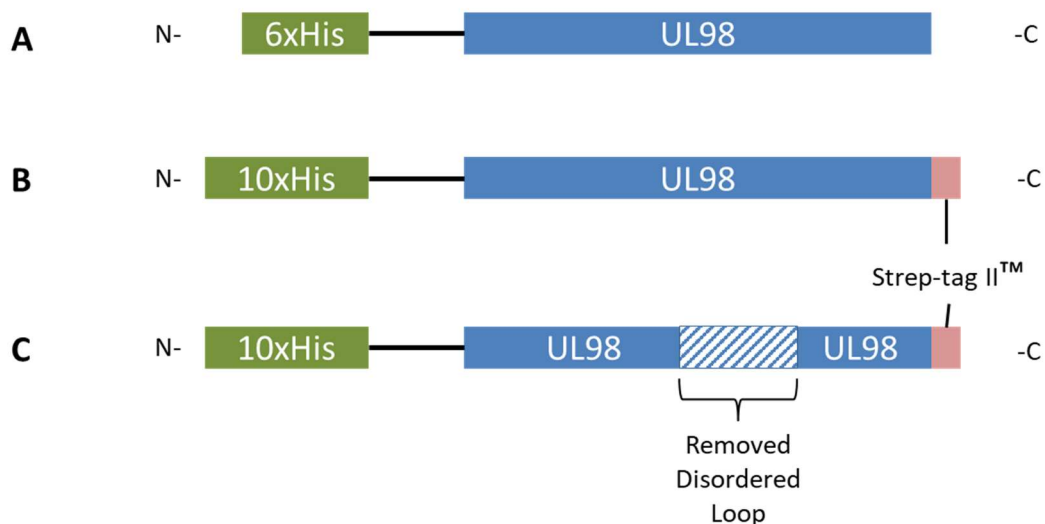


Figure 26. Schematic of (A) 6x-His-pUL98, (B) DTS-UL98 containing a Strep-tag II™ at the C-terminal and an enlarged 10xHis-tag at the N-terminal, and (C) DTS-CTL-UL98 with the deleted loop at position 6367-6513 shown in the protein.

On advice of Prof. Thomas Krey, our crystallization collaborators at the Medizinische Hochschule Hannover (Germany), I also deleted a 147 bp region from position 6367 to position 6513 encoding for a 49-amino acid loop present within the DTS-UL98 protein. This region is known to not be present in the crystal structure of SOX (87) and was thought to potentially interfere with the crystallization effort. This region was removed by fusion PCR of the surrounding pUL98 coding regions, which resulted in a construct referred to as Double-Tagged Strep, C-terminal Deletion-UL98 or DTS-CTL-UL98 (Figure 26C). These constructs were then purified first by the NiNTA-based system followed by purification using the StrepTactin/StrepTag-II system. The resulting batches were then kept for further analysis of purity and activity.

5.2.7 The double-purified pUL98 shows activity

As with the 6x-His-pUL98, it was important to show that the additional tag did not impair the nuclease activity of the double-purified constructs. This is especially true of the DTS-CTL-UL98 construct, as a large sequence region had been removed from the AN. To this end I used the same activity assay given in Section 5.2.4, testing the nuclease activity of 1 μ g of DTS-UL98 or DTS-CTL-UL98 with 250 ng plasmid DNA in nuclease buffer for 6 hours at 37 $^{\circ}$ C. As an undigested control I used 250 ng plasmid DNA incubated with no protein.

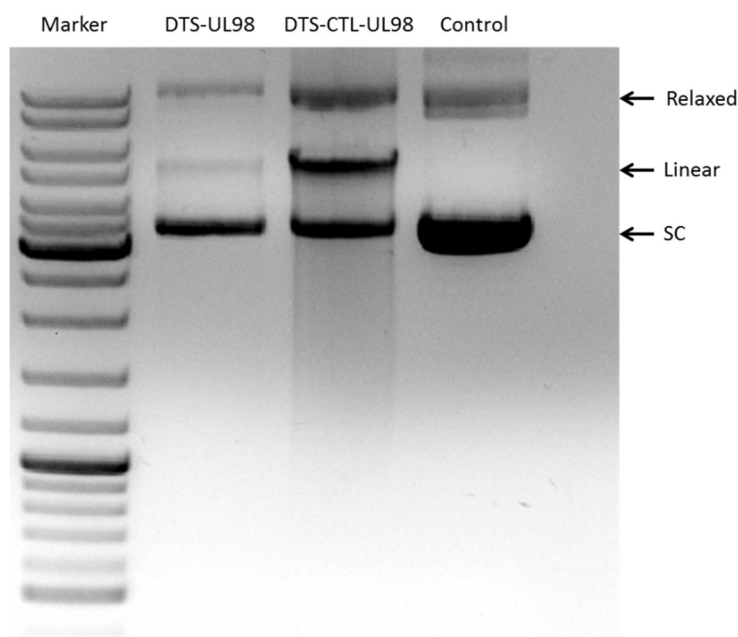


Figure 27. 250 ng pcDNA3 was added to 1 μ g of either DTS-UL98 protein or DTS-CTL-UL98 protein in 20 μ l nuclease buffer or nuclease buffer only (Empty Control) and incubated for 6 hrs at 37 $^{\circ}$ C. The resulting products were then run on a 1% Agarose gel in TAE buffer. Both DTS-UL98 and DTS-CTL-UL98 showed nuclease activity as seen in the presence of linear bands which were absent in the Control well. DTS-CTL-UL98 protein showed a reduced nuclease activity compared to that of the DTS-UL98 protein as seen by the increased amount of linear and relaxed bands compared to the DTS-UL98 protein.

Both DTS-UL98 and DTS-CTL-UL98 show functional nuclease activity, as linear plasmid bands are present in both conditions but absent in the control. This means that both proteins are able to degrade the plasmid, linearizing it in the process. DTS-CTL-UL98 has denser linear and relaxed bands than the full-length DTS-UL98, meaning that it has a reduced nuclease activity, as full nuclease activity would mean that the bands should fade and disappear as the DNA is degraded (see Section 5.2.4 for another example of this). Therefore I concluded that adding the double-tag to the pUL98 construct does not impair its alkaline nuclease activity. In addition, while the DTS-CTL-UL98 showed reduced nuclease activity, it was not completely abrogated, indicating that the enzymatic active site was probably still intact. As DTS-CTL-UL98 was meant to be used only for crystallographic analysis, these data indicated that the deleted region may be of use in increasing the chances of crystallization while maintaining the overall functional structure of pUL98.

5.2.7.1 Double-Tagged Full-Length pUL98 shows no extraneous bands.

I decided to visualize the purity of the DTS-UL98 protein by running a sample of the protein after NiNTA purification as well as the flow-through remaining after the pDTS-UL98 was

bound to the StrepTactin beads. Running these two samples along with the NiNTA and Strep-purified pDTS-UL98 on a SDS-PAGE gel and immunostaining the bands with α -6x-His antibody would reveal the purity of the pDTS-UL98.

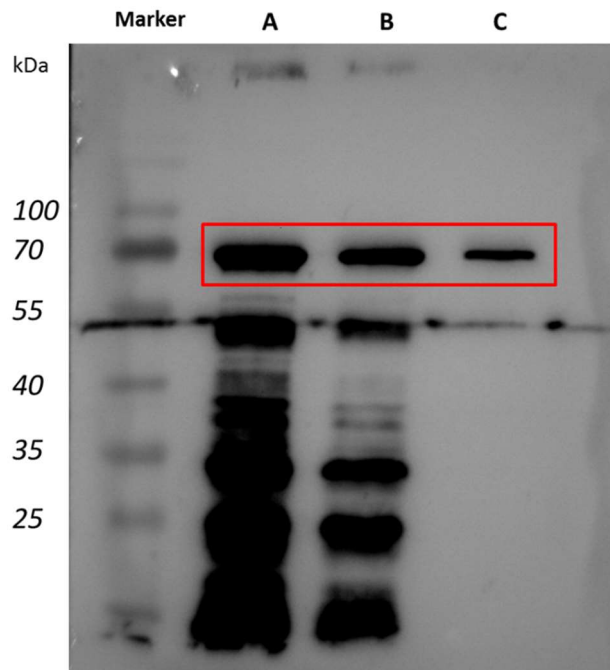


Figure 28. Immunoblotting of DTS-UL98 stained with Mouse α -6x-His antibody. pDTS-UL98 bands are shown at 65 kDa within the red box. Lane A) DTS-UL98 purified using the NiNTA method only. Lane B) Supernatant of protein product post-streptavidin binding. Lane C) Eluate post-streptavidin purification. Lane C demonstrated no carryover of extraneous bands present in A bands post-streptavidin purification, with these bands only present in lane B.

The pUL98 band at 65 kDa was visible in all three fractions (Figure 28 A-C, highlighted in the red box) indicating that pUL98 was not lost during the secondary purification or due to the addition of the secondary tag, even if not all of the protein is able to bind to the streptavidin beads. Moreover, the expected extraneous bands were present in the NiNTA-only purified DTS-UL98 fraction from 60 to 10 kDa lane (A). These bands were still present in the supernatant post-streptavidin bead binding (lane B), but no carryover of these bands was detected upon elution of the full-length pUL98-DTS from the streptavidin beads, which showed only the expected pUL98 band at 65 kDa (lane C). A band was also visible at around 55-60 kDa (*) but as this band was present throughout the blot, including the marker lane, it was assumed that this band was an artifact rising from the transfer of the protein from the SDS-PAGE gel to the nitrocellulose membrane.

These data demonstrated that double-purification of pDTS-UL98 yielded a highly pure fraction of DTS-pUL98, which was evidenced by the lack of extraneous bands from 60 to 10

kDa. The protein yield of DTS-UL98 was much lower than that of the NiNTA-only purified protein, as was seen in lane C, where the pUL98 band was less dense than that seen in lane A. Indeed, it was so low as to be undetectable in the Coomassie stain procedure. This made this purification procedure unsuitable for a high-throughput assay, as not enough protein could be generated for further use. Ongoing work is focusing on increasing yield for further crystallization work, which also requires a large amount of protein. Because the extraneous bands are unlikely to be the source of DNase activity in the purified fractions (Figure 24), and purified pUL98 fractions are stable in the presence of protease inhibitors (Figure 25), I decided to use only 6x-His-pUL98 purified only with the NiNTA system to develop a high-throughput screening system.

5.2.8 Conceptualizing a high-throughput screening system of pUL98 inhibitors.

Targeting the pUL98 protein during infection leads to a significantly reduced replication or death of the viral infection (Figure 19), making the pUL98 pathway a viable target for novel HCMV antivirals. Additionally, the pET28b (+)/BL21(DE3) expression system generated large amounts of free and functional pUL98 with substantial DNase activity. With this knowledge, I decided to design a high-throughput system based on the use of fluorescently tagged DNA substrates incubated with active pUL98. This system is widely used in Taqman qPCR, where a DNA probe to a genetic target of interest is bound to both a tag containing a fluorophore and a respective quencher in close proximity. While the probe is intact, the quencher absorbs the light emitted by the fluorophore, meaning that no fluorescence is detected. However, the 5' – 3' exonuclease activity of the Taqman polymerase destroys the probe by replicating the target of interest, removing the fluorophore, and fluorescence can be detected.

Using this principle, I intended to use a DNA substrate tagged with both a fluorophore and a respective quencher. I hypothesized that when purified and active pUL98 is added to this substrate the protein would degrade the substrate, leading to the disassociation of the fluorophore from the quencher and an increase in fluorescence. However, if the pUL98 is in presence of an inhibitor that can abrogate the activity of the protein the fluorescence will not increase, leading to a baseline or reduced fluorescence response. This principle is summarized in Figure 29:

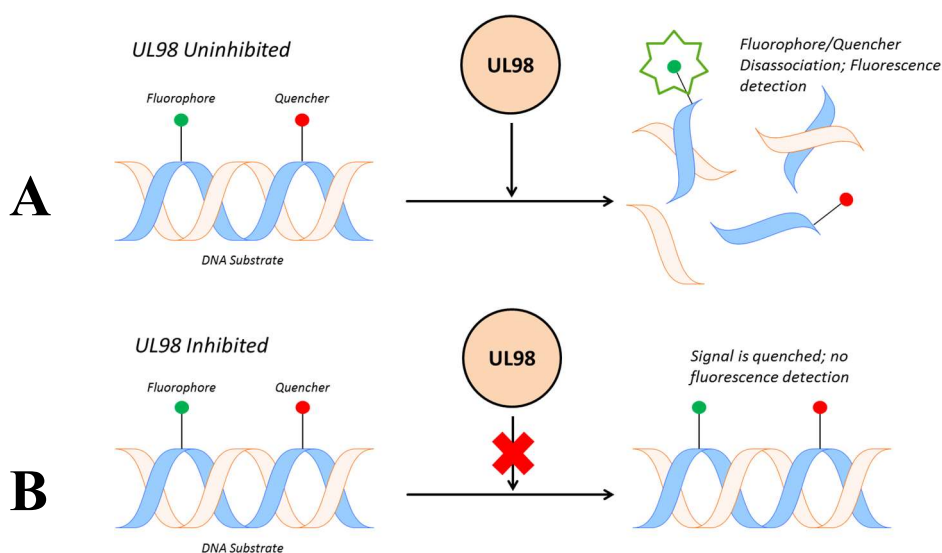


Figure 29. Graphical schematic of the principle behind the proposed high-throughput screening system for identifying small molecular inhibitor compounds of pUL98. In both A and B a known amount of pUL98 is incubated with a known concentration of fluorophore-tagged substrate as well as a compound to be tested. In A) the compound has no effect on pUL98 activity, leading to the disassociation of the fluorophore and quencher as the DNA substrate is degraded, leading to an increase in fluorescent signal. In B) the compound inhibits or impairs the activity of pUL98, leading to a reduced or absent increase in fluorescent signal.

5.2.9 Proof-of-Concept of High-throughput fluorescence-based assay

In order to prove whether the proposed high-throughput screening system was viable, I used the DNase Alert™ QC system (ThermoFisher Scientific) as a prototype system. This system contained a pre-designed fluorescently-tagged substrate which was used to detect the presence of contaminating DNases in a similar manner as described in Figure 29. 6x-His-pUL98 was then used in place of the supplied DNase in increasing amounts. This was to test if such a system would detect increasing activity of pUL98. Additionally, in order to test if the system can detect inhibition of pUL98, I decided to use the known inhibitor Atanyl Blue PRL (also known as Acid Blue 129). This anthraquinone dye has been shown by Alam et al. (183) to inhibit HCMV infection by targeting pUL98, making it an ideal control compound for detecting the inhibition of pUL98 in my system. I then incubated increasing amounts of pUL98 with 50 μ M Atanyl Blue for 10 minutes at room temperature before testing for activity with the DNase Alert kit.

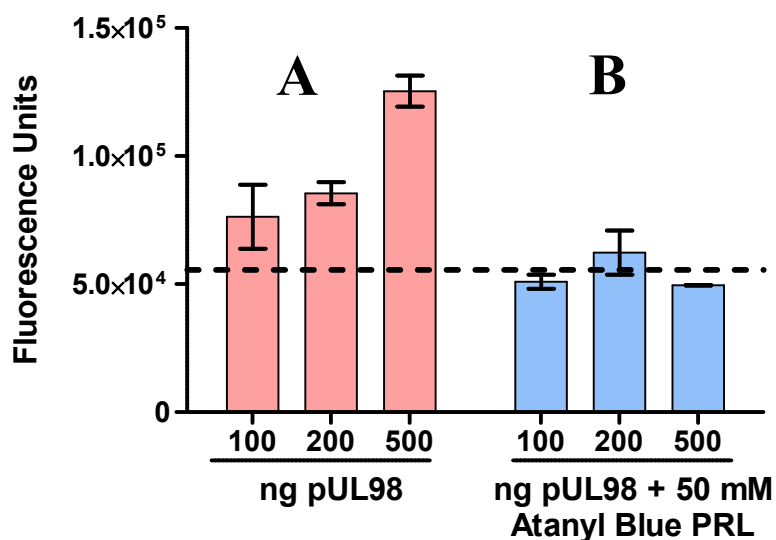


Figure 30. The commercial DNase Alert kit was able to detect increasing amounts of pUL98 as well as the inhibition of pUL98. In A) 100, 200 or 500 ng 6x-His-pUL98 was added to wells containing substrate alone. In B) 100, 200 or 500 ng 6x-His-pUL98 was added to wells containing substrate and 50 mM Atanyl Blue PRL. The no-enzyme control reading of wells containing substrate only is given as a dashed line. The increasing amount of pUL98 added in Condition A lead to an overall increase in fluorescent signal, while in Condition B the pUL98 was inhibited by the Atanyl Blue PRL with signals at or near the no-enzyme reading. The experiments were done in triplicates. Means \pm SEM are shown.

Adding an increasing amount of pUL98 to the substrate provided in the kit lead to an increase in fluorescent signal over the no-enzyme control with the highest signal seen when 500 ng pUL98 was added (Figure 30A). In contrast, none of the tested amounts of pUL98 showed any fluorescent activity when in the presence of 50 μ M Atanyl Blue PRL, with all three signals either at or near the no-enzyme reading (Figure 30B). This indicates that a fluorescently based system as described in Figure 29 would be able to detect whether pUL98 activity is inhibited in the presence of no-inhibition and no-enzyme controls.

5.2.10 Substrates Used in Fluorescence Assay

As the concept of the high-throughput screening was shown to be robust, I decided to use alternative substrates. Substrates used by Kuchta et al. and Alam et al. (90,183) in similar systems were known to differentiate between the 5'-3' exonuclease activity and the endonuclease activity exhibited by pUL98 (Figure 31). The first, an endonuclease-only sensitive substrate, prevented exonuclease activity by addition of a phosphorothioate bond after the 5' adenosine (seen as a * in the sequence in Figure 31A), a bond which cannot be cleaved by most nucleases. The second forms a hairpin loop which only allows for 5'-3'

degradation of the substrate (Figure 31B). Both were coupled with a FAM fluorophore and an Iowa Black quencher.

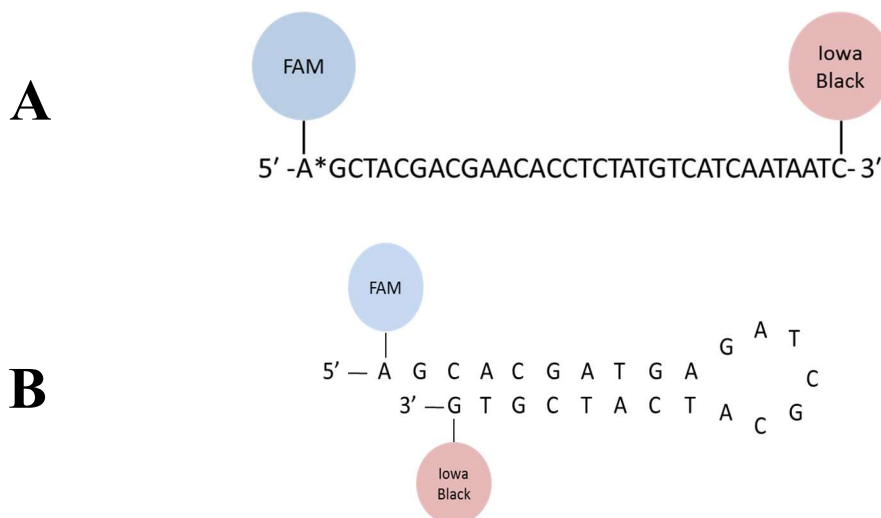


Figure 31. Molecular structure of A) the endonuclease-sensitive substrate containing a 5' phosphorothioate bond preventing 5'-3' exonuclease activity, and B) the hairpin-forming exonuclease-sensitive substrate.

By using these substrates I hoped to be able to determine whether a potential inhibitor may have had an effect on only one or both DNase activities of pUL98. As Kuchta et al. found that alteration of the pUL98 active site mostly impacted its endonuclease activity, I decided to use the endonuclease substrate in the high-throughput screen.

5.2.11 Determining the optimal incubation time of the high-throughput screen.

In order to optimize the high-throughput system, it was important to determine the optimal incubation period for detection. This was because incubation for too little time would increase the false positive-inhibition rate by not allowing the enzyme enough time to degrade the substrate. Conversely, incubating for too long would increase the false negative-inhibition rate by allowing partially-inhibited protein enough time to degrade the substrate. I therefore determined that the ideal incubation time was the point at which the protein was just able to degrade all available substrate.

I added 1 μ g 6x-His-pUL98 to 200 nM endonuclease substrate in nuclease buffer, in triplicate. Each triplicate series containing a sister triplicate well containing only 200 nM endonuclease substrate in nuclease buffer as a no-enzyme control, which also tests the stability of the substrate alone over time. The reactions were performed in a 96-well plate. The plate was read

every half hour in an Omega plate reader, generating a time course demonstrating the progression of digestion of the endonuclease substrate.

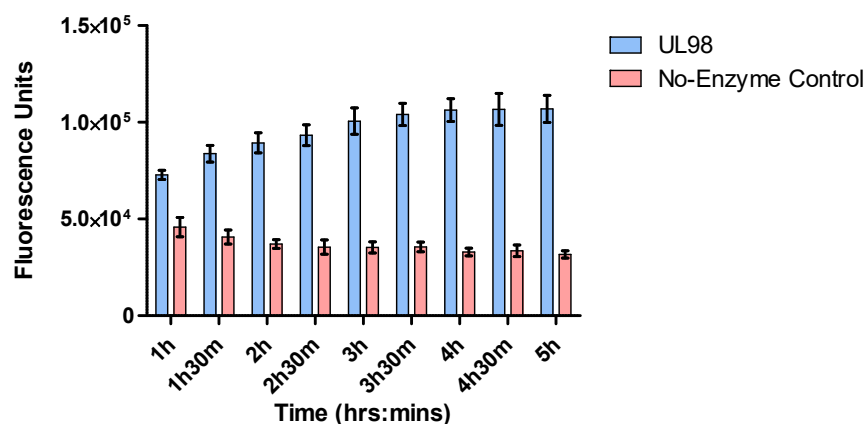


Figure 32. Time course of 200 nM endonuclease substrate added to either 1 μ g 6x-His-pUL98 in nuclease buffer (blue) or nuclease buffer only (red). The activity of pUL98 peaks at around 3-4 hrs. and plateaus beyond 4 hrs., indicating total digestion of the substrate beyond that point. The experiments were done in triplicates. Means \pm SEM are shown.

The time course given in Figure 32 showed that the fluorescent signal steadily increased from 1 hr. onwards in the pUL98-containing wells (blue bars) compared to their no-enzyme controls (red bars). The fluorescent signal reached a peak at around 1×10^5 fluorescent units at 4 hours, after which the signal attained a plateau at 4 hours 30 mins or 5 hours. I decided to incubate the screen for 4 hours, which is the minimal time for full degradation of the substrate. At this time, inhibited pUL98 would be expected to have fluorescent signal below that of the no-inhibition controls.

5.2.12 pUL98 shows strong activity at 200 ng

In order to determine the optimal amount of 6x-His-pUL98 for the assay, I decided to investigate the activity of different amounts of protein against the endonuclease substrate. This would allow me to determine a protein amount per well which would ideally give a fold-change value of 2-3 times the unit of fluorescence of the no-enzyme control. This parameter was important, because using an excess amount of protein may have masked any potential effects of an inhibitor. This would also allow me to select the minimal amount of protein necessary to use in order to reduce the amount of protein required for the entire high-throughput screen. To this end I tested the activity of 6x-His-pUL98 at the amounts of 100, 200, 400, 600, 800 ng, and 1 μ g, incubated with 200 nM endonuclease substrate against a 200 nM substrate-only no-enzyme control.

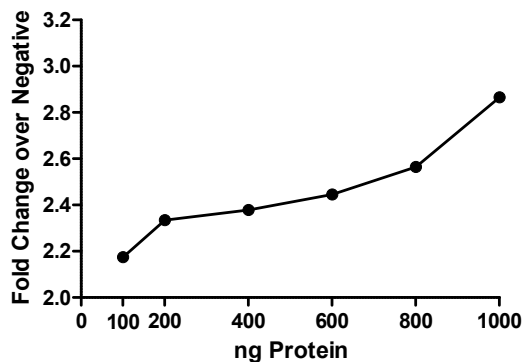


Figure 33. Fold change of activity of different amounts of 6x-His-pUL98 incubated for 4 hrs with 200 nM endonuclease substrate against a no-enzyme control of 200 nM substrate only. All amounts show activity above a fold-change of 2 but below 3. 200 ng (fold-change 2.33) was selected for use in further screens as it exhibits a good no-inhibition/no-enzyme ratio for a minimal amount of protein needed. The experiments were done in triplicate.

The fold-change of the 6x-His-pUL98 protein was above two at amounts as low as 100 ng, while increasing amounts gradually increased the fold-change distance (Figure 33). While 1 μ g demonstrated a fold-change of 2.8, it required a large amount of protein which would prove prohibitive in larger assays. I opted to use 200 ng of pUL98 in further screens, which showed a fold-change of 2.3 and allowed for a reduction in future material needed.

5.3 Identifying inhibitors of pUL98

5.3.1 High-throughput screen of a small-molecular compound library

Using the fluorescent system I designed in section 5.2.8 I then carried out a high-throughput screen of a small molecular compound library of 27690 compounds at the Medizinische Hochschule Hannover. For each compound, 200 ng of 6x-His-pUL98 was incubated with 10 μ M of the compound for 10 min at room temperature to allow for any potential interaction of the inhibitors with the protein before being added to 200 nM endonuclease substrate in nuclease buffer. Each plate contained two no-inhibition controls, two no-enzyme controls, and two inhibition controls. The no-inhibition controls contained 200 ng 6x-His-pUL98 with 200 nM substrate in nuclease buffer. The no-enzyme controls contained only 200 nM substrate in nuclease buffer, and the inhibition controls contained 200 ng 6x-His-pUL98 incubated with 50 μ M Atanyl Blue PRL and 200 nM substrate in nuclease buffer. Each inhibitor was tested in duplicate, and activity was measured as fluorescent activity using a Cytation5 plate reader. The results of the large screen were then normalized as fold change of the compounds relative to each inhibition control (Figure 34).

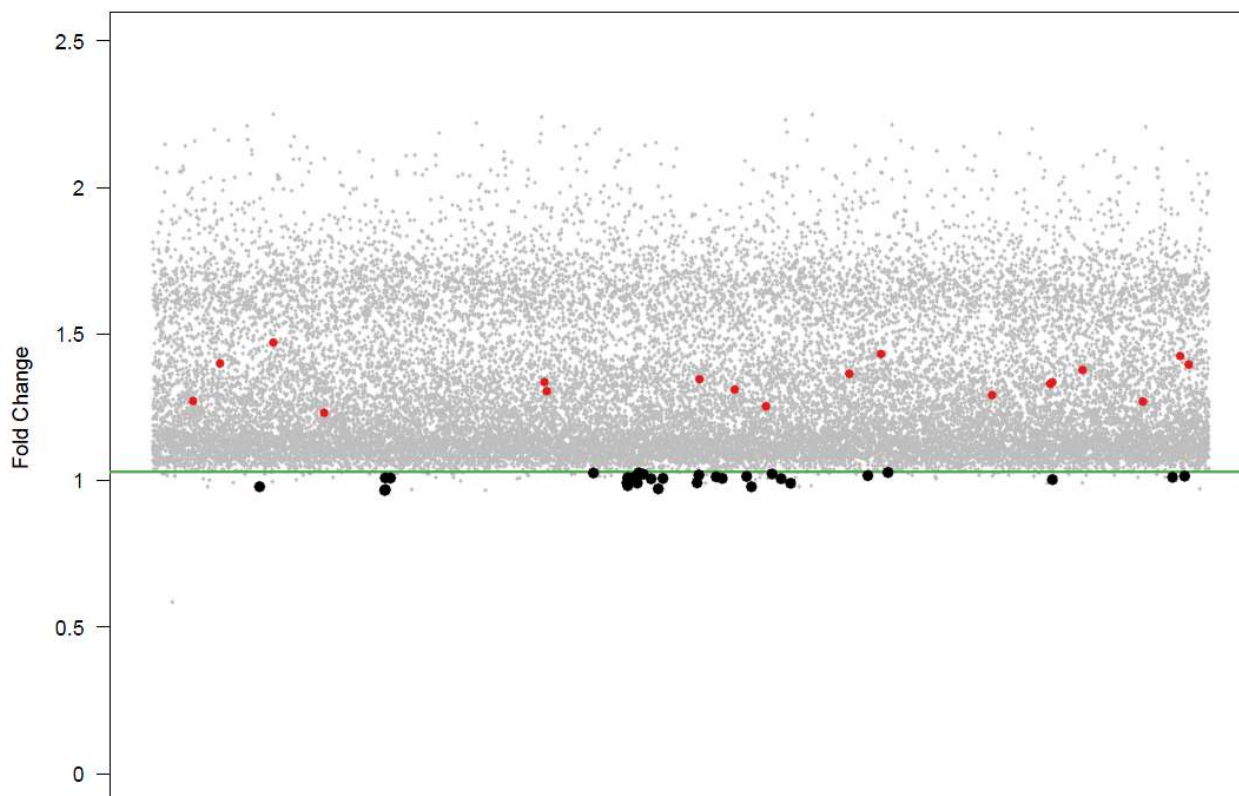


Figure 34. Fold change of 27690 small molecular compounds and their respective fluorescence activity against their respective inhibition controls. Putative inhibitors were chosen below the threshold of 1.03 (green line). Potential inhibitors with less than 10% variation between replicates, shown in black, were selected as potential candidate inhibitory compounds for further evaluation. No-inhibition controls of uninhibited pUL98 were averaged in clusters of 10 and plotted in red.

As the results are compared with the inhibition control (50 μ M atanyl blue PRL), it would show a fold change of 1, indicating full inhibition of pUL98. I expected that the no-inhibition control should demonstrate a fold-change of 2.3 times the inhibitor control. However, the results in Figure 34 showed that the majority of compounds clustered around fold-changes between 1.2 and 1.4, which was lower than the fold change usually seen using the endonuclease substrate. While the no-inhibition controls (red points) largely demonstrated a high fold-change, they do not reach the levels seen in Figure 33, indicating that the overall background fluorescence was elevated and that there is an increased level of noise present in the system. This was probably due to the different handling conditions present during upscaling for a high-throughput screen such as repeated refrigeration and handling of the substrate, which may have impacted the activity the pUL98 protein or destabilized the endonuclease substrate. Due to this elevated noise, I decided to use a very stringent cutoff of 1.03 (green line), meaning inhibition of pUL98 to 3% higher than the inhibition control.

Therefore, only compounds at or very near the activity of the inhibitor controls would be considered as potential candidates. This analysis then showed that 90 compounds demonstrated a fold-change below 1.03. However, each compound thus identified was then investigated individually to rule out compounds that showed large differences between their replicates (defined as more than 10% difference between the replicates) because these likely represented pipetting errors during the high-throughput screen. In addition, care was taken if inhibitors appeared in a cluster of more than three per cluster per plate. As the compounds are randomly distributed throughout the plates, with dissimilar structures being tested with each other, clusters of inhibited results are unlikely. These clusters are then deemed to be more likely due to the plate effect, where sections of the plate demonstrated different properties due to variation in ambient conditions. For example, if a plate is unevenly heated then cooler areas will show lower fluorescent values. While this represents a very conservative analysis of the large screen results, it was important to eliminate any known false inhibition signals present, and certainly some true inhibitors may have been omitted. However, even with these measures, 33 compounds satisfied these exclusion criteria and were considered to be potential pUL98 molecular inhibitor candidates. Out of the 33 identified, only 28 were commercially available, which were then tested further.

5.3.2 Validation of the identified compounds

As the large screen showed high noise it was important to validate the 28 compounds I identified. I ran the identified compounds in a repeat screen using the same endonuclease substrate in 96 well plates, allowing me to easily modify testing parameters, if necessary, and to confirm the validity of the identified compounds. I therefore tested the compounds at 10 μM using the same enzymatic system and the same conditions as in the high-throughput screen in section 5.3.1. I then normalized the results to the 50 μM Atanyl Blue PRL inhibition response. I decided to use a fold-change threshold of 1.3 in this screen, as I did not wish to exclude compounds that may have exhibited a weaker inhibition of pUL98 than originally detected.

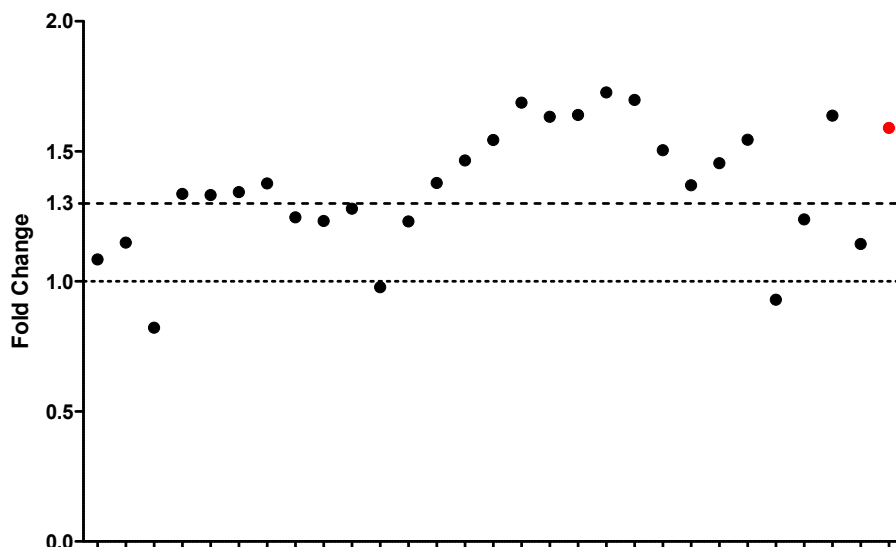


Figure 35. Fold change dot plot of enzymatic screening of 28 small molecular compounds identified as inhibitors of pUL98. Fluorescent signal was normalized to that of the inhibitor control (50 μ M Atanyl Blue PRL) and plotted as a fold change increase. Three compounds showed a fold-change below 1.0 (dotted line) of the inhibitor control, while an additional 8 showed fold-change of below 1.3 (dashed line), indicating lesser activity against pUL98. The remaining 17 identified compounds demonstrated fold-change above 1.3 and were therefore excluded from further investigation. Average no-inhibition control is plotted in red. The experiments were done in triplicate.

Of the 28 identified compounds, 11 showed fold-change below 1.3, indicating an inhibition of activity of around 30% compared to the inhibitory control (Figure 35). These compounds were then termed Compounds A to K. Three of these compounds, Compounds A, E, and I showed fold change values below 1.0, indicating that these have an increased inhibitory effect on pUL98 at 10 μ M compared to 50 μ M Atanyl Blue PRL. The remaining 17 identified compounds showed fold-change values above 1.3. This indicated that these compounds were likely falsely identified inhibitors in the primary screen and were therefore excluded from further analysis.

5.3.3 Inhibitors require further screening

It was imperative that a further screen of the identified compounds needs to be carried out to ensure that the compounds were active against pUL98 activity within an infective model. This was necessary to know because the enzymatic screen does not convey any information on the bioavailability of the identified compounds. For example, it may be that the identified compounds were unable to cross the cellular membrane, rendering them ineffective in treating HCMV infection.

I therefore used an assay called the Plaque Reduction Assay, or PRA. The PRA is dependent on infecting a monolayer with a defined titer of virus and covering the monolayer with a semi-solid overlay containing the compounds to be tested. This overlay prevents the release of replicating infectious virions from the cells into the supernatant, restricting viral growth to spreading to adjacent cells at sites of primary infection. Viral stocks can be titrated in this manner to calculate a plaque-forming unit (PFU) titer at which a standard amount of plaques are formed in that cell line. Addition of the compounds of interest to the overlay in varying concentrations shows whether the compound is bioavailable by inhibiting the formation of the plaques relative to the number of an untreated positive control and an untreated, uninfected negative control. This can be used to quantify the effectiveness of the compound against HCMV growth. This effectiveness is determined by calculating the half maximal inhibitory concentration, or IC_{50} , defined as the concentration of treatment compound where the number of infectious plaques is reduced by half (see section 3.8).

5.3.4 Toxicity of the 11 Identified Compounds

As the compounds were to be investigated using the PRA method required the use of live cells it was essential to determine the cytotoxicity of the identified compounds. I therefore designed a toxicity assay using the ATP luminescence-based cell viability method to test the cytotoxicity of the eleven compounds in MRC-5 fibroblasts, ranging from concentrations of 2 μ M, 5 μ M, 10 μ M, and 20 μ M for a period of 72 hours. This incubation time was selected as it allows for visualization of cytotoxic effect of the compounds, even if they are unstable at longer times, as cells may recover if incubated for a longer period of time if the compound is degraded or metabolized. The results were normalized to an untreated cell control, with a cut-off of 85% cell viability selected as an indicator of unsuitable toxicity. The results are given in Figure 36:

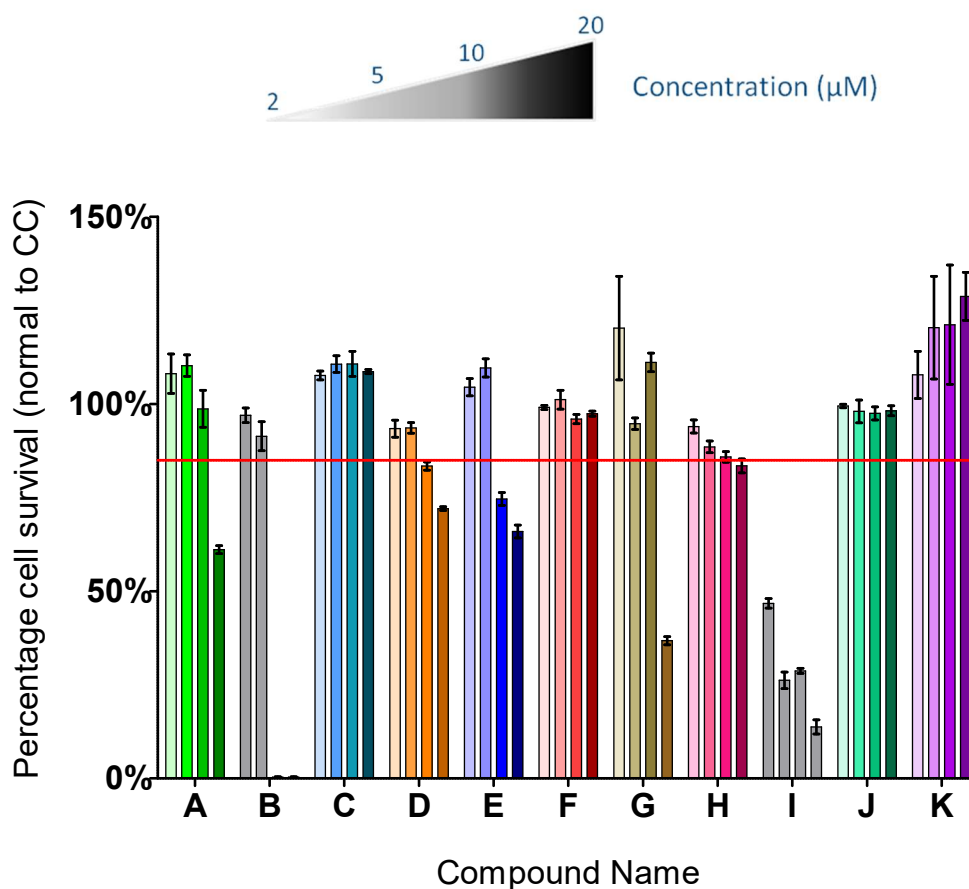


Figure 36. Cell viability of 11 compounds as determined by the ATP luminescence method. Compounds were tested on MRC-5 cells at 2 μ M, 5 μ M, 10 μ M, and 20 μ M and incubated for 72hrs. The results were then normalized as a percentage against an untreated cell control set at 100%. Darker colors indicate higher concentrations, and greyed-out bars indicate compounds excluded due to high toxicities at lower concentrations. The experiments were done in triplicates. Means \pm SEM are shown.

The results of the toxicity test demonstrated that most compounds were non-toxic at concentrations between 2 and the 10 μ M, the concentration at which the compounds were screened. Compounds K and J showed no toxicity at any concentration or had values higher 100%, indicating increased cell growth regardless of compound presence. In contrast, compounds A, D, E, and G showed viability lower than 85% at concentrations of 10 μ M or higher. I decided not to exclude these, as it may still have been possible that their IC_{50} values would be far below these values, as was seen in the fact that three compounds exhibited a fold change of less than 1 in the validation screen in section 5.3.2. However, I realized that care must be taken in interpreting any cell-based results of these compounds. Compound I showed low cell viability at all concentrations, and Compound B demonstrated a high reduction in cell viability at 10 μ M, and I excluded these from further PRA analysis.

5.3.5 Plaque Reduction Assay screening of compounds reveals *in vivo* effectiveness

I then carried out a PRA containing the nine remaining compounds against the TB40/E strain of HCMV in the infection of MRC-5 fibroblasts. I decided to use the TB40/E strain as it is more representative of clinical strains isolated from patients with HCMV viremia and does not contain the large genetic deletions as seen in other laboratory-attenuated strains of HCMV (24). Adding a known inhibitor of viral growth will reduce the number of these plaques, and if a series of increasing concentrations of the compound is added to the overlay, the IC_{50} can be calculated, which estimates the concentration at which the compound reduces the infectious plaques to 50 %.

In this assay, I therefore infected MRC-5 fibroblasts with HCMV strain TB40/E and tested the nine identified compounds at concentrations of 2, 5, 10, or 20 μM added to a methylcellulose overlay. After 14 days, the overlay was carefully removed, and the plaques were fixed and stained with Crystal Violet stain. Plaques were then counted, with the IC_{50} values calculated as a non-linear regression of log (inhibitor) vs response-variable slope (four parameters) least-squares ordinary curve fit with a bottom constrained to 0. These results are given in Figure 37:

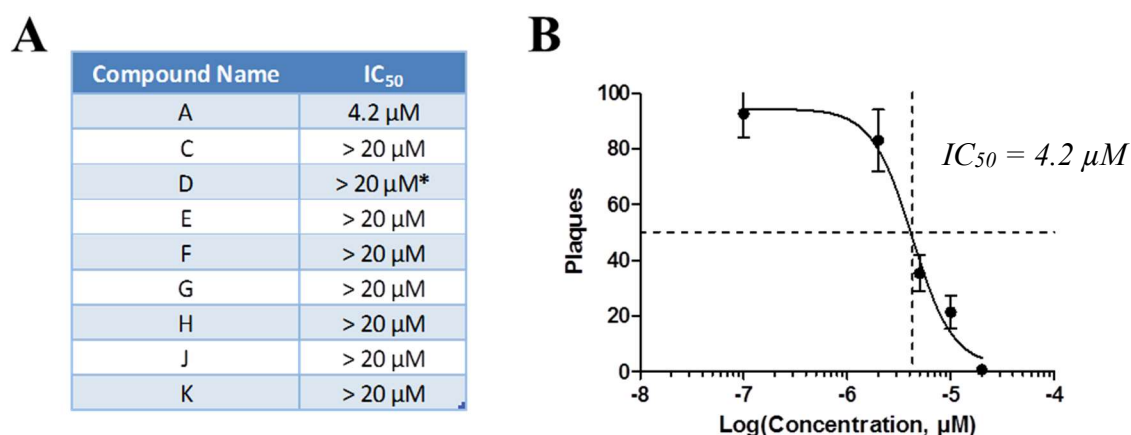


Figure 37. A) Calculated IC_{50} results for the nine identified compounds. IC_{50} values above 20 μM indicated an ambiguously calculated IC_{50} value, indicating no inhibition of HCMV strain TB40/E at the concentrations tested. One compound, Compound D, showed instability and variable results upon replication (ranging from IC_{50} 14 μM to over 20 μM) and was excluded from further analysis. Compound A showed a good inhibition of HCMV infection in MRC-5 cells *in vitro* with an IC_{50} value calculated as 4,2 μM . B) *In silico* calculation of the IC_{50} value of Compound A, calculated as a non-linear regression analysis of the log(concentration) versus the plaque count per condition. Bottom is constrained to 0. The experiments were done in triplicates. Means \pm SEM are shown.

As the data above show, most compounds demonstrated an IC_{50} value of over 20 μM , calculated as an ambiguous *in silico* result. This indicated that the compounds showed no inhibition of HCMV strain TB40/E plaque spread in the concentrations tested. This means

that if they did exhibit an *in vivo* activity against HCMV infection, their IC₅₀ concentrations would be above 20 μM, which is above the accepted standard of a low-micromolar maximum (ideally around 5 μM) for preliminary lead compounds (187). These compounds were therefore excluded from further investigation. The ineffectiveness of these compounds may have been caused by several reasons, from cellular metabolism of the compound to an ineffective form or an inability to cross the cellular membrane to the viral replication mechanisms. One compound, Compound D, showed suspected instability during testing, giving alternate IC₅₀ values of 14- >20 μM between experimental replicates. While Compound D was therefore not further investigated as part of this work it cannot be definitively excluded from further investigation. In contrast, Compound A exhibited an IC₅₀ of 4.2 μM (Figure 37B), indicating adequate effectiveness and activity against pUL98 in this infectious system. I therefore decided to further investigate the inhibitory effects of Compound A against HCMV.

5.4 Characterization of Compound A

5.4.1 Compound A Impacts the Growth of HCMV TB40/E

In order to confirm the antiviral activity of Compound A, I designed an assay to investigate the compound's effect on viral growth *in vivo*. If Compound A is a true inhibitor of viral growth, I expected that an increase in compound concentration would lead to lower viral growth. I performed a multistep growth curve in MRC-5 cells at an MOI of 0.2 in the presence of increasing concentrations of Compound A. Medium and fresh compound was changed and added every second day. Virus in the supernatant was titrated at different days post infection.

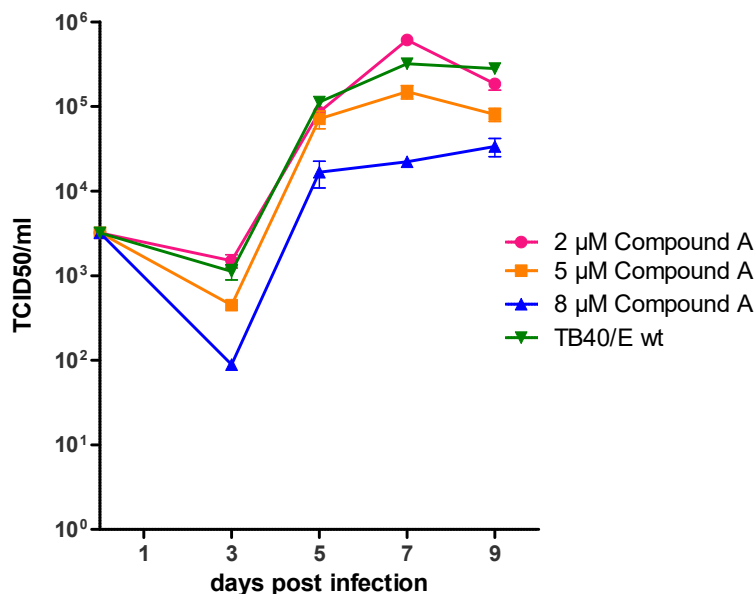


Figure 38. Growth rates of HCMV-TB40/E replicating in the presence of 2, 5 or 8 μ M Compound A or no compound (green line). While TB40/E + 2 μ M compound (red line) showed comparable growth kinetics to that of the TB40/E a reduction of around half a log TCID₅₀ titer is seen starting at day 7 in TB40/E + 5 μ M Compound A (orange line), and a large reduction of one log TCID₅₀ is seen at day 5 in TB40/E + 8 μ M Compound A (blue line). This indicated that Compound A reduced viral growth as suggested in the PRA assays. The experiments were done in triplicates. Means \pm SEM are shown.

The viral growth kinetics in Figure 38 showed that treatment of TB40/E with 2 μ M Compound A did not show a significant difference between the untreated control between days 0 to 9, indicating that this concentration was too low to effectively inhibit HCMV growth. Treatment of TB40/E with 5 μ M Compound A showed an increased effect, with viral titers showing a drop of half a log from the TB40/E beginning at day 7, while treatment with 8 μ M compound A reduced viral growth by a full log titer beginning at day 3. This indicated that Compound A did have an inhibitory effect on TB40/E growth. While this data showed that Compound A has an effect on TB40/E viral growth kinetics it must be noted that this assay is not directly comparable with the PRA, as secondary infections take place in this assay, leading to infection of new cells in the plates by newly produced virus. The assay is therefore not comparable as an indicator of IC₅₀ but instead showed that Compound A is a true inhibitor of viral growth.

5.4.2 The Inhibitory Activity of Compound A is comparable to Ganciclovir

In order to compare the calculated IC₅₀ of Compound A to a known current anti-HCMV drug, I decided to test the efficacy of Ganciclovir using the same PRA protocol. This will lend

context to the IC_{50} of Compound A as a lead candidate against HCMV infection. Ganciclovir was tested at concentrations of 500 nM to 20 μ M and the IC_{50} was determined by nonlinear regression (Figure 39).

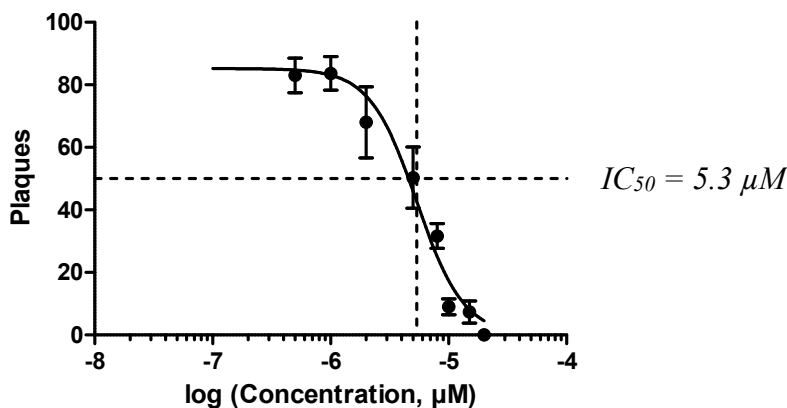


Figure 39. IC_{50} result of Ganciclovir (GCV), calculated as a non-linear regression analysis of the log (concentration) versus the plaque count per condition. The IC_{50} of GCV was determined to be 5.3 μ M, indicating that Compound A has a comparable effectiveness to ganciclovir in the PRA method used to identify IC_{50} values. Bottom is constrained as 0. The experiments were done in triplicates. Means \pm SEM are shown.

The IC_{50} of Ganciclovir was then determined to be 5.3 μ M, which is comparable to Compound A's IC_{50} of 4.3 μ M. This showed that the effectiveness of Compound A was comparable to that of a currently used drug in this PRA system, meaning that it has potential as a candidate compound.

Compound A is effective against other herpesviruses.

As Compound A was shown to be effective against HCMV infection in the PRA, I hypothesized that it may also be effective against other pathogenic herpesviruses, as the alkaline nucleases are highly conserved in the herpesviruses. I first decided to test HSV as the prototype of alpha-herpesviruses, as well as MCMV, as eventual *in vivo* work would rely on the use of the mouse animal model.

I used Compound A at concentrations 2-20 μ M in a PRA against the HSV-1 in Vero green monkey fibroblasts, as well as in a PRA against the Smith strain of MCMV in M2-10B4 bone-marrow stromal cells. The subsequent IC_{50} s are shown below:

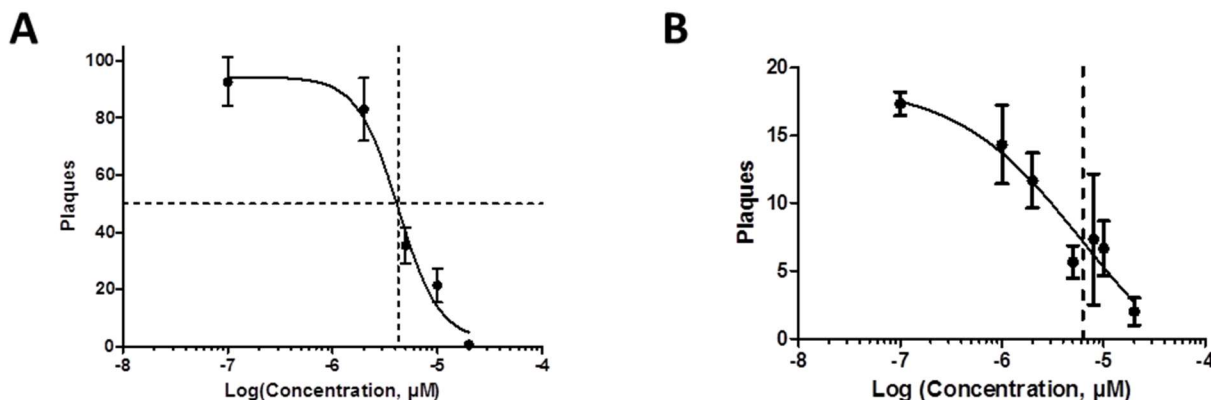


Figure 40. IC₅₀ values calculated as a non-linear regression analysis of the log (concentration) versus the plaque counts per condition for A) HSV-I (5.2 μM) and B) MCMV strain Smith (6.2 μM). Bottom constrained to 0. The experiments were done in triplicates. Means ±SEM are shown.

The results of the PRA given in Figure 40 indicated that Compound A shows inhibitory activity against both HSV-I and MCMV, with IC₅₀ values of 5.3 and 6.2 μM respectively. While this inhibition was clear in HSV-1 in MCMV, the non-linear regression indicated that there is a trend towards inhibition, but high variation existed within the data. This may be because the MCMV viral alkaline nuclease, M98, is not essential, with knockouts of M98 known to not attenuate viral growth in a temperature-sensitive mutant (188). This is in contrast to HCMV UL98 knockout mutants, which show a lethal phenotype. However, this trend did indicate that Compound A has an effect against MCMV and showed that it is likely that Compound A exhibits activity against other herpesviruses in an infectious system.

5.4.3 Compound A is a likely non-competitive inhibitor of pUL98

Determining whether Compound A is a competitive or non-competitive inhibitor of pUL98 was of interest: a competitive inhibitor must compete with the target substrate for binding with the target protein in order to have an inhibitory effect and may be reversible, while a non-competitive compound either binds irreversibly to the protein's active site or may bind elsewhere in the protein and change its conformation in a way that abrogates its DNase activity. In order to investigate this, I first designed an experiment that investigates the inhibitory effect of Compound A on pUL98 at different concentrations at 30-minute intervals over a period of 4.5 hours. I incubated 200 ng of 6x-His-pUL98 and 200 nM of exonuclease substrate with either 2, 4, 6, 8, 10, or 20 μM Compound A in nuclease buffer, along with a non-inhibition control of pUL98 containing only protein and substrate in nuclease buffer, and a

no-enzyme control containing only substrate in nuclease buffer. Fluorescence was then read every 30 minutes.

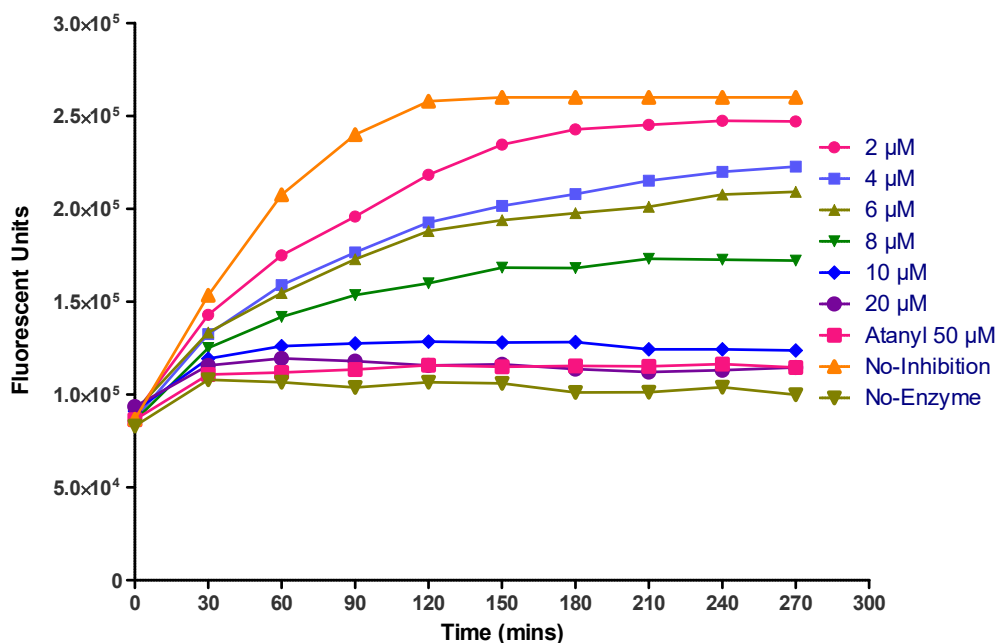


Figure 41. Kinetics of pUL98 incubated with increasing concentrations of Compound A. “No-inhibition”: 200 ng 6x-His-pUL98 incubated with no inhibitor and 200 nM substrate in nuclease buffer; **“No-Enzyme”:** 200 nM substrate in nuclease buffer. pUL98 activity was measured as arbitrary fluorescent units in 30 min intervals over 4.5 hours. No one condition reached an activity comparable to the no-inhibition control and most show parallel curves to the no-inhibition control, suggesting that Compound A displays a non-competitive inhibition of pUL98 activity.

If Compound A is competitive, I expected to see that all of the substrate would be slowly degraded overtime, with pUL98 showing lower activity at earlier timepoints, forming an exponential curve. In contrast, the curves in Figure 41 instead reached a plateau, indicating that the inhibitory effect of the compound is independent of the amount of substrate present in the assay. This indicated that Compound A may be an inhibitor with non-competitive inhibition kinetics.

To confirm this, I designed a second experiment using the same timepoints and experiment time but with testing a constant amount of Compound A against an increasing amount of substrate. In this experiment, I decided to test at a concentration of 8 μM, as I hypothesized that at this concentration activity would not be fully abrogated. This would rule out any potential issues from using excessive Compound A, which would make an increase in signal undetectable if the compound were to show competitive inhibition kinetics. An additional

consideration is that an increase in substrate concentration also increases the substrate background fluorescence, due to the density of fluorophores present. This means that every substrate condition also required a no-enzyme control with the same substrate concentration in nuclease buffer only. Due to this, I also decided to investigate the fold-change of the activity with regards to its no-enzyme control for each condition, as this controls for any increase in background that may give an elevated fluorescent signal. I expected that if the compound was a competitive inhibitor, the increase in activity would lead to higher fold-changes than the previously-tested pUL98 + 8 μ M Compound A and 200 nM substrate. If it was non-competitive, it would demonstrate the same fold-change response, as it would be insensitive to the amount of substrate present. I therefore tested the activity of 200 ng 6x-His-pUL98 with 8 μ M Compound A at substrate concentrations of 150, 200, 300, 400, 500, 600, 700, 800, 900, or 1000 nM exonuclease substrate in nuclease buffer. 6x-His-pUL98 was incubated with 50 μ M Atanyl Blue as an independent inhibition control, and pUL98 with 200 nM substrate only served as a no-inhibition control. Fluorescence was then read every 30 minutes for 4.5 hours, and the results were then calculated as the ratio of the fluorescent activity of each condition at each timepoint against its respective no-enzyme control at that timepoint.

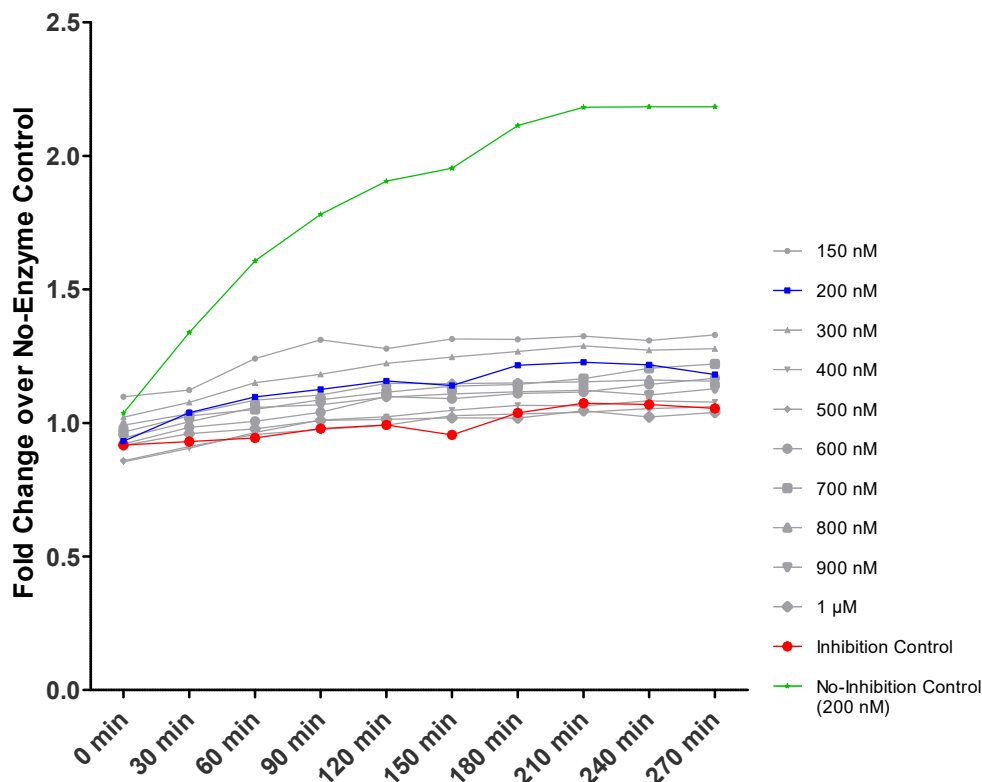


Figure 42. Kinetic of pUL98 incubated with increasing concentrations of exonuclease substrate. 200 ng of 6x-His-pUL98 was incubated with 8 μ M Compound A and either 150 or 200 - 1000 nM exonuclease substrate in 100 nM intervals in nuclease buffer. 200 ng 6x-His-pUL98 was incubated with no inhibitor and 200 nM substrate in nuclease buffer as a no-inhibition control. Each test condition had its own no-enzyme control of substrate at the same concentration tested with no pUL98 or inhibitor. Fold-change increase in activity for pUL98 + 8 μ M Compound A + 200 nM substrate (blue line) showed an increase in activity over the 50 μ M Atanyl Blue PRL inhibition control curve (red line), showing slight activity. Regardless of the concentration of substrate used no condition (gray lines) showed a significant increase over time approaching the no-inhibition control (green line) with only 150 nM and 300 nM showing slightly increased activity.

The results in Figure 42 demonstrate that the different experimental conditions show inhibition kinetics almost identical to that of the 200 nM curve, regardless of the substrate concentration. These curves, as expected, are below the no-inhibition control curve but above the inhibition control curve. This was strong evidence that pUL98 activity was reduced to a similar level at 8 μ M regardless of the substrate concentration, as in a competitive inhibition model the fold-change activity would increase with an increase in substrate concentration. The data in Figures 41 and 42 therefore suggest that Compound A is highly likely to have non-competitive inhibitory kinetics against the activity of pUL98.

5.4.4 Inhibition of double-tagged protein rules out residual effects of background bands

In order to prove that Compound A acts directly on the purified pUL98 and not any contaminating band present in the purification, the inhibitory effect of 10 μM Compound A was tested against DTS-UL98 (see section 5.2.6) using the enzymatic assay:

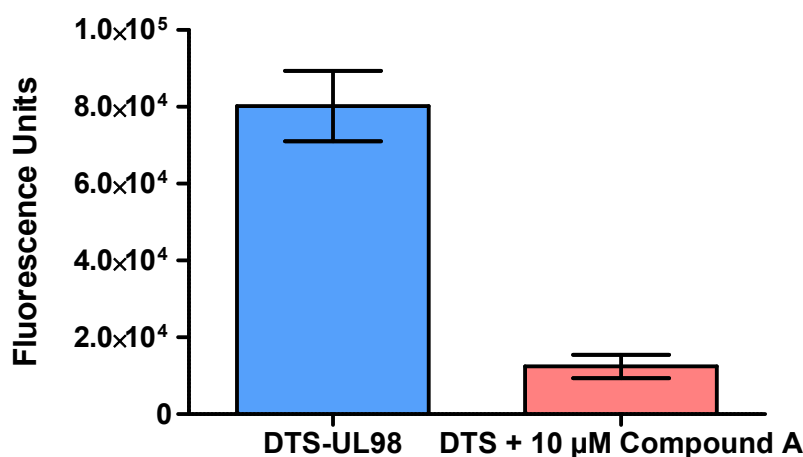


Figure 43. Difference in enzymatic activity of 200 ng DTS-UL98 in nuclease buffer only or with 10 μM Compound A after subtraction of the no-enzyme control. Compound A was able to abrogate DTS-UL98 activity to near-no-enzyme levels (at 0 fluorescence), indicating that Compound A acts on pUL98 directly. Means \pm SEM of two independent experiments are shown.

Compound A drastically reduced the enzymatic activity of DTS-UL98, with DTS-UL98 in the presence of the compound showing a seven-fold decrease in enzymatic activity compared to that of the uninhibited protein (Figure 26). This demonstrated that Compound A acts directly on purified pUL98, as DTS-UL98 contains no contaminating bands compared to 6x-His-pUL98 (see Figure 28), which also demonstrated that the contaminating bands present in the 6x-His-pUL98 most likely do not interfere with the detection of pUL98 activity.

5.4.5 The Cytotoxicity of Compound A.

In order to determine whether Compound A could be classified as a suitable lead compound against HCMV infection, I determined its cytotoxic concentration (50%) (CC_{50}) value, the concentration at which 50% of exposed cells exhibit cytotoxicity. The ATP luminescence assay was used to test compound A in MRC-5 fibroblasts ranging from concentrations of 2, 5, 10, 20, 25, and 50 μM for 72 hrs. I chose not to use concentrations higher than 50 μM as the total amount of DMSO in the wells would exceed 1%, which is toxic for the cells. I

normalized the results as a percentage of viable cells compared to an untreated cell control and analyzed the CC_{50} *in silico*.

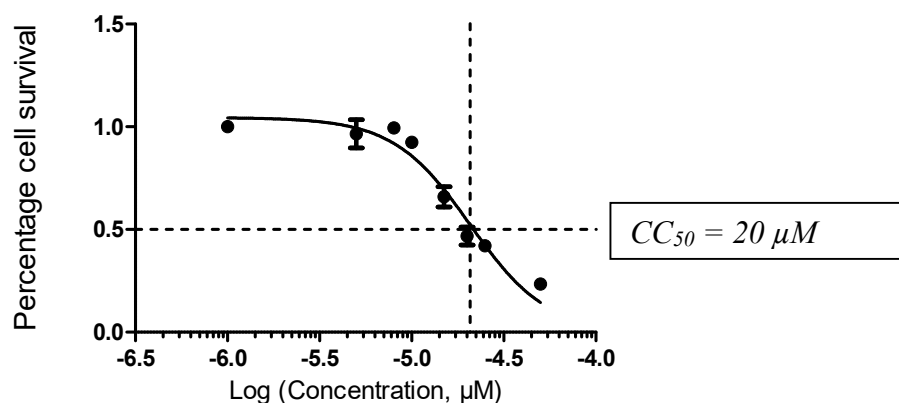


Figure 44. CC_{50} value calculated for Compound A using a nonlinear regression curve fit. Cytotoxicity was measured as the percentage cell survival normalized to an untreated control plotted against the log of the concentration of Compound A used. The curve bisects $y = 0.5$ (50%) at -4.68 , the antilog of which is the CC_{50} value of $20 \mu\text{M}$. Bottom constrained to 0. The experiments were done in triplicates. Means \pm SEM are shown.

Compound A shows 50% cytotoxicity in MRC-5 cells at $20 \mu\text{M}$ (Figure 44). As the DMSO concentration does not exceed 1% in any of the wells, it was unlikely that this cytotoxicity is caused by the DMSO and can be assumed to be caused by the Compound A alone.

The calculated toxicity of Compound A was of concern, as it affects the Selectivity Index (SI) of the compound, defined as the ratio of the CC_{50} to the IC_{50} . This value defines the propensity of the compound to target the pathogen before exerting cytopathic effect against the host cells. In this case, the SI of Compound A was calculated to be 4.7, while only compounds with a SI higher than 10 are deemed to be lead compounds. This means that Compound A must be optimized before it can be considered as a lead compound, and structural derivatives of Compound A must be considered.

5.4.6 Quantifying structural derivatives of Compound A

Small chemical alterations may optimize the compound and improve its IC_{50} and CC_{50} values. To investigate this, 100 compounds which contain the core structure of Compound A, and have only small alterations such as extra carbons, a halogen substitution etc., were purchased from a commercial chemical supplier (Chemdiv, USA). Of these 100 compounds, 48 were insoluble in DMSO, and 52 could be further analyzed.

5.4.6.1 Enzymatic activity of the 100 compounds

While small chemical alterations may lead to an improved SI of the compound, I hypothesized that certain alterations may lead to a loss of pUL98 inhibitory activity. Additionally, identifying compounds with higher IC₅₀ values than Compound A would be optimal. I designed a small screen similar to the high-throughput screen and tested the derivative compounds at 5 μ M concentration against pUL98. It was then possible to identify those compounds that would exhibit improved activities compared to that of Compound A. I then normalized the resulting signals to the respective 50 μ M Atanyl Blue PRL screening inhibition control (Figure 45). I selected compounds displaying a fold change of less than 1.3 in order to account for variation.

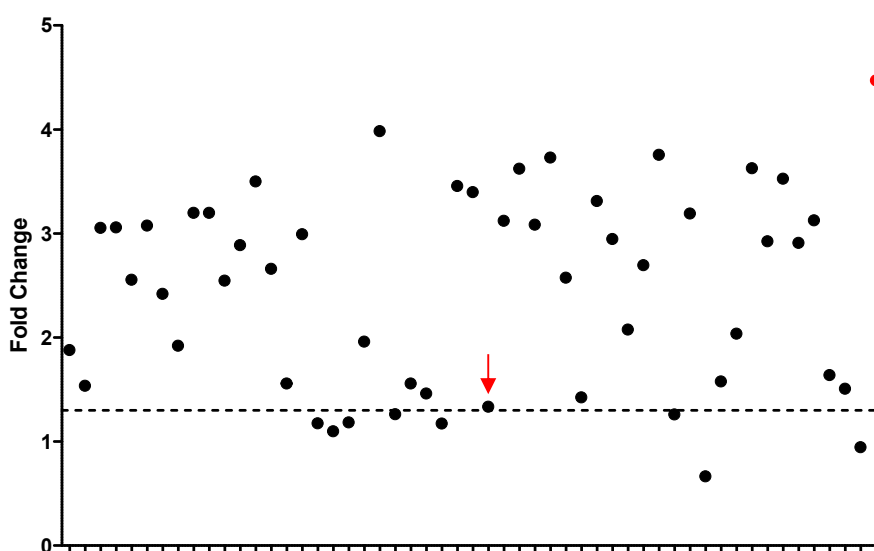


Figure 45. Fold change dot plot of enzymatic screening of 52 small molecular derivatives of Compound A. Fluorescent signal was normalized to that of the inhibitor control (=1)(50 μ M Atanyl Blue PRL) and plotted as a fold change increase. Eight compounds demonstrating fold change of 1.3 (dotted line) were detected, with a ninth (AD-66, red arrow), demonstrating a fold change of 1.33 and selected as a borderline case. Average no-inhibition control is plotted in red. The experiments were done in triplicate.

Of the 52 derivatives tested, only eight showed a fold change reduction below 1.3 of the inhibition control. A ninth compound, compound AD-66, showed a fold change reduction of 1.33 which I deemed a borderline case. As these nine compounds showed good inhibition of pUL98 at 5 μ M, I hypothesized that these compounds may demonstrate improved effectiveness against pUL98 *in vivo* and decided to quantify these compounds in an infection model.

5.4.6.2 Toxicity analysis of the Compound A derivatives

Before testing the Compound A derivatives (ADs) in a PRA, I first had to determine their cytotoxicity. I designed an assay similar to that done in section 5.3.4 using the ATP luminescence-based cell viability method to test the cytotoxicity of the nine compounds against MRC-5 fibroblasts ranging from concentrations of 1 μ M, 2 μ M, 5 μ M, 10 μ M, and 20 μ M incubated for 72 hours.

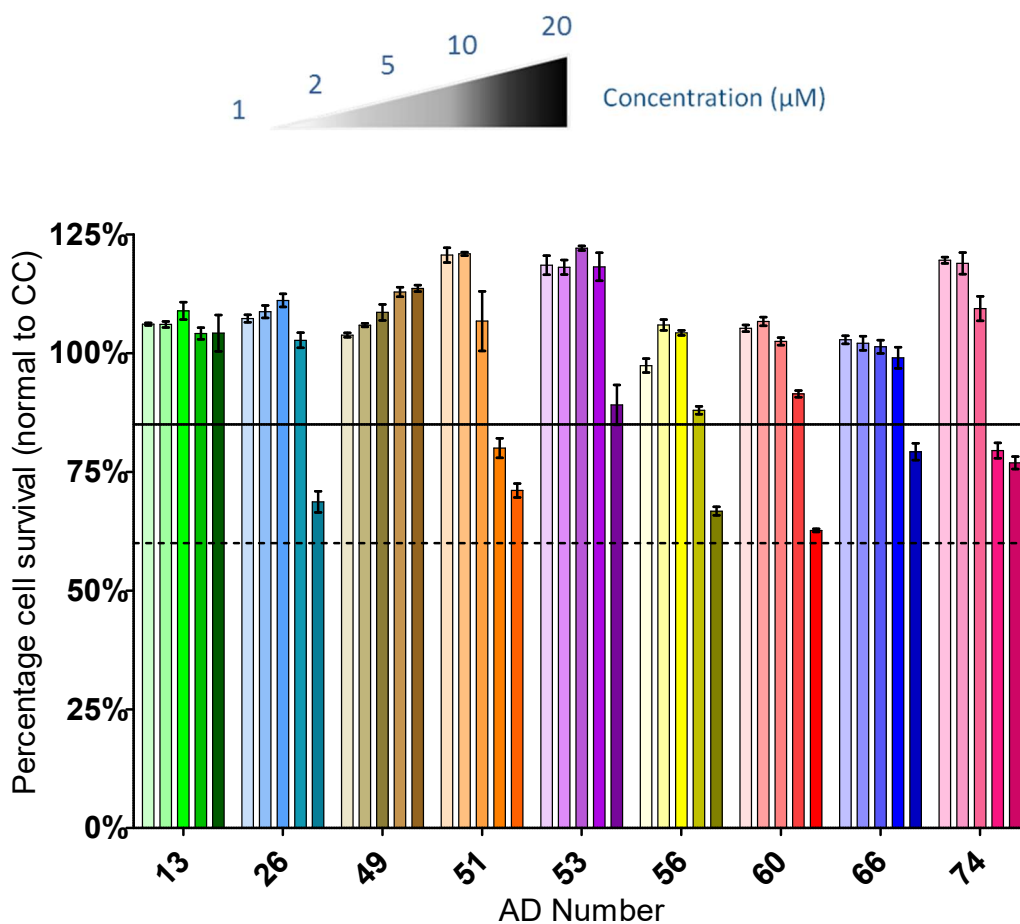


Figure 46. Cell viability of 9 compounds as determined by the ATP luminescence method. Compounds were tested on MRC-5 cells at 1 μ M, 2 μ M, 5 μ M, 10 μ M, and 20 μ M and incubated for 72hrs. The results were then normalized as a percentage against an untreated cell control. Darker colors indicate higher concentrations. Both the 85% viable cutoff and the STS negative are given as a solid line and a dotted line respectively.

The toxicity of the nine derivatives showed a similar pattern to that of Compound A, with AD-26, -51, -74, -56, -60, and -66 demonstrating viability below 85% at 20 μ M concentration (Figure 46). These were not grounds for exclusion in this assay, as their IC_{50} s may lie far above this level, but care must be taken in interpreting further results using this concentration. In contrast, AD-13, -49, and -53 demonstrated good tolerance at 20 μ M.

5.4.6.3 Plaque reduction assay and SI calculation show a promising lead candidate.

A PRA using the TB40/E strain infecting MRC-5 fibroblasts and a cytotoxicity analysis were then carried out as described in sections 5.3.4 and 5.3.5, with the nine compounds as described before.

Compound Name	IC ₅₀ (μM)	CC ₅₀ (μM)	Ro5 Compliant?	S.I.
AD-13	>20	>20	Yes	N/A
AD-26	>20	23	Yes	N/A
AD-49	>20	>20	Yes	N/A
AD-51	1.14	17	Yes	14.9
AD-53	4.1	31	No	7.5
AD-56	5.2	26	Yes	5
AD-60	5.3	23	Yes	4.3
AD-66	>20	28	Yes	N/A
AD-74	4.8	30	Yes	6.25

Table 3. Summary of identified derivatives and their calculated IC₅₀, CC₅₀, Ro5 compliance and SI values. Compounds that showed very little to no activity in the PRA are given a value of >20 μM, and compounds that showed no toxicity at 20 μM are given a CC₅₀ value of >20 μM. SI values that cannot be calculated due to high IC₅₀ or CC₅₀ values are given as N/A.

PRA of the derivatives and CC₅₀ results show improved compound properties and satisfaction of Lipinski's Rule of Five, a checklist that determines whether lead-like small molecular compounds may be orally bioavailable by considering a list of structural criteria (189):

1. No more than 5 hydrogen donors,
2. No more than 10 hydrogen acceptors,
3. Molecular weight must be no more than 500 Da,
4. Octanol-water partition coefficient LogP must be no more than 5

Several compounds do not exhibit any activity in infection (Table 3), probably due to their chemical alteration impairing their ability to inhibit pUL98 activity in an infectious model. These compounds, namely AD-13, -26, -49, and -66, were therefore excluded from further consideration. However, two compounds exhibited IC_{50} either at or lower than Compound A, with AD-53 showing an IC_{50} of 4.3 μ M while AD-51 exhibited an IC_{50} of 1.14 μ M with a CC_{50} of 31 and 17 μ M respectively. Unfortunately, while AD-53 showed reduced toxicity compared to that of Compound A (20 μ M), the compound still only exhibited an SI of 7.5, which is still below the accepted range of 10. This is also seen in AD-56, -60, and -74, which showed SI values of 5, 4.3, and 6.25 respectively, making them unsuitable as lead candidates.

Out of the 9 derivatives tested, only AD-51 satisfied all requirements: even though its CC_{50} value was higher than that of Compound A, its IC_{50} value was 1.14 μ M, resulting in an SI value of 14.9. As AD-51 also satisfied the Ro5 it therefore qualified as a lead small molecular compound.

6 Discussion

6.1 UL98 alkaline nuclease activity is essential for HCMV growth

The results given in this work have shown that the HCMV viral alkaline nuclease pUL98 is essential for viral replication and thus a valid drug target. Previous studies that disrupted the UL98 genetic region, such as the transposon disruption of various HCMV genes done by Yu et al. and the systemic deletion study done in the Towne strain by Dunn et al., found that disruption of the UL98 genetic region is lethal to viral growth (92,93). The phenotype displayed by the DD mutant in this work is consistent with these previous findings. These approaches of disrupting the UL98 genetic region do introduce the problem of affecting other downstream genes by disrupting a potential promoter of those genes. This is especially true of the UL98 genetic region which shares a 64 nucleotide base pair overlap with the essential UL99 region, which encodes for a protein responsible for the proper envelopment of the viral particle and abrogation of which is known to cause a lethal viral phenotype (190,191). This means that simple disruption of the UL98 region is not a true indicator of whether the UL98 gene is essential, as it is unknown whether the UL99 region relies on a promoter present within this region which may be lost during disruption of the UL98 region. Additionally, it is currently unknown whether pUL98 exhibits functions other than its alkaline nuclease activity. This means that simple disruption of the UL98 region, whether by simple removal of the genetic region or by introducing a stop codon to the region in order to prevent expression of the full region would not be able to specifically demonstrate that the alkaline nuclease activity of pUL98 is essential to viral growth. In contrast, this work shows only the alkaline nuclease activity of pUL98 is essential for viral growth, as the point mutations are introduced in the predicted AN active site (D254A, E278A and DD) and do not affect the UL99 genetic region but do affect viral growth. Indeed, the attenuated growth of the D254A and E278A active site mutants implies that the expression of UL99 is most likely not affected by the alterations in the UL98 region. Ideally, a viral growth curve quantifying the difference in viral growth between the mutants and the wild-type virus by titration of the virus titer at different times should be performed. However, the low growth of each of the single mutants makes the generation of virus stocks unfeasible, and generation of functional stocks of the double-residue active site mutant DD is impossible due to its lethal phenotype. Further studies of the role of pUL98 in the viral life cycle therefore need to be tested by other means. For example, a destabilizing domain could be attached to the protein, rendering pUL98 sensitive to proteasomal degradation unless in the presence of a stabilizing ligand. The protein can then be

removed during the viral life cycle at will, allowing for observation of potential differences in growth with or without the presence of pUL98 while eliminating the risk of disrupting other essential viral genes (192). The creation of a destabilization-sensitive form of pUL98 would also aid understanding the exact function of pUL98 in the HCMV viral life cycle. As this work was mostly focused on finding inhibitors of the pUL98 protein, it could not answer questions relating to pUL98's exact role in HCMV replication. However, the antiviral compounds identified in this work can be used as tools in investigating the effect of inhibiting pUL98 during infection. Defining its exact role would establish its precise localization within the nucleus, allowing for better understanding as to whether the protein can be reached by specific compounds. Moreover, it would assist in designing and optimizing compounds that may target specific exo- and endonuclease functions of pUL98.

6.1.1 Timing of expression of pUL98 during the viral life cycle

Work done on the ANs of alpha-herpesviruses and gamma-herpesviruses have led to insights in their potential inhibition, an example of which can be seen in Grady et al. who were able to link the inhibitory activity of small molecular compounds against the HSV-1 alkaline nuclease pUL12 with the protein's function in processing branched DNA structures necessary for viral genome replication (74). As the ANs are highly conserved in the herpesviruses, these data from UL12 suggests that pUL98 plays a similar function in the HCMV lifecycle. Indeed, this is supported by the fact that pUL98 is expressed with early-late kinetics, placing it in the timeframe of viral genome replication rather than viral packaging of genomic DNA into nucleocapsids that takes place during the Late phase (193). In addition, Neuber et al. did not identify pUL98 in their survey of the HCMV terminase complex, making an direct or indirect role of pUL98 in this complex unlikely (100). An alternative role for pUL98 in the HCMV viral life cycle is posited by Strang, who speculates that pUL98 may be involved in the rearrangement and compacting of host chromatin upon assembly of the viral replication compartment, but little is known about the process of this chromatin partitioning as of the writing of this work (57).

6.2 Advantages of a potential pUL98 crystal structure

Due to the sequence similarity among the various herpesvirus alkaline nucleases, it is possible to use the crystal structure of the KSHV SOX protein as a template to model the binding of potential inhibitory compounds, as well as to predict the overall structure of an AN of interest. Indeed, the pUL98 structure generated by Kuchta et al. used this as a basis for their prediction

(90). However, use of the SOX protein in this manner does not completely substitute for a native crystal of the other alkaline nucleases, as it must be noted that the SOX protein also functions to degrade host cellular transcription (the “host-shutoff function”), which is not demonstrated by other herpesviral ANs (83). This means that structural prediction of pUL98 has to be carefully interpreted, as they may incorporate aspects of this host-shutoff function, reducing the accuracy of the prediction. The generation of a crystal structure of native pUL98 would therefore be an important aid in finding additional small molecular inhibitory compounds against the protein, as this would make it possible to accurately visualize the active site and allow for a more tailored approach in the design of the compounds.

While this work was able to generate batches of pUL98 potentially suitable for crystallography, it was not possible to generate enough total protein to begin crystallographic studies, which often requires a high amount of total protein in solution. Indeed, Dahlroth et al.’s generation of the crystal that solved the structure of the KSHV-SOX protein required a total of 30 mg of protein in a 8 mg/ml protein solution, a relatively high value compared to the maximum of 6 mg that was attained in this work. While another system such as the baculovirus/insect cell protein expression system may be able to generate higher concentrations of pUL98, this is not guaranteed. Additionally, switching to a new expression system may not produce functional pUL98, as eukaryotic-based systems tend to introduce post-translational modifications which may artificially alter protein activity in a way not present *in vivo* into the expressed protein, procedures which are absent in prokaryotic systems. This gives the bacterial expression system used in this work a distinct advantage over eukaryotic systems, as it is shown that pUL98 generated using the pET28b(+) in BL21(DE3) expression system retains functional nuclease activity. A simple way to increase the amount of protein generated by this system is to increase the amount of bacteria containing the expressed protein, for example by optimizing the protocol for use in a fermenter system, which can generate very high amounts of biomass containing the protein compared to non-fermenter systems. Use of the double-tagged protein is important in this setting, as the protein batch must be very pure for successful crystallization; the contaminant band can interfere with the formation of an ordered crystal. In addition to this analysis, collaborative work has revealed several domains which may prove to be disordered. Disordered domains within proteins are known to be unstable and mobile elements within the structure, meaning that these domains have to be removed in order to improve the likelihood of successful crystallization (unpublished data). This work has generated one such mutant, the double-tagged C-terminal domain deletion DTS-CTL-UL98. However, deletion of this domain

severely reduces the function of the protein compared to the full-length double-tagged protein, but does not completely abolish it, indicating that other regions within the protein also play a role in its activity. As the disordered loops are not situated within the predicted active site, they can be used as a primary crystallization step in order to define the exact nature of the active site, and potentially also be co-crystallized with an inhibitor. This in turn requires a higher amount of the protein to be expressed and purified, as double-tagged purification systems tend to recover low amounts of protein.

6.3 Improvement of the high-throughput screen

Although it was not possible to investigate compounds by modeling them to a known active site, this work was still able to identify potential compounds using the fluorescent-based high-throughput screen. While this screen was able to identify multiple small molecular inhibitors of pUL98, some problems emerged upon translating the system to a high-throughput format. This is seen in the reduction in fold-change values for the no-inhibition controls in the high-throughput screen relative to those obtained in the optimization. A large majority of the compounds showing no inhibition have a fold change around 1.2 to 1.3 in the high-throughput screen, while they were above 2 during optimization. This can be due to several factors linked to switching to a high-throughput system. For example, handling the substrate during the screen requires that the substrate be kept from 0 – 4 °C, which is not possible when using the pipetting robot, as that unit has no refrigeration capability. This may render the phosphorothioate-linked endonuclease substrate unstable, leading to increased noise within the screening system as the general background fluorescence increases in all wells. This then reduces the calculated fold change present in the system, leading to the observed drop. Careful analysis of the results can still identify potential inhibitors of pUL98 by strictly selecting compounds that show fluorescent signal close to the inhibition controls, but this tradeoff will also potentially exclude true inhibitors as well as several falsely identified inhibitors. In general, use of a more stable substrate may overcome this problem in future screening. Indeed, the exonuclease substrate used in the secondary screening the Compound A derivatives in this work shows a much higher fold-change difference between the inhibition control and the no-inhibition controls, indicating that it may be more stable. This also implies that both the endo- and exonuclease substrates are similarly capable of identifying inhibitors of pUL98 and are somewhat interchangeable. However, as Kuchta et al found that the endonuclease function of pUL98 may be of more importance than the exonuclease activity in its AN function, it was not used as the primary screening substrate in the high-throughput

assay (90). It must be noted that the exonuclease substrate has also not been tested in a high-throughput capacity and may also demonstrate a drop in its fold-change response if subjected to the same conditions as the endonuclease substrate. However, if the exonuclease substrate proves to be more robust than the endonuclease substrate, then any future use of this system will benefit from using the exonuclease substrate as the primary substrate followed by a confirmatory screen of any identified inhibitors using the endonuclease substrate.

6.4 Identification and characterization of compounds inhibiting pUL98

While the high-throughput screen was able to identify nine confirmed inhibitors of pUL98 in the fluorescent-based enzymatic system, only two compounds, Compounds A and D, were shown to have an effect against HCMV infection *in vitro*. This is to be expected, as testing the nine compounds in an infectious model is in effect a third screen which filters out compounds unable to inhibit pUL98 in an infectious model. Compounds known to have an inhibitory effect against purified pUL98 may be metabolized to a non-inhibitory form within the cell or may be unable to cross the cellular membrane. Indeed, the low number of effective compounds identified in this work is the expected result of carrying out a targeted approach to identifying novel antiviral compounds. In this model, the antiviral target is known, as opposed to a phenotypic-based screen which simply investigates which small molecular compounds show an inhibitory effect against HCMV infection as a whole. A phenotypic screen therefore may identify several compounds demonstrating an effect against viral infection at the cost of not knowing their exact antiviral targets, while a targeted screen only searches for compounds showing an effect against a known antiviral target at the cost of identifying a higher number of inhibitors.

Even with its drawbacks, the screening methodology used in this work was able to identify the small molecular Compounds A and D as inhibitors of pUL98 both in the enzymatic - based screen as well as in an infectious model based on the HCMV plaque reduction assay. Unfortunately, Compound D was excluded from further investigation in this work due to inconsistent inhibition of viral growth in experimental replicates of the plaque reduction assay, likely pointing to an issue of chemical stability. This by no means indicates that the compound will not be further investigated, as alterations can be made to the compound in order to further stabilize it in a cellular assay. This can be argued of the eight remaining compounds identified in the high-throughput assay that demonstrated no effect in the plaque reduction assay, as it is known that they exhibit inhibitory activity against purified pUL98, and further investigations to their chemical structures may give insights into how to render

then effective in a cellular assay. However, this work presents only a beginning step in defining Compound A's inhibition of pUL98 activity, as this work has also shown that the compound has a low SI, indicating that it shows a level of toxicity against host cells which renders it unfit as a treatment compound in its current form. While this work could not discuss or present the actual structure of Compound A, or any other compounds used, due to confidentiality issues which may jeopardize ongoing work on these compounds, it must be noted that alterations of Compound A's structure may lead to more favorable biological properties. This was done in a limited way within this work by screening 100 derivatives of Compound A, each with only small chemical alterations. These small alterations were selected on a simple basis of difference, as this approach aimed to investigate the effect of each individual difference on the activity of Compound A as well as to identify any compounds that show markedly more favorable SI values. Very little is known about Compound A, as it is one of several thousand small molecular compounds generated by mass chemistry as part of the generation of a small molecular compound library. Compound A itself is then in effect a tool which serves as a primary indicator that its structure demonstrates an inhibitory property against pUL98. Therefore, the data generated by the 100 A-derivative (AD) compounds tested is valuable even if an AD demonstrated no inhibitory effect against pUL98 activity or even rendered the compound insoluble in DMSO, as these changes bring insight into which alterations of Compound A are detrimental to the compound. This allows for a strategy of alteration to be developed. The discovery of the low SI seen in the AD-51 derivative is especially enlightening, as this compound actually proved to be more toxic than that of Compound A, which would normally be grounds for excluding the compound from further analysis. However, the alteration introduced in this derivative proved to greatly improve its anti-pUL98 activity in an infectious model by around fourfold compared to the unaltered Compound A. Analysis of this change in the AD may lead to insights in this increase in efficacy – for example, perhaps the derivative binds more effectively to the enzyme, leading to a significant decrease in its IC_{50} value. This structural analysis of the compound falls outside of the scope of this work, as well as the field of virological research, as expertise in medicinal chemistry is needed to accurately analyze the effect of structural changes in Compound A and design improved derivatives of Compound A. Indeed, as of the writing of this work, I am already collaborating with a group of medicinal chemists in order to optimize the efficacy of Compound A. In addition, questions of binding efficacy may be only definitively answered by solving the crystal structure of pUL98, which would allow for an

accurate modeling of binding to the pUL98 active site, again underlining the importance for a successful crystallographic analysis of pUL98.

6.5 Optimization of Compound A and future directions

The optimization of Compound A is especially important as the compound has yet to be tested in a whole-organism model. This is important as the effect of Compound A and its derivatives are only known in one cell type, and it may be ineffective or even demonstrate undesirable side effects in a whole biological systems model. In the case of HCMV, this is the murine model utilizing MCMV and its UL98 AN homolog, M98. M98 presents a special challenge, as it is known that it is not essential for viral growth and proliferation, like pUL98 is in HCMV. This can be seen in the work carried out by Timoshenko et al. who demonstrated that mutating a conserved residue in the M98 AN in the temperature-sensitive *Tsm5* MCMV strain demonstrated growth kinetics comparable to the *wt* virus (188). This can also be seen in this work, where Compound A does seem to reduce MCMV replication in a plaque reduction assay, suggesting that M98 may be inhibited, but demonstrates high variation and can be described more as a trend of inhibition rather than a full inhibition. This means that a direct analysis of the effectiveness of Compound A in MCMV infection *in vivo* is not possible, and will require a different approach. One possible approach would be to generate a chimeric MCMV virus susceptible to Compound A that replaces the M98 genetic region with that of the HCMV UL98 region. A potential drawback of this approach may be that a chimeric virus does not function in the same manner as the *wt* virus and may not be viable, which then require additional *in vitro* investigation of the virus. An additional problem is the fact that M98 overlaps with the essential gene M99 ORF, like UL98 overlaps with UL99 in HCMV, meaning that a replacement of M98 could disrupt an essential promoter. Another approach that would not rely on a chimeric murine/human virus is the use of a mouse xenograft model, as used by Lischka et al. in their work on letermovir in a murine model, as letermovir shows no inhibition of MCMV (165). In this model, human fibroblasts are seeded and grown on a collagen gelfoam matrix with vascularization factors, following which they are infected with HCMV. The matrices are then implanted subcutaneously into immunodeficient SCID mice. This allows for the compound to be administered orally, and the matrices can be removed and digested post-sacrifice to investigate the effect of the compound in *in vivo* infection. While either method presented here can be considered as artificial, both methods allow for an *in vivo* investigation of Compound A and its derivatives. One insight into the mechanism of action of Compound A seen in this work is the manner of inhibition of pUL98, which is shown here to

likely be non-competitive with regards to the nuclease substrate. Inhibitors with non-competitive aspects are not unknown in the treatment of HCMV; indeed, the antiviral drug foscarnet inhibits the pUL54 viral polymerase by binding at the pyrophosphate binding site and is non-competitive for nucleoside substrates, unlike the mechanism of activity of GCV/VGCV or CDV (142). However, foscarnet is a reversible inhibitor of pUL54 and does compete with pyrophosphate and is therefore not a true non-competitive inhibitor of pUL54. The data shown in this work indicates that Compound A is not likely to compete with any other factor present in infection. Firstly, Compound A demonstrates good inhibition in the enzymatic assay, which contains only the compound, DNA substrate, protein, and Nuclease buffer, which is a simple mixture of buffered Tris at pH 8, magnesium chloride and DTT. As pUL98 evidently does not require any other components for its AN activity, it is highly unlikely that Compound A would need to compete with another cellular and/or viral factor in order to inhibit pUL98. Secondly, the IC_{50} of Compound A in the enzymatic assay is very close to that of the IC_{50} in the infectious PRA with only 1 μ M difference. If Compound A were to compete with another factor in the manner of foscarnet it would be expected that a large difference in the IC_{50} results between the enzymatic and the PRA would be seen, as the competing factor would not be present in the enzymatic assay. While this aspect can be postulated from the results shown in this work, what cannot be answered is the exact nature of the non-competitive binding to pUL98. Two major possibilities exist: first, Compound A may bind to the viral DNA polymerase in a similar manner to foscarnet, where it does not target the active site of pUL98 but instead targets another unidentified site in the protein, which then interferes with the protein's ability to bind and/or process the DNA substrate. Another possibility would be that Compound A does bind to the pUL98 active site, but irreversibly so, preventing the protein from binding to the DNA substrate. This question of activity can only be solved by successful co-crystallization of the protein bound to Compound A, which would allow for an accurate visualization of the exact method of interaction of the drug with the protein.

6.6 Closing Remarks

The discovery of Compound A and its derivative AD-51 as novel inhibitors of the pUL98 AN in this work shows that there exist alternative viral pathways viable for antiviral treatment of HCMV. While the development of Compound A and its derivatives as an antiviral drug is still in its infancy, Compound A, and especially AD-51, fulfill preliminary requirements of drug-like compounds. Most notably, they satisfy Lipinski's Rule of Five, meaning that they are likely to be orally bioactive as drugs (189). This suggests that if medicinal chemistry is able to

generate an effective and selective derivative of Compound A to be functional and non-toxic in an animal model, it may be able to advance to clinical trials. It is my hope that Compound A forms the basis of a future antiviral drug in treating HCMV infection.

7 Materials

7.1.1 Cells

Name	Description	Reference
MRC-5	Primary human lung fibroblasts	American Type Culture Collection (ATCC), CCL-171
M2-10B4	Mouse (<i>Mus musculus</i>) bone marrow/stroma cells	ATCC, CRL-1972
Vero	African green monkey (<i>Cercopithecus aethiops</i>) kidney epithelium cells	ATCC, CCL-81

7.1.2 Cell culture media and reagents

Description	Supplier
Dulbecco's Modified Eagle Medium (DMEM), high glucose	Thermo Fisher Scientific
Dulbecco's Phosphate Buffered Saline (PBS) (1 x)	Thermo Fisher Scientific
Fetal calf serum (FCS)	PAN Biotech
OptiMEM-I	Thermo Fisher Scientific
10 x MEM	Thermo Fisher Scientific
L-Glutamine	Thermo Fisher Scientific
Penicillin/Streptomycin (100 x)	Thermo Fisher Scientific
Trypsin-EDTA (1x)	Thermo Fisher Scientific
Crystal Violet Solution	Th. Geyer GmbH & Co. KG
Methylcellulose	Th. Geyer GmbH & Co. KG

Cells were grown in growth media consisting of DMEM + 1% (v/v) penicillin/streptomycin and 10% (v/v) FCS. Reduced growth media was used in plaque reduction assays and consist of DMEM + 1% (v/v) Penicillin/streptomycin and 3% (v/v) FCS.

7.1.3 Methylcellulose overlay for plaque reductions

Description	Components	Application
Methylcellulose (dissolved)	2.5 % (w/v) Methylcellulose in ddH ₂ O	Overlay for Plaque Reduction Assays
Methylcellulose Overlay	Methylcellulose (dissolved) 10 % 10 x MEM 1 % Penicillin / Streptomycin 1.5 % L-Glutamine 10 mM NaHCO ₃ 5 % FCS	

7.1.4 Bacteria

Name	Genotype	Growth temperature	Reference
<i>E. coli</i> GS1783	F- <i>mcrA</i> Δ(<i>mrr</i> - <i>hsdRMSmcrBC</i>) Φ80Δ <i>lacZ</i> Δ <i>M15</i> Δ <i>lacX74</i> <i>endA1 recA1</i> <i>deoR</i> Δ(<i>ara,leu</i>)7697 <i>araD139 galU GalK</i> <i>nupG rpsL</i> λ- <i>cI857</i> Δ(<i>crobioA</i>)<> <i>araC</i> - PBADI- <i>sceI</i>	30 °C	(194)
<i>E. coli</i> BL21(DE3)	F- <i>ompT gal dcm lon hsdSB(rB-mB-)</i> λ(DE3 [<i>lacI lacUV5-T7p07 ind1 sam7</i> <i>nin5</i>]) [<i>malB+</i>] _{K-12} (λS)	37 °C	Shankar Kumar, HPI Hamburg

7.1.5 Bacterial growth media

Description	Reference
Lysogeny broth (LB) medium (Lennox)	Carl Roth
Agarose	Carl Roth
Lysogeny broth (LB) agar	LB medium plus 15 g/l agar

7.1.6 Antibiotics

Name	Application	Concentration	Reference
Chloramphenicol	Selection of bacteria	15 µg/ml	Carl Roth
Kanamycin	Selection of bacteria	100 µg/ml	Carl Roth
Penicillin	Cell culture supplement	100 U/ml	Sigma- Aldrich
Streptomycin	Cell culture supplement	100 µg/ml	Sigma- Aldrich
L-(+)-Arabinose	Selection of bacteria	1% (w/v)	Sigma- Aldrich

7.1.7 Viruses

Name	Description	Reference
TB40/E	HCMV clinical strain TB40/E	(24)
TB40/E _{wt} -GFP	HCMV clinical strain TB40/E expressing GFP, cloned as BAC	(186)

7.1.8 Viruses generated in this work

Name	Description
wt-GFP	HCMV TB40/E _{wt} -GFP with HA-tag added to N-terminus of UL98
D254A	wt-GFP with amino acid mutation introduced to mutate UL98, D254A
E278A	wt-GFP with amino acid mutation introduced to mutate UL98, E278A
DD	wt-GFP with two amino acid mutations introduced to mutate UL98, D254A & E278A

7.1.9 Plasmids

Name	Description	Reference
pET28b(+)	Expression vector, kanR	Shankar Kumar, HPI Hamburg
pEP-Kan-S1	Template plasmid for <i>en passant</i> mutagenesis, contains I-Sce-aphA1 cassette, kanR	(194)

7.1.10 Plasmids generated in this work

Name	Vector	Characteristics
6x-His-pUL98	pET28b(+)	Expresses 6x-His-tagged pUL98
6x-His-pUL98-D254A	6x-His-pUL98	Expresses 6x-His-tagged pUL98 with an aspartic acid at position 254 replaced with an alanine
10xHis-UL98	6x-His-pUL98	Expresses 10xHis-tagged pUL98
DTS-UL98	10xHis-UL98	Expresses 10xHis and StrepTagII-tagged pUL98

D254A Rev	CAGCAAGGTGCGACCGCTGCCCTGCTTGA GCACGCCGAAGCACAGGGCCATGGAAGC GCCAGCAGCCC GCCAGTGTTACAACCAATTAACC	To mutate the aspartic acid at position 254 to alanine in the UL98 sequence of wt-GFP by <i>en passant</i> mutagenesis
E278A Fwd	GCAGCGGTCGCACCTTGCTGGTGGAAACCG TGCGCGCGCTCTACGCGATCAAGTGCCG CTACAAATATTTAGGGATAACAGGGTAAT CGATTT	To mutate the glutamic acid at position 278 to alanine in the UL98 sequence of wt-GFP by <i>en passant</i> mutagenesis
E278A Rev	AAAGGGGTCCTCCTTTTTGCGCAAATATTT GTAGCGGCACTTGATCGCGTAGACGCGCG CGCACGGTTCGCCAGTGTTACAACCAATT AACC	
Check Fwd	GGCGACAGAGAAGGTACAAA	For sequence verification of the D254A & E278A mutant BACs
Check Rev	GAGGGATGTTGTCGTAGG	
10x His Fwd	TATACCATGGGCAGCAGCCATCATCATCA TCATCACCACCACCACCATAGCAGCGGCC TGGTGCCG	To alter the 6x-His-tag UL98 to 10x-His in pET28b(+)
10x His Rev	GCGAAGCTTCGGCGGCGTGCC	
Strep-Tag Rev	TATAGCGGCCGCTATTATTTTCGAACTGC GGGTGGCTCCAAGCGCTGGGGCTACCCG GCGTGGTACCG	For adding a streptavidin tag and generating DTS-UL98 in pET28b(+) (Forward primer is pET Fwd)
Fusion 1 Fwd	GGCGACGGCGCTGGCGGGCGGCGCTGATCA CGCGCGCTTTTCACTGCCGG	For deletion of the region of DTS-UL98 to by fusion PCR to generate DTS-CTL-UL98 in pET28b(+)
Fusion 1 Rev	ATTGACAAAAGCCGGCAGTGAAAAGCGC GCGTGATCAGCGCCGCCGC	

Fusion 2 Fwd	AGCGACGGGGACGCCACGATCACTATTAA CGCGCGCTTTTCACTGCCGG	For deletion of the region of DTS-UL98 to by fusion PCR to generate DTS-CTL-UL98 in pET28b(+)
Fusion 2 Rev	ATTGACAAAAGCCGGCAGTGAAAAGCGC GCGTTAATAGTGATCGTGGCGT	
D254A Quikchange Fwd	TGGGCGCTTCCATGGCCCTGTGCTT	To mutate the aspartic acid at position 254 to alanine in 6x-His-pUL98 in pET28b(+)
D254A Quikchange Rev	AAGCACAGGGCCATGGAAGCGCCCA	
Inner Seq Fwd	TCGGTATCAAACACGAGGGC	For sequence verification of the D254A & E278A 6x-His-pUL98 mutants in pET28b(+)
Inner Seq Rev	ATACAGCAGATCGGCCAGGT	

7.1.12 Enzymes

Description	Reference
Fast Digest restriction enzymes and buffer	Thermo Fisher Scientific
PRECISOR DNA polymerase and buffer	BioCat
T4-DNA-ligase and buffer	Thermo Fisher Scientific

7.1.13 Reagents for small-scale plasmid and BAC extraction (“Mini-prep”)

Buffer	Components	Application
S1	50 mM Tris	Resuspending bacterial pellet
	10 mM EDTA	
	100 µg/ml RNase A	
	ddH ₂ O	
	pH 8.0	
S2	200 mM NaOH	Lysing bacterial pellet
	1% (v/v) SDS	
	ddH ₂ O	
S3	2.8 M potassium acetate	Neutralizing lysis buffer
	ddH ₂ O	
	pH 5.1	
Tris-HCl	10 mM Tris	For dissolving DNA
	ddH ₂ O	
	pH 8.0	

7.1.14 Protease Inhibitors

Description	Reference
Aprotinin	Carl Roth
Leupeptin	Carl Roth
Pefabloc SC	Carl Roth
Pepstatin A	Sigma-Aldrich
Protease inhibitor cocktail cOmplete™ mini, EDTA-free	Roche

7.1.15 Reagents for protein purification

Buffer	Components	Application
Buffer A	50 mM NaH ₂ PO ₄	Lysing bacterial pellet
	300 mM NaCl	
	15 % (v/v) Glycerol	
	1 % Nonidet P-40	
	ddH ₂ O	
	pH 8.0	
Lysis buffer	Buffer A + 20 mM Imidazole	
His-Elution buffer	Buffer A + 300 mM Imidazole	For elution of protein from NiNTA beads
Buffer B-2	50 mM KH ₂ PO ₄	For dialyzing/suspension of protein
	50 mM NaCl	
	15 % (v/v) Glycerol	
	100 μM EDTA	
	pH 8.0	
Buffer C	50 mM Tris	For dialyzing/suspension of protein
	50 mM NaCl	
	15 % (v/v) Glycerol	
	100 μM TCEP	
	pH 8.0	
Strep-Elution buffer	Buffer C w/o TCEP + 50 mM biotin	For elution of protein from StrepTactin beads
HisPur Ni-NTA beads	Supplier: Thermo Fisher Scientific	For His-tag protein purification
StrepTactin-XT beads	Supplier: IBA Lifesciences	For strep-tag protein purification

7.1.16 Reagents for agarose gel electrophoresis

Buffer	Components	Application
50 x TAE	2 M Tris, pH 8.0	Diluted to 1 × with ddH ₂ O before using, used for preparing agarose gel and as running buffer
	50 mM EDTA	
	5.7 % (v/v) acetic acid	
	ddH ₂ O	
GeneRuler™ DNA Ladder Mix	Supplier: Thermo Fisher Scientific	DNA Size ladder for agarose gels

7.1.17 Reagents for SDS-PAGE polyacrylamide gel electrophoresis

Buffer	Components	Application
4 x SDS sample loading buffer	150 mM Tris	Diluted to 1 x with ddH ₂ O before using. Loading buffer for SDS-PAGE gel electrophoresis
	2 mM EDTA	
	20 % (v/v) glycerol	
	4 % (v/v) SDS	
	10% β-mercaptoethanol	
	0.4 % bromophenol blue	
	ddH ₂ O	
	pH 6.8	
10 x Laemmli running buffer	250 mM Tris	Diluted to 1 x with ddH ₂ O before using. Running buffer for SDS-PAGE gel electrophoresis
	1,92 M Glycine	
	1 % (w/v) SDS	
	ddH ₂ O	
10 x TBS-T	100 mM Tris	Diluted to 1 x with ddH ₂ O before using. For preparing antibody dilutions and washing membranes
	1,5 M NaCl	
	1 % (v/v) Tween-20	
	ddH ₂ O	
	pH 7.5	
Transfer buffer	50 mM Tris	For semi-dry blotting
	40 mM Glycine	
	0.04 % (v/v) SDS	
	20% (v/v) Methanol	
12 % running gel precursor	12% (v/v) Acrylamide/Bisacrylamide	For making 12% SDS-PAGE running gels
	375 mM Tris	
	0.1 % (v/v) SDS	
	ddH ₂ O, pH 8.8	

4 % stacking gel precursor	4% (v/v) Acrylamide/Bisacrylamide	For making 4% SDS-PAGE stacking gels
	125 mM Tris	
	0.1 % (v/v) SDS	
	ddH ₂ O	
	pH 6,8	
Coomassie Fixing Buffer	50 % Methanol 10 % Acetic acid 40 % ddH ₂ O	For fixing SDS-PAGE gels for Coomassie staining
Coomassie Staining Buffer	Coomassie Fixing Buffer 0.1 % (w/v) Coomassie R-250	For staining SDS-PAGE gels for Coomassie staining
Coomassie Destaining Buffer	40 % Methanol 10 % Acetic acid 50 % ddH ₂ O	For destaining SDS-PAGE gels for Coomassie staining
PageRuler™ Prestained Protein Ladder Mix	Supplier: Thermo Fisher Scientific	Protein size ladder for SDS-PAGE gels

7.1.18 Primary Antibodies

Antigen	Species	Application (dilution)	Reference
6x-His	Mouse	Immunoblot (1:1000)	Clontech

7.1.19 Secondary Antibodies

Antigen	Species	Conjugate	Application (dilution)	Reference
Mouse Ig	Goat	HRP	Immunoblot (1:5000)	Jackson ImmunoResearch

7.1.20 Fluorescently-Tagged DNA Substrates

Primers	5' - 3'	Reference
Endonuclease substrate	5'-/5 6- FAM/A*GCTACGACGAACACCTCTATGTCATC AATAATC/3IABIFQ/-3'	Integrated DNA Technologies

Exonuclease substrate	5'-/56- FAM/AGCACGATGAGATCGCATCATCGTG/3IA BkFQ/-3'	Integrated DNA Technologies
-----------------------	--	-----------------------------

7.1.21 Compounds

Compounds were purchased from ChemDiv (San Diego, United States) or MolPort (Riga, Latvia).

7.1.22 Reagents for fluorescence-based protein activity assay (“Enzymatic assay”)

Buffer	Components	Application
Nuclease buffer	50 mM Tris	Buffer for alkaline nuclease-based assays
	6 mM MgCl ₂ *6H ₂ O	
	1 mM DTT	
	ddH ₂ O	
Atanyl Blue PRL (Acid Blue 129)	Dissolve in DMSO	Inhibition control. Supplier: Sigma-Aldrich

7.1.23 Commercial kits

Description	Supplier
BCA Protein Assay Kit	Thermo Fisher Scientific
NucleoBond Gel and PCR Clean-up	Macherey-Nagel
NucleoBond Xtra Midi	Macherey-Nagel
CellTiter-Glo® Luminescent Cell Viability Assay	Promega

7.1.24 Other materials used

Description	Reference
Nitrocellulose membrane (0.2 µm)	GE Healthcare Life Science
Whatman® gel blotting paper, Grade GB003	Sigma-Aldrich

Commonly used chemicals were purchased from Carl Roth, Merck, or Sigma-Aldrich.

8 Methods

8.1 Molecular biology methods

8.1.1 Primer synthesis

Primers were synthesized and desalted by Thermo Fisher Scientific. The lyophilized primers were resuspended in ddH₂O at stock concentration of 100 μ M. Primers were stored at -20 °C for long-term storage.

8.1.2 Polymerase Chain Reaction (PCR)

PCR was performed using a Biometra T3000 thermal cycler as per the manufacturer's instructions. PRECISOR DNA polymerase is used for all PCRs.

8.1.2.1 Reaction conditions and setup

PRECISOR setup	
5 x GC-Rich buffer	10 μ l
dNTP Mix (25 mM each)	1.25 μ l
Template (10 - 100 ng)	x μ l
Primers (10 μ M)	2 μ l Each
DMSO	1.5 μ l
PRECISOR High-Fidelity DNA Polymerase	1 μ l
ddH ₂ O	to 50 μ l

PRECISOR cycling conditions			
Cycle Step	Temperature (°C)	Time	Cycle(s)
Initial denaturation	98	2 min	1
Denaturation	98	30 s	25-30
Annealing	T _m -3 °C	30 s	
Extension	72	15 - 30 s /kb of template	
Final extension	72	5 min	1

8.1.3 Fusion PCR

Fusion PCR was carried out using the principles outlined by Heckman and Pease (195).

Briefly, overlapping primers were used to amplify the regions upstream and downstream of the sequence to be removed. These two regions were then annealed in a second PCR, creating a fragment that did not contain the internal region.

8.1.4 DNA restriction digestion

DNA restriction digestion is performed using the FastDigest™ restriction enzymes and buffers manufactured by Thermo Fisher Scientific as per the manufacturer's instructions.

FastDigest Setup	
10 x FastDigest Green Buffer	3 µl
DNA	1 µl
FastDigest Enzyme	1 µl
ddH ₂ O	up to 30 µl

Reactions are incubated at 37 °C for 1 hr before loading on an agarose gel for further analysis.

8.1.5 Agarose gel electrophoresis

PCR products and DNA fragments are analyzed by running them on 1% (w/v) TAE agarose gels containing 0.5 µg/ml ethidium bromide (EB) and using O'GeneRuler as a DNA size ladder. DNA in gels was visualized under UV light using a UV-Transilluminator (ECX-F20.M, VILBER). Pictures of TAE gels were taken using a GelDoc XR+ (BioRad) and the ImageLab software suite (BioRad).

8.1.6 Purification of DNA

DNA fragments, PCR, and ligation products were purified using a NucleoSpin Gel and PCR Clean-up kit according to the manufacturer's instructions and resuspended in Tris-HCl. The concentration of the purified DNA was measured by a NanoDrop-1000 spectrophotometer (Peqlab). DNA is frozen at -20 °C for long-term storage or kept at 4 °C for short-term use.

8.1.7 DNA ligation

Linearized vectors and inserts were ligated using T4-DNA ligase according to the manufacturer's instructions at a molar ratio of 1 : 5 vector : insert. Ligation was performed overnight at 16 °C or 1 hr at 22 °C using a Thermomixer (Eppendorf).

8.1.8 Storage of bacterial stocks

500 μ l of bacterial overnight culture was added to 300 μ l autoclaved 60% (v/v) glycerol and stored long-term at -80 °C as a bacterial stock.

8.1.9 Generation of electrocompetent *E. coli*.

A single colony of was inoculated in 10 ml LB-broth medium complemented with chloramphenicol and cultured overnight at 30 °C if GS1783, or with kanamycin at 37 °C if BL21(DE3). The inoculate was then diluted 1:20 in LB-medium and continuously cultured at 30 °C in a shaking incubator HT (Infors). When the bacteria reached an OD₆₀₀ of 0.5 - 0.6 the culture was immediately placed in an ice-water bath for 20 min. In case of GS1783 the culture was transferred beforehand to a shaking water bath at 42 °C for 20 min in order to induce the *Red* recombinase system. The culture was then centrifuged at 5,000 x g and 4 °C and media is decanted. The pellet was then resuspended and washed twice in sterile ice-cold double-distilled (ddH₂O) twice and ice cold 10% (v/v) glycerol once, and was centrifuged between each step at 5000 x g at 4 °C. Bacteria were then pelleted and resuspended in 1 ml 10% glycerol (v/v), aliquoted in 80 μ l volumes and stored at -80 °C.

8.1.10 Bacterial Transformation

Bacteria were transformed by electroporation. 40 μ l of aliquoted electrocompetent bacteria were thawed on ice and mixed with either 10 ng ligated product, 10 ng supercoiled plasmid or 150 ng linear DNA product. Bacteria-DNA mixtures were incubated on ice for 10 mins before transferring to pre-chilled 2 mm electroporation cuvettes and pulsed using a Gene Pulser XCell (BioRad) at 2.5 kV, 25 μ F and 200 Ω . 1 ml LB broth was immediately added to the cuvettes to resuspend the bacteria-DNA mixture and transferred to a 1.5 ml Eppendorf tube. The suspension was then incubated on a Thermomixer comfort 5355 (Eppendorf) at an appropriate temperature for 1 hour. The suspension was then plated on LB agar containing appropriate antibiotics and incubated overnight in a bacterial incubator (IPP400, Memmert).

8.1.11 Cloning Procedure

Firstly, two unique restriction enzyme recognition sites were identified in the Multiple Cloning Site (MCS) of the vector. Use of two enzymes with different sticky ends prevents the insertion of the sequence of interest in the reverse orientation. Specific primers were then designed for the sequence of interest, with each primer containing a recognition site for one of the selected enzymes. The primers were then used to amplify an “insert” PCR product

consisting of the sequence flanked by the unique recognition sites. The insert and the vector were then separately digested with the two selected restriction enzymes. The linearized vector and the digested insert are then purified and ligated before transformation into bacteria.

Correct cloning was verified by DNA sequencing of bacterial clones as described in section 8.1.16.

8.1.12 Quikchange™ Cloning protocol

Point mutations were generated using the PRECISOR DNA polymerase (BioCat) in 6x-His-pUL98 plasmids using the Quikchange™ (Agilent Technologies) protocol as described by the manufacturer. Mutated plasmids were transfected into BL21(DE3) strain *E. coli* and plated on LB-agar plates containing kanamycin. Clones were screened for correct mutation by Sanger sequencing (see section 8.1.16).

8.1.13 Creation of mutant virus strains using *en passant* mutagenesis

Modifications of the viral genome were introduced using the “*en passant*” system and protocol described in Tischer et al. (194). An overview is given in Figure 47:

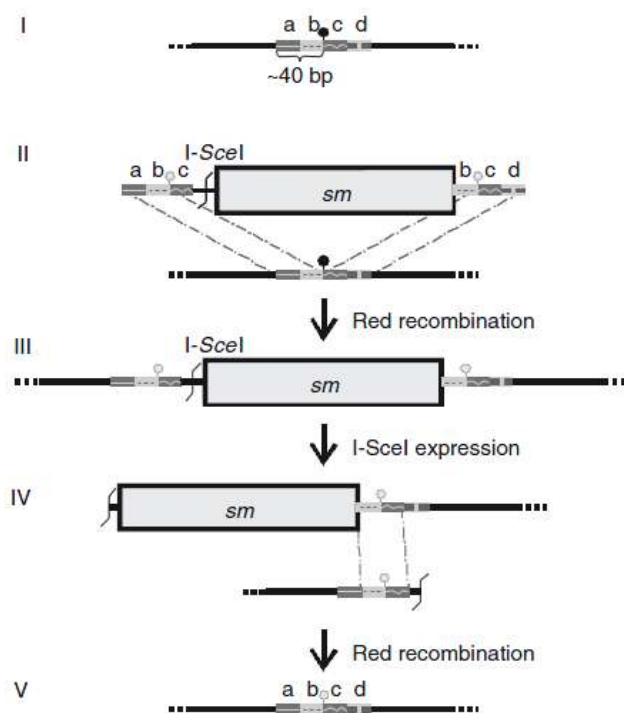


Figure 47. Overview of introduction of a point mutation using the *en passant* mutagenesis system. Adapted from (194).

Firstly, four regions of around 20 bp each immediately flanking the point mutation or deletion were selected and termed *a-d*, with the mutation being situated between *b* and *c* (Figure 47I).

A forward and reverse primer were then synthesized that contained three of the homologous regions and a sequence for amplifying the kanamycin cassette of the pEP-KanS1 plasmid, which includes a recognition site for the *I-SceI* restriction enzyme. PCR amplification then generated an insert comprised of 5' - *a* - *b* - *c* - *I-SceI* - *Kan* cassette - *b* - *c* - *d* - 3' (Figure 47II). 200 ng of this insert was then transformed into the *E.coli* strain GS1783 containing the wt-GFP BAC. Due to the presence of the *Red* recombinase system the insert will be introduced by homologous recombination into the BAC (Figure 47II). Bacteria are then plated on LB-agar plates containing kanamycin and chloramphenicol and grown overnight. Clones were verified by PCR amplification of the region of interest, with those demonstrating a 1000 bp shift being deemed as containing the insert.

Positive clones then underwent second recombination., Briefly, clones were grown in 2 ml LB-medium containing chloramphenicol for 1h 30 min or until cloudy. 2 ml of LB medium containing 2% (v/v) filter-sterilized L-arabinose and chloramphenicol was then added and the culture was grown for 1 h. This allowed for the expression of the *I-SceI* restriction enzyme, which cleaves the recognition site found within the insert (Figure 47III). The culture was then transferred to a waterbath and grown at 42 °C for 25 min in order to ensure the *Red* recombinase system was expressed. The culture was then returned to 30 °C and grown for a further 2 hours. This procedure allowed for the *Red* recombinase system to repair the cleaved strand by homologous recombination, removing the kanamycin cassette in the process and leaving a “scarless” region containing the mutation of interest (Figure 47IV). Culture was then plated on LB-agar plates containing chloramphenicol and 1 % (v/v) L-arabinose and incubated overnight. Clones were verified by Sanger sequencing after PCR amplification of the region of interest (See section 8.1.16).

8.1.14 Isolation of Plasmid DNA (“Miniprep”)

A single clone of *E. coli* containing the plasmid or BAC of interest was inoculated in 5 ml LB medium with appropriate antibiotics and cultured overnight. 4 ml overnight culture is then transferred to a 2 ml Eppendorf tube and pelleted by centrifuging at 5000 x *g* for 10 min at 4 °C. The pellet was then resuspended in 300 µl S1 buffer on ice. 300 µl of S2 buffer was then added and the tubes mixed by inversion and lysed for 4 min at room temperature (RT). 300 µl of S3 buffer was then added and the tubes mixed by inversion and then incubated for 2 min on ice. The mixture was then centrifuged at 16 000 x *g* and 4 °C in a benchtop centrifuge for 15 min and the clarified supernatant (ca. 800 µl) transferred to a new 2 ml Eppendorf tube. 400 µl isopropanol was added to the supernatant and the mixture centrifuged in a benchtop

centrifuge at 16 000 x g and 4 °C for 90 min, pelleting the DNA. The supernatant is then removed from the tube and the pellet is washed in 70% ethanol/ddH₂O. The ethanol mixture is then discarded, and the pellet dried in a benchtop heating block at 37 °C and dissolved in Tris-HCl. The pellets are kept at 4 °C for short-term use or at -20 °C for long-term storage.

8.1.15 Isolation of plasmid and BAC DNA (“Midiprep”)

A single clone of *E. coli* containing the plasmid or BAC of interest was inoculated in 200 ml LB medium with appropriate antibiotics and cultured overnight. Bacteria were harvested by centrifuging at 5000 x g for 15 min at 4 °C. Plasmid or BAC DNA was then isolated using the NucleoBond Xtra Midi kit using the “low-copy” protocol as per the manufacturer’s instructions. DNA concentration was quantified and BAC DNA was stored in 70% ethanol mixture at -20 °C and resuspended in Tris-HCl before use while other plasmids are stored at -20 °C in Tris-HCl.

8.1.16 DNA sequencing

In order to verify if DNA sequences generated in this work were correct Sanger sequencing was performed by Microsynth Seqlab GmbH (Göttingen, Germany) on a PCR product of the altered region (if a BAC) or on the purified plasmid using primers detailed in section 7.1.11.

8.1.17 Expression of UL98 Protein

An inoculate of UL98 cloned within the pET28b+ vector system in the BL21(DE3) strain was cultured in an LB media with kanamycin in an incubator overnight at 37 °C. The inoculate was then diluted to an appropriate volume in LB medium containing kanamycin. The bacteria were cultured until OD₆₀₀=0.6. Filter-sterilized IPTG was then added to a final concentration of 1 mM and the bacteria were then cultured for 3hrs at 25 °C shaking. The bacteria was then centrifuged at 6,000 x g at 4 °C and the pellets frozen at -80 °C for further processing.

8.2 Protein Biochemistry

8.2.1 His-tag purification of UL98 Protein

Pellets frozen after expression of UL98 protein were resuspended on ice in Lysis buffer, and incubated on ice for 30 mins. The lysate was then homogenized 4x with a lance sonicator at a pulse length of 15s per cycle. The lysate was then cleared by centrifuging at 15 000 x g at 4 °C for 30 mins, following which the lysate is transferred to 50 ml tubes (BD Falcon). An appropriate amount of HisPur™ nickel-nitriloacetic acid (NiNTA, Thermo Fisher Scientific)

beads is centrifuged at 200 x g at 4 °C and washed 6 x in lysis buffer before adding to the cleared lysate. The mixture is then incubated at 4 °C on a rotator for 1 hr. The tubes are then centrifuged at 200 x g at 4 °C for 3 mins in a benchtop centrifuge and the supernatant is discarded. The beads are then washed 3 x in wash buffer and centrifuged as above after every step. Finally, an appropriate amount of elution buffer is added, and the beads are centrifuged for 5 min at 300 x g at 4 °C, with the supernatant then dialyzed against the desired final buffer in SnakeSkin™ (Thermo Fisher Scientific) 10k MWCO overnight at 4 °C. Protein concentration is determined as given in section 8.2.3 and aliquoted and frozen at -80 °C for long-term storage.

8.2.2 Strep-tag purification of double-tagged protein

Protein was purified as described in section 8.2.1 but is dialyzed in C buffer at the final step. An appropriate volume of StrepTactin XT™ beads (IBA Lifesciences) was centrifuged at 200 x g at 4 °C and washed 6 x in C buffer. The beads were then added to the dialyzed protein and the mixture was transferred to a 2 ml Eppendorf tube. The mixture was then incubated on a rotator for 1 hr at 4 °C. The beads were then centrifuged at 200 x g for 3 mins and washed 3x in C buffer. The C buffer was removed and protein was eluted with an appropriate amount of strep-elution buffer. The supernatant was then dialyzed in C buffer overnight at 4 °C. Protein concentration was then determined as described in section 8.2.3 and aliquoted and stored at -80 °C for long-term storage.

8.2.3 Determination of protein concentration of purified protein

Protein concentration was determined using the BCA assay kit (Thermo Fisher Scientific) according to the manufacturer's instructions.

8.2.4 SDS polyacrylamide gel electrophoresis (Immunoblot)

8.2.4.1 Preparation of samples

4 x SDS loading buffer is then added to the desired amount of protein with ddH₂O to a final concentration of 1 x SDS loading buffer. Samples are then denatured by heating at 95 °C for 10 min, following which they are cooled down to room temperature. Samples are either used directly or stored at -20 °C.

8.2.4.2 Gel preparation and electrophoreses.

12 % resolving / 4 % stacking gels are cast according to the procedures outlined in Laemmli (196). The desired amount of protein is then loaded into each well. Samples and a protein size ladder are then run in 1 x running buffer using a MiniPROTEAN Tetra Cell-System (BioRad) at 80V for 20 min to stack samples. The voltage is increased to 100-110 V after the samples enter the resolving gel and begin to separate. Gels are run for 60 min until the protein is well separated as verified by the protein ladder.

8.2.4.3 Semi-dry blotting

Protein was transferred from SDS-PAGE gels to nitrocellulose membranes with 0.2 μ M pore sizes (Hybond ECL, GE Healthcare). Gels were transferred by semi-dry blot in transfer buffer under constant current of 0.1A per membrane for 1 hr using a Trans-Blot SD semi-dry transfer cell (BioRad) as per the manufacturer's instructions. Membranes were blocked in 5% (w/v) non-fat milk powder in TBS-T for 1 hr, following which they were incubated with primary antibody at an appropriate dilution in 5% (w/v) non-fat milk powder in TBS-T overnight at 4 °C. Primary antibody was then washed 3x for 10 min each out using TBS-T and the membrane was then incubated in secondary antibody specific against the primary antibody coupled with horseradish peroxidase (HRP) in 5% (w/v) non-fat milk powder in TBS-T for 1 hr at room temperature. The membrane was then washed 3 x in TBS-T for 5 min. ECL Western Blotting Substrate was then added and pictures were taken using a Fusion SL-4 3500WL Molecular Imaging camera (Peqlab).

8.2.4.4 Coomassie Staining

Protein was run on a SDS-PAGE gel as described in section 8.2.4. The gels were then fixed in Coomassie Fixing Buffer for 30 min at RT. Gels were then transferred to Coomassie Staining Buffer and stained for 30 min at RT. Gels were then repeatedly washed in Coomassie Destaining Buffer until the background stain was removed and protein bands were visible. Gels were then imaged using a flatbed scanner (Epson).

8.2.5 Quantification of activity of purified protein

The nuclease activity of the purified protein was confirmed by incubating 1 μ g of purified protein with 250 ng pcDNA3 plasmid DNA in Nuclease Buffer for 16hrs at 37 °C. A negative control containing only 250 ng of pcDNA3 plasmid DNA in Nuclease Buffer was incubated

under the same conditions. The resulting mixture was then run on a 1% agarose gel matrix and the resulting bands visualized using a UV camera.

8.2.6 Proof of concept of the enzymatic assay

Proof of concept of the enzymatic assay was carried out by using the reagents found in the DNase Alert™ kit (ThermoFisher Scientific) and 1 µg purified protein as per the manufacturer's instructions.

8.2.7 Quantification of enzymatic nuclease activity of purified protein

Purified protein was added to 200 nM exonuclease-substrate in varying amounts ranging from 180 - 220 ng protein in triplicate in Nuclease Buffer in a 96-well plate. A no-enzyme control containing only 200 nM substrate in Nuclease Buffer was also added to the same plate in triplicate. The plate was then incubated at 37 °C for 4 hrs. Fluorescence signal was detected using an Omega plate reader with an E_x of 458 nm and E_m of 520 nm.

8.2.8 Quantification of optimal substrate concentration

Optimal substrate concentration was determined by incubating increasing amounts of concentrations of substrate with 1 µg of purified pUL98 protein in nuclease buffer. No-inhibition controls only containing the same increasing concentrations tested with no purified pUL98 protein in nuclease buffer was added to the same plate. The plate was then sealed with a foil cover to exclude light and incubated at 37 °C for 4 hours before reading at an appropriate Ex/Em setting in an Omega plate reader. Both the protein results and the no-inhibition controls were plotted for each concentration, with the optimal substrate concentration determined as the concentration with the highest protein signal/no-inhibition signal ratio.

8.2.9 Substrate Synthesis

Endonuclease and Exonuclease DNA substrates were synthesized by Integrated DNA Technologies (USA) as HPLC-purified DNA fragments. Lyophilized substrate was reconstituted in Tris-HCl buffer to 100 µM. Substrate was aliquoted and stored in black-opaque Eppendorf tubes at -80 °C for long-term storage.

8.2.10 Compounds

Compounds tested were dissolved in DMSO to a final stock concentration of 10 mM, with the exception of Compound A which was dissolved at a concentration of 5 mM. Compounds were aliquoted to minimize freeze-thaw cycles and stored at -20 °C for long-term storage.

8.2.11 Fluorescence-based enzymatic assay for testing inhibitors of purified protein

Purified protein and putative inhibitor was suspended in Nuclease buffer in a 1.5 ml Eppendorf tube. The following controls are also used, all in Nuclease buffer: An no-inhibition control consisting of purified protein only, a no-enzyme control consisting of only Nuclease buffer, an inhibition control consisting of purified protein incubated with 50 µM of the known inhibitor Atanyl Blue PRL (Acid Blue 129), and a DMSO control consisting of purified protein incubated with the highest amount of DMSO used in the assay. These are then incubated at room temperature for 10 mins. Meanwhile, the desired substrate concentration was diluted in Nuclease buffer and aliquoted in an appropriate number of wells in a black-walled and –bottomed U-bottom 96-well plate (BD Falcon). The inhibitors and the controls were then added to the wells containing substrate to a final volume of 100 µl, with each condition aliquoted in triplicate. Plates are then sealed with an opaque foil and incubated at 37 °C for 4 hrs. Fluorescence activity is detected by using an Omega plate reader with an Ex of 458 nm and Em of 520 nm.

8.2.12 Screening of the small molecular compound library

Screening of the small molecular compound library was done at the Medizinische Hochschule Hannover (Germany) using the system described in section 8.2.11 with the following alterations: Compounds and controls were plated in black walled- and bottomed 364- well plates in duplicate in a final volume of 50 µl with inhibitors tested at a final volume of 10 µM per condition. Plates were pipetted using a Biomek FX (Beckman Coulter) pipetting robot in a KOJAIR tech BLII laminar flow unit. Fluorescent signal was read using a Cytation 3 (Biotek) plate reader at an E_x of 493 nm and E_m of 518 nm.

8.3 Cell biology and virology methods

8.3.1 Cell culture

All cell culture was performed in a laminar flow hood (HeraSafe, Heraeus). Cells were grown on tissue culture dishes (Ø 100 mm or Ø 145 mm) or plates (6-well, 24-well or 96-well) at 37 °C in a Hera Cell CO₂ incubator (Heraeus) with a constant 5% CO₂ supply and

approximately 95% humidity. All cells were cultured with high glucose DMEM media supplemented with 10% FCS, 100 IU/ml Penicillin and 100 µg/ml Streptomycin. Cells were split using 0.25% Trypsin-EDTA solution when reaching approximately 90% confluence as a monolayer. Trypsin was neutralized by adding growth medium containing FCS.

8.3.1.1 Determining cell concentration

10 µl of cell suspension was loaded onto a counting slide and cell number was analyzed by a TC20™ Automated Cell Counter (BIO-RAD).

8.3.1.2 Freezing cells for storage

Cell suspension was spun down at 37 °C, 300 x g for 6 min. Supernatant was discarded and the cell pellet was suspended in 1 ml FCS containing 10% DMSO and transferred to a cryotube. It was then immediately stored at -80 °C. Cells were further transferred to liquid nitrogen for long-term storage.

8.3.1.3 Thawing frozen cells

Cells from -80 °C freezer or liquid nitrogen were immediately placed in a water bath at 37 °C. After fully thawing cell suspension was transferred to a Ø 100 mm culture dish containing 10 ml growth media. Media was replaced the next day.

8.3.2 Transfection of viral BACs into mammalian cells

Mammalian cells were transfected by electroporation to reconstitute virus. 2-5 µg of viral genome-containing BAC was added to 1.5 µg pp71-expressing plasmid. The mixture is then transferred to a 4 mm electroporation cuvette, and MRC-5 cells (at a passage no higher than p28) are then trypsinized and centrifuged for 10 mins at 200 x g at room temperature. Growth media is then gently aspirated from the cellular pellet and the cells are resuspended in 200 µl of non-supplemented Opti-MEM. The resuspended cells are added to the cuvette containing the BAC-DNA mix and the final volume is made up to 260 µl using Opti-MEM. The mixture is then pulsed with a setting of 220 V and 950 µF. The cuvette is then incubated for 5 min at room temperature. 1 ml of Opti-MEM is then gently added to the cuvette, and the electroporated cells are then transferred to a Ø 100 mm culture dish containing 10 ml Growth medium. Cells are then incubated in a cell incubator at 37 °C and 5% CO₂. Growth medium was replaced every two days.

8.3.3 Culture of virus stock

HCMV stocks were generated by infecting 2×10^6 cells/plate of MRC-5 cells with 2×10^5 TCID₅₀ virus to make an infectious multiplicity of infection (MOI) of 0.01 TCID₅₀/cell. The mixture was then equally distributed on 5 Ø 145 mm cell culture dishes and supernatant was collected after 6 days, 9 days and 12 days infection. Fresh growth medium was added after each collection. Supernatant was first centrifuged at 6000 x g at 4 °C for 15 min to remove cell debris. The supernatant was then either frozen at -80 °C for short-term storage or directly added to a sterile bucket and centrifuged at 10 000 x g at 4 °C for 4 hr to pellet the virus. The pellet was then resuspended in 1 ml growth medium overnight at 4 °C before aliquoting and storage at - 80 °C.

8.3.4 Determination of HCMV TCID₅₀

The concentration of HCMV in a solution was determined by the TCID₅₀/ml method (Munch, Spearman, Karber), which is defined as the tissue culture viral dose which will infect 50 % of cells in a monolayer. To this end 1000 MRC-5 cells were seeded in each well of a 96-well plate and incubated overnight in a cell incubator. The next day HCMV was serially diluted from 1:10² to 1:10⁹ in 2 ml growth medium. 100 µl of dilution was added to each well so that each dilution consisted of an entire row of 12 wells in the 96-well plate. This procedure was repeated 3 times, and the three plates were then incubated in a cell incubator. After 14 days the number of infected wells of each dilution was counted and the viral titer was calculated based on the Spearman-Kärber method (197,198)

$$\text{Titer} = \frac{10^N}{\text{inoculation volume [ml]}} \text{TCID}_{50}\text{ml}^{-1},$$

$$N = \text{highest dilution giving 100\% cytopathic effect (CPE)} + \left[\frac{\text{total number of test units showing CPE}}{\text{number of test units per dilution}} \right] - \frac{1}{2}$$

8.3.5 Cell viability assay

Cell viability assays were performed on 1×10^3 cells/well MRC-5 cells in a 96-well black-walled and transparent-bottomed plate. 2 µM Staurosporine (STS) was used as a toxicity control and untreated wells were used as a non-toxic control. An amount of DMSO equivalent to the compound dilution containing the highest percentage of DMSO was added alone to cells as a DMSO control. Plates were incubated for 72 hrs in a cell incubator before reading using the CellTiter Glo® Luminescent Cell Viability Assay kit (Promega) according to the manufacturer's instructions. Briefly, the 96-well plate was kept at RT for 30 min. before

reading. Meanwhile, the two CellTiter Glo® reagents was thawed at RT and reconstituted before use. 100 µM of the mixed reagents are then added to each well and the cells lysed by orbital shaking in an Omega plate reader for 30 seconds. The plate was then kept in the dark for 10 min at RT to stabilize the luminescent signal before reading with an Omega plate reader.

8.3.6 CMV plaque-reduction assay (PRA)

8.3.6.1 Determination of CMV plaque titer

In order to determine the amount of plaques formed by the virus a 48-well plate was seeded with 5×10^4 cells/well of MRC-5 fibroblasts (HCMV) or M2-10B4 cells (MCMV) and incubated in a cell incubator overnight. The next day HCMV or MCMV was diluted from 1:10³ to 1:10¹⁴ in 2ml restricted growth media. This was repeated 4 times. All except 100 µl Growth media is aspirated from the 48-well plate and 100 µl viral dilution is added to each well so that each row of 4 wells consist of an independently-diluted dilution step of virus. The plate was then incubated 3 hrs in a cell incubator. Following this 300 µl of methylcellulose overlay is added to each well and the plate was incubated in a cell incubator. After 14 days the methylcellulose was gently removed and cells were washed in D-PBS until all methylcellulose was removed. 300 µl CV stain was then added and cells are incubated for 10 min at room temperature to fix and stain cells. CV stain was then discarded and wells washed with H₂O and dried overnight at RT before plaques were counted using a light microscope. The dilution at which 20-30 plaques are generated was determined as the PRA titer, as this amount of plaques was easy to read and also allowed for easy detection of inhibition of plaque formation.

8.3.6.2 CMV plaque-reduction assay

The CMV plaque-reduction assay (PRA) was carried out in a similar manner, but with the following alterations: Serial dilutions of required compound are dissolved in 5 ml methylcellulose along with a DMSO control consisting of the amount of DMSO present in the highest concentration of compound and incubated at RT overnight to allow compounds to dissolve. 44 of the 48-well plate were then infected with a PRA titer of virus in 100 µl restricted growth media, with 100 µl restricted growth media only being added to the remaining 4 wells. The plate was then incubated as described above. 300 µl of compound-containing methylcellulose was then plated so that each row of four wells consisted of a dilution of compound. Methylcellulose containing no compound was added to two wells of

uninfected cells as an uninfected cell control and two infected wells as a virus infection control, while methylcellulose containing DMSO was added to two wells of uninfected cells as an DMSO cell control and two infected wells as a virus + DMSO infection control. Plates were then incubated, stained and read as described in section 8.3.6.1.

8.3.6.3 Determination of HSV-1 plaque titer

HSV-1 titer was determined as described in section 8.3.6.1 with the following alterations: 1.7×10^7 VERO cells were plated in a 6-well plate in growth media and incubated overnight. HSV-1 (a kind gift from Dr. Beate Sodeik, Hannover) was diluted in DMEM supplemented with antibiotics and 1 % FCS from 1:10⁴ to 1:10⁷, which was repeated three times, making a dilution series of three wells of independently-diluted HSV-1. The plates were incubated as described in section 8.3.6.1 and 1 ml of methylcellulose was added per well. The plates are stained at three days post infection as described in section 8.3.6.1.

8.3.6.4 HSV-1 Plaque reduction assay

HSV-1 plaque reduction assay was performed as described in Section 8.3.6.2 but with the following alterations: 1.7×10^7 VERO cells were plated in a 6-well plate in growth media and incubated overnight. A PRA titer of HSV-1 (a kind gift from Dr. Beate Sodeik, Hannover) was diluted in DMEM supplemented with antibiotics and 1 % FCS. Compounds were diluted in methylcellulose as described in section 8.3.6.2 and 1 ml was added to each well so that each row of three wells constituted a dilution of compound. Controls were as described in section 8.3.6.2. Cells were stained and read after 3 days as described in section 8.3.6.3.

8.3.7 Viral growth kinetic of Compound A

In order to determine the impact of Compound A on HCMV growth a 6-well plate was seeded with 1×10^5 cells/well MRC-5 fibroblasts in growth medium and incubated overnight. The next day all wells except for three were infected with three independent dilutions of TB40/E at an MOI of 0.2 TCID₅₀/cell in 3 ml growth media/well so that each well in a row represented a separate dilution of HCMV. The remainder of the virus dilutions were frozen at – 80 °C as the Input control. Plates were incubated in a cell incubator for 3 hrs, after which the media was aspirated and cells washed 3x in warm D-PBS. 3 ml growth media containing diluted Compound A was then added so that each row of three wells consisted of one dilution of Compound A. 3 ml of growth medium containing no compound was added to one row as an no-inhibition control. 1 ml of each well was removed and frozen at – 80 °C at days 1, 3, 5, 7 and 9, at which the remaining media was aspirated, cells washed 1x in warm D-PBs and

fresh media containing compound was added to the wells. The supernatants were the titrated for TCID₅₀ as described in section 8.3.4 in order to determine virus titer at specific days.

8.4 Statistical Analysis and Figure Generation

Statistical analysis was carried out using GraphPad Prism version 5.03 (GraphPad Software, La Jolla California, USA) and Microsoft Excel (Microsoft Corporation, USA). IC₅₀ calculations were done by non-linear regression (log (inhibitor) vs. response – Variable slope (four parameters)) analysis of the log (compound concentration) versus the plaque count per condition with the bottom constrained to 0. CC₅₀ values were calculated by nonlinear regression analysis (log(agonist) vs. response – Variable slope (four parameters)) of the log (compound concentration) vs the percentage survival per condition with bottom constrained to 0.

Figures were generated in GraphPad Prism version 5.03 or R version 3.6.1.

9 References

1. Roizmann B, Pellet PE. The Family Herpesviridae: A Brief Introduction Herpesviridae. In: Knipe DM, Howley PM, editors. *Fields Virology*. 4th ed. Philadelphia: Lippincott Williams & Wilkins; 2001. p. 2381–97.
2. Adler B, Sattler C, Adler H. Herpesviruses and Their Host Cells: A Successful Liaison. *Trends Microbiol*. 2017 Mar 1;25(3):229–41.
3. Whitley RJ. Herpes Simplex Viruses. In: Knipe D, Howley PM, editors. *Fields Virology*. 4th ed. Philadelphia: Lippincott Williams & Wilkins; 2001. p. 2461–509.
4. Arvin AM. Varicella-Zoster Virus. In: Knipe DM, Howley PM, editors. *Fields Virology*. 4th ed. Philadelphia: Lippincott Williams & Wilkins; 2001. p. 2731–67.
5. Rickinson AB, Kieff E. Epstein-Barr Virus. In: Knipe D, Howley PM, editors. *Fields Virology*. 4th ed. Philadelphia: Lippincott Williams & Wilkins; 2001. p. 2575–627.
6. Cesarman E. Gammaherpesviruses and Lymphoproliferative Disorders. *Annu Rev Pathol Mech Dis*. 2014 Jan 24;9(1):349–72.
7. Barton E, Mandal P, Speck SH. Pathogenesis and Host Control of Gammaherpesviruses: Lessons from the Mouse. *Annu Rev Immunol*. 2011 Apr 23;29(1):351–97.
8. Moore PS, Chang Y. Kaposi's Sarcoma-Associated Herpesvirus. In: Knipe DM, Howley PM, editors. *Fields Virology*. 4th ed. Philadelphia: Lippincott Williams & Wilkins; 2001. p. 2803–33.
9. Pass RF. Cytomegalovirus. In: Knipe DM, Howley PM, editors. *Fields Virology*. 4th ed. Philadelphia: Lippincott Williams & Wilkins; 2001. p. 2675–705.
10. Yamanishi K. Human Herpesvirus 6 and Human Herpesvirus 7. In: Knipe DM, Howley PM, editors. *Fields Virology*. 4th ed. Philadelphia: Lippincott Williams & Wilkins; 2001. p. 2785–801.
11. Andrä CJ (ed). *Verhandlungen des naturhistorischen Vereines der preussischen Rheinlande und Westfalens*. 1881;Achtunddreissigster Jahrgang. Vierte Folge: 8. Jahrgang. Max Cohen & Sohn, Bonn.:161–162.
12. Jesionek A, Kiolemenoglou B. Ueber einen Befund von protozoenartigen Gebilden in den Organen eines hereditaerluetischen Foetus. *Muenchner Med Wochenschr*. 1904;51:1905–7.
13. Minder W. Die Aetiologie der Cytomegalia infantum. *Schweizer Med Wochenschr*. 1953;(83):1180–2.
14. von Glahn WC, Pappenheimer AM. Intranuclear Inclusions in Visceral Disease. *Am J Pathol*. 1925 Sep;1(5):445-466.3.
15. Smith M. Propagation of salivary gland virus of the mouse in tissue cultures. *Proc Soc Exp Biol Med*. 1954;86:435–40.
16. Smith M. Propagation in tissue cultures of a cytopathogenic virus from human salivary gland virus (SGV) disease. *Proc Soc Exp Biol Med*. 1956 Jun 1;92(2):424–30.
17. Rowe W, Hartley J, Waterman S, Turner H, Huebner R. Cytopathogenic agent

- resembling human salivary gland virus recovered from tissue cultures of human adenoids. *Proc Soc Exp Biol Med*. 1956 Jun;92(2):418–24.
18. Weller TH, MacAuley JC, Craig JM, Wirth P. Isolation of Intranuclear Inclusion Producing Agents from Infants with Illnesses Resembling Cytomegalic Inclusion Disease. *Exp Biol Med*. 1957 Jan 1;94(1):4–12.
 19. Chee MS, Bankier AT, Beck S, Bohni R, Brown CM, Cerny R, et al. Analysis of the Protein-Coding Content of the Sequence of Human Cytomegalovirus Strain AD169. In: *Current topics in microbiology and immunology*. 1990. p. 125–69.
 20. Stern-Ginossar N, Weisburd B, Michalski A, Le VTK, Hein MY, Huang S-X, et al. Decoding human cytomegalovirus. *Science*. 2012 Nov 23;338(6110):1088–93.
 21. Cha TA, Tom E, Kemble GW, Duke GM, Mocarski ES, Spaete RR. Human cytomegalovirus clinical isolates carry at least 19 genes not found in laboratory strains. *J Virol*. 1996 Jan;70(1):78–83.
 22. Bradley AJ, Lurain NS, Ghazal P, Trivedi U, Cunningham C, Baluchova K, et al. High-throughput sequence analysis of variants of human cytomegalovirus strains Towne and AD169. *J Gen Virol*. 2009 Oct 1;90(10):2375–80.
 23. Li G, Nguyen CC, Ryckman BJ, Britt WJ, Kamil JP. A viral regulator of glycoprotein complexes contributes to human cytomegalovirus cell tropism. *Proc Natl Acad Sci*. 2015 Apr 7;112(14):4471–6.
 24. Sinzger C, Hahn G, Digel M, Katona R, Sampaio KL, Messerle M, et al. Cloning and sequencing of a highly productive, endotheliotropic virus strain derived from human cytomegalovirus TB40/E. *J Gen Virol*. 2008 Feb 1;89(2):359–68.
 25. Murrell I, Tomasec P, Wilkie GS, Dargan DJ, Davison AJ, Stanton RJ. Impact of sequence variation in the UL128 locus on production of human cytomegalovirus in fibroblast and epithelial cells. *J Virol*. 2013 Oct 1;87(19):10489–500.
 26. Wilkinson GWG, Davison AJ, Tomasec P, Fielding CA, Aicheler R, Murrell I, et al. Human cytomegalovirus: taking the strain. *Med Microbiol Immunol*. 2015 Jun 17;204(3):273–84.
 27. Krmpotic A, Bubic I, Polic B, Lucin P, Jonjic S. Pathogenesis of murine cytomegalovirus infection. *Microbes Infect*. 2003 Nov 1;5(13):1263–77.
 28. Cannon MJ, Schmid DS, Hyde TB. Review of cytomegalovirus seroprevalence and demographic characteristics associated with infection. *Rev Med Virol*. 2010 Jun 18;20(4):202–13.
 29. Colugnati FA, Staras SA, Dollard SC, Cannon MJ. Incidence of cytomegalovirus infection among the general population and pregnant women in the United States. *BMC Infect Dis*. 2007 Dec 2;7(1):71.
 30. Hyde TB, Schmid DS, Cannon MJ. Cytomegalovirus seroconversion rates and risk factors: implications for congenital CMV. *Rev Med Virol*. 2010 Sep 1;20(5):311–26.
 31. Lachmann R, Loenenbach A, Waterboer T, Brenner N, Pawlita M, Michel A, et al. Cytomegalovirus (CMV) seroprevalence in the adult population of Germany. *PLoS One*. 2018;13(7):e0200267.
 32. Cannon MJ. Congenital cytomegalovirus (CMV) epidemiology and awareness. *J Clin Virol*. 2009 Dec 1;46(SUPPL. 4):S6–10.

33. Boppana SB, Ross SA, Fowler KB. Congenital Cytomegalovirus Infection: Clinical Outcome. *Clin Infect Dis*. 2013 Dec 15;57(suppl 4):S178–81.
34. Goderis J, De Leenheer E, Smets K, Van Hoecke H, Keymeulen A, Dhooge I. Hearing Loss and Congenital CMV Infection: A Systematic Review. *Pediatrics*. 2014 Nov 1;134(5):972–82.
35. Kenneson A, Cannon MJ. Review and meta-analysis of the epidemiology of congenital cytomegalovirus (CMV) infection. *Rev Med Virol*. 2007 Jul 1;17(4):253–76.
36. Britt WJ, Prichard MN. New therapies for human cytomegalovirus infections. *Antiviral Res*. 2018 Nov 1;159:153–74.
37. Ljungman P, Boeckh M, Hirsch HH, Josephson F, Lundgren J, Nichols G, et al. Definitions of cytomegalovirus infection and disease in transplant patients for use in clinical trials. Snyderman DR, editor. *Clin Infect Dis*. 2017 Jan 1;64(1):87–91.
38. Stern M, Hirsch H, Cusini A, van Delden C, Manuel O, Meylan P, et al. Cytomegalovirus serology and replication remain associated with solid organ graft rejection and graft loss in the era of prophylactic treatment. *Transplantation*. 2014 Nov 15;98(9):1013–8.
39. Santos CAQ, Brennan DC, Yusen RD, Olsen MA. Incidence, Risk Factors and Outcomes of Delayed-onset Cytomegalovirus Disease in a Large Retrospective Cohort of Lung Transplant Recipients. *Transplantation*. 2015 Aug;99(8):1658–66.
40. Reischig T, Kacer M, Hruby P, Jindra P, Hes O, Lysak D, et al. The impact of viral load and time to onset of cytomegalovirus replication on long-term graft survival after kidney transplantation. *Antivir Ther*. 2017;22(6):503–13.
41. Onor IO, Todd SB, Meredith E, Perez SD, Mehta AK, Marshall Lyon G, et al. Evaluation of clinical outcomes of prophylactic versus preemptive cytomegalovirus strategy in liver transplant recipients. *Transpl Int*. 2013 Jun 1;26(6):592–600.
42. Marty FM, Ljungman P, Chemaly RF, Maertens J, Dadwal SS, Duarte RF, et al. Letermovir Prophylaxis for Cytomegalovirus in Hematopoietic-Cell Transplantation. *N Engl J Med*. 2017 Dec 21;377(25):2433–44.
43. Mocarski ES, Courcelle CT. Cytomegaloviruses and Their Replication. In: Knipe DM, Howley PM, editors. *Fields Virology*. 4th ed. Philadelphia: Lippincott Williams & Wilkins; 2001. p. 2629–73.
44. Ryckman BJ, Rainish BL, Chase MC, Borton JA, Nelson JA, Jarvis MA, et al. Characterization of the human cytomegalovirus gH/gL/UL128-131 complex that mediates entry into epithelial and endothelial cells. *J Virol*. 2008 Jan 1;82(1):60–70.
45. Li L, Nelson JA, Britt WJ. Glycoprotein H-related complexes of human cytomegalovirus: identification of a third protein in the gCIII complex. *J Virol*. 1997 Apr 1;71(4):3090–7.
46. Huber MT, Compton T. Characterization of a novel third member of the human cytomegalovirus glycoprotein H-glycoprotein L complex. *undefined*. 1997;
47. Saffert RT, Kalejta RF. Inactivating a cellular intrinsic immune defense mediated by Daxx is the mechanism through which the human cytomegalovirus pp71 protein stimulates viral immediate-early gene expression. *J Virol*. 2006 Apr 15;80(8):3863–71.
48. Kalejta RF. Tegument Proteins of Human Cytomegalovirus. *Microbiol Mol Biol Rev*.

- 2008 Jun 1;72(2):249–65.
49. Ogawa-Goto K, Tanaka K, Gibson W, Moriishi E, Miura Y, Kurata T, et al. Microtubule network facilitates nuclear targeting of human cytomegalovirus capsid. *J Virol.* 2003 Aug 1;77(15):8541–7.
 50. Stenberg RM, Witte PR, Stinski MF. Multiple spliced and unspliced transcripts from human cytomegalovirus immediate-early region 2 and evidence for a common initiation site within immediate-early region 1. *J Virol.* 1985 Dec 1;56(3):665–75.
 51. Meier JL, Stinski MF. Major Immediate-Early Enhancer and Its Gene Products. In: Reddehase M, Lemmermann N, editors. *Cytomegaloviruses: From Molecular Pathogenesis to Intervention.* Caister Academic Press; 2013. p. 152–73.
 52. Marchini A, Liu H, Zhu H. Human Cytomegalovirus with IE-2 (UL122) Deleted Fails To Express Early Lytic Genes. *J Virol.* 2001 Feb 15;75(4):1870–8.
 53. White EA, Clark CL, Sanchez V, Spector DH. Small internal deletions in the human cytomegalovirus IE2 gene result in nonviable recombinant viruses with differential defects in viral gene expression. *J Virol.* 2004 Feb 15;78(4):1817–30.
 54. White EA, Rosario CJ Del, Sanders RL, Spector DH. The IE2 60-Kilodalton and 40-Kilodalton Proteins Are Dispensable for Human Cytomegalovirus Replication but Are Required for Efficient Delayed Early and Late Gene Expression and Production of Infectious Virus. *J Virol.* 2007 Mar 15;81(6):2573–83.
 55. Kang H, Kim ET, Lee H-R, Park J-J, Go YY, Choi CY, et al. Inhibition of SUMO-independent PML oligomerization by the human cytomegalovirus IE1 protein. *J Gen Virol.* 2006 Aug 1;87(8):2181–90.
 56. Kim Y-E, Lee J-H, Kim ET, Shin HJ, Gu SY, Seol HS, et al. Human Cytomegalovirus Infection Causes Degradation of Sp100 Proteins That Suppress Viral Gene Expression. *J Virol.* 2011 Nov 15;85(22):11928–37.
 57. Strang BL. Viral and cellular subnuclear structures in human cytomegalovirus-infected cells. *J Gen Virol.* 2015 Feb 1;96(2):239–53.
 58. Çam M, Handke W, Picard-Maureau M, Brune W. Cytomegaloviruses inhibit Bak- and Bax-mediated apoptosis with two separate viral proteins. *Cell Death Differ.* 2010 Apr 9;17(4):655–65.
 59. Brune W, Andoniou C. Die Another Day: Inhibition of Cell Death Pathways by Cytomegalovirus. *Viruses.* 2017 Sep 2;9(9):249.
 60. Marshall EE, Bierle CJ, Brune W, Geballe AP. Essential Role for either TRS1 or IRS1 in Human Cytomegalovirus Replication. *J Virol.* 2009 May 1;83(9):4112–20.
 61. Pari GS. Nuts and Bolts of Human Cytomegalovirus Lytic DNA Replication. In Springer, Berlin, Heidelberg; 2008. p. 153–66.
 62. Lehman IR, Boehmer PE. Replication of herpes simplex virus DNA. Vol. 274, *Journal of Biological Chemistry.* American Society for Biochemistry and Molecular Biology; 1999. p. 28059–62.
 63. Ahn JH, Jang WJ, Hayward GS. The human cytomegalovirus IE2 and UL112-113 proteins accumulate in viral DNA replication compartments that initiate from the periphery of promyelocytic leukemia protein-associated nuclear bodies (PODs or ND10). *J Virol.* 1999 Dec 1;73(12):10458–71.

64. Penfold MET, Mocarski ES. Formation of Cytomegalovirus DNA Replication Compartments Defined by Localization of Viral Proteins and DNA Synthesis. *Virology*. 1997 Dec 8;239(1):46–61.
65. Zarrouk K, Piret J, Boivin G. Herpesvirus DNA polymerases: Structures, functions and inhibitors. *Virus Research*. 2017.
66. Woon H-G, Scott GM, Yiu KL, Miles DH, Rawlinson WD. Identification of putative functional motifs in viral proteins essential for human cytomegalovirus DNA replication. *Virus Genes*. 2008 Oct 10;37(2):193–202.
67. Appleton BA, Loregian A, Filman DJ, Coen DM, Hogle JM. The Cytomegalovirus DNA Polymerase Subunit UL44 Forms a C Clamp-Shaped Dimer. *Mol Cell*. 2004 Jul 23;15(2):233–44.
68. Sinigalia E, Alvisi G, Mercorelli B, Coen DM, Pari GS, Jans DA, et al. Role of Homodimerization of Human Cytomegalovirus DNA Polymerase Accessory Protein UL44 in Origin-Dependent DNA Replication in Cells. *J Virol*. 2008 Dec 15;82(24):12574–9.
69. Strang BL, Sinigalia E, Silva LA, Coen DM, Loregian A. Analysis of the Association of the Human Cytomegalovirus DNA Polymerase Subunit UL44 with the Viral DNA Replication Factor UL84. *J Virol*. 2009 Aug 1;83(15):7581–9.
70. Strang BL, Coen DM. Interaction of the human cytomegalovirus uracil DNA glycosylase UL114 with the viral DNA polymerase catalytic subunit UL54. *J Gen Virol*. 2010 Aug 1;91(8):2029–33.
71. Prichard MN, Lawlor H, Duke GM, Mo C, Wang Z, Dixon M, et al. Human cytomegalovirus uracil DNA glycosylase associates with ppUL44 and accelerates the accumulation of viral DNA. *Virol J*. 2005 Jul 15;2(1):55.
72. Prichard MN, Duke GM, Mocarski ES. Human cytomegalovirus uracil DNA glycosylase is required for the normal temporal regulation of both DNA synthesis and viral replication. *J Virol*. 1996 May 1;70(5):3018–25.
73. Strang BL, Boulant S, Chang L, Knipe DM, Kirchhausen T, Coen DM. Human cytomegalovirus UL44 concentrates at the periphery of replication compartments, the site of viral DNA synthesis. *J Virol*. 2012 Feb 15;86(4):2089–95.
74. Grady LM, Szczepaniak R, Murelli RP, Masaoka T, Le Grice SFJ, Wright DL, et al. The Exonuclease Activity of Herpes Simplex Virus 1 UL12 Is Required for Production of Viral DNA That Can Be Packaged To Produce Infectious Virus. *J Virol*. 2017;91(23).
75. Bujnicki JM, Rychlewski L. The Herpesvirus Alkaline Exonuclease Belongs to the Restriction Endonuclease PD-(D/E)XK Superfamily: Insight from Molecular Modeling and Phylogenetic Analysis. *Virus Genes*. 2001;22(2):219–30.
76. Weller SK, Coen DM. Herpes simplex viruses: mechanisms of DNA replication. *Cold Spring Harb Perspect Biol*. 2012 Sep 1;4(9):a013011.
77. Severini A, Scraba DG, Tyrrell DL. Branched structures in the intracellular DNA of herpes simplex virus type 1. *J Virol*. 1996 May 1;70(5):3169–75.
78. Wilkinson D, Weller S. The Role of DNA Recombination in Herpes Simplex Virus DNA Replication. *IUBMB Life (International Union Biochem Mol Biol Life)*. 2003

- Aug 1;55(8):451–8.
79. Smith S, Reuven N, Mohni KN, Schumacher AJ, Weller SK. Structure of the herpes simplex virus 1 genome: manipulation of nicks and gaps can abrogate infectivity and alter the cellular DNA damage response. *J Virol*. 2014 Sep 1;88(17):10146–56.
 80. Reuven NB, Weller SK. Herpes simplex virus type 1 single-strand DNA binding protein ICP8 enhances the nuclease activity of the UL12 alkaline nuclease by increasing its processivity. *J Virol*. 2005 Jul 1;79(14):9356–8.
 81. Reuven NB, Staire AE, Myers RS, Weller SK. The herpes simplex virus type 1 alkaline nuclease and single-stranded DNA binding protein mediate strand exchange in vitro. *J Virol*. 2003 Jul 1;77(13):7425–33.
 82. Porter IM, Stow ND. Virus particles produced by the herpes simplex virus type 1 alkaline nuclease null mutant ambUL12 contain abnormal genomes. *J Gen Virol*. 2004 Mar 1;85(3):583–91.
 83. Glaunsinger B, Ganem D. Lytic KSHV infection inhibits host gene expression by accelerating global mRNA turnover. *Mol Cell*. 2004 Mar 12;13(5):713–23.
 84. Glaunsinger B, Ganem D. Highly selective escape from KSHV-mediated host mRNA shutoff and its implications for viral pathogenesis. *J Exp Med*. 2004 Aug 2;200(3):391–8.
 85. Rowe M, Glaunsinger B, van Leeuwen D, Zuo J, Sweetman D, Ganem D, et al. Host shutoff during productive Epstein-Barr virus infection is mediated by BGLF5 and may contribute to immune evasion. *Proc Natl Acad Sci U S A*. 2007 Feb 27;104(9):3366–71.
 86. Everly DN, Feng P, Mian IS, Read GS. mRNA degradation by the virion host shutoff (Vhs) protein of herpes simplex virus: genetic and biochemical evidence that Vhs is a nuclease. *J Virol*. 2002 Sep 1;76(17):8560–71.
 87. Dahlroth SL, Gurmu D, Haas J, Erlandsen H, Nordlund P. Crystal structure of the shutoff and exonuclease protein from the oncogenic Kaposi's sarcoma-associated herpesvirus. *FEBS J*. 2009 Nov 1;276(22):6636–45.
 88. Glaunsinger B, Chavez L, Ganem D. The exonuclease and host shutoff functions of the SOX protein of Kaposi's sarcoma-associated herpesvirus are genetically separable. *J Virol*. 2005 Jun 15;79(12):7396–401.
 89. Uppal T, Meyer D, Agrawal A, Verma SC. The DNase Activity of Kaposi's Sarcoma-Associated Herpesvirus SOX Protein Serves an Important Role in Viral Genome Processing during Lytic Replication. *J Virol*. 2019 Apr 15;93(8):e01983-18.
 90. Kuchta AL, Parikh H, Zhu Y, Kellogg GE, Parris DS, Mcvov MA. Structural modelling and mutagenesis of human cytomegalovirus alkaline nuclease UL98. *J Gen Virol*. 2012 Jan 1;93(1):130–8.
 91. Sheaffer AK, Weinheimer SP, Tenney DJ. The human cytomegalovirus UL98 gene encodes the conserved herpesvirus alkaline nuclease. *J Gen Virol*. 1997 Nov 1;78(11):2953–61.
 92. Yu D, Silva MC, Shenk T. Functional map of human cytomegalovirus AD169 defined by global mutational analysis. *Proc Natl Acad Sci U S A*. 2003 Oct 14;100(21):12396–401.

93. Dunn W, Chou C, Li H, Hai R, Patterson D, Stolc V, et al. Functional profiling of a human cytomegalovirus genome. *Proc Natl Acad Sci.* 2003 Nov 25;100(24):14223–8.
94. Ligat G, Cazal R, Hantz S, Alain S. The human cytomegalovirus terminase complex as an antiviral target: a close-up view. *FEMS Microbiol Rev.* 2018 Mar 1;42(2):137–45.
95. McVoy MA, Adler SP. Human cytomegalovirus DNA replicates after early circularization by concatemer formation, and inversion occurs within the concatemer. *J Virol.* 1994 Feb;68(2):1040–51.
96. Hwang J-S, Bogner E. ATPase activity of the terminase subunit pUL56 of human cytomegalovirus. *J Biol Chem.* 2002 Mar 1;277(9):6943–8.
97. Bogner E, Reschke M, Reis B, Mockenhaupt T, Radsak K. Identification of the gene product encoded by ORF UL56 of the human cytomegalovirus genome. *Virology.* 1993 Sep;196(1):290–3.
98. Borst EM, Wagner K, Binz A, Sodeik B, Messerle M. The essential human cytomegalovirus gene UL52 is required for cleavage-packaging of the viral genome. *J Virol.* 2008 Mar 1;82(5):2065–78.
99. Bogner E, Radsak K, Stinski MF. The gene product of human cytomegalovirus open reading frame UL56 binds the pac motif and has specific nuclease activity. *J Virol.* 1998 Mar;72(3):2259–64.
100. Neuber S, Wagner K, Goldner T, Lischka P, Steinbrueck L, Messerle M, et al. Mutual Interplay between the Human Cytomegalovirus Terminase Subunits pUL51, pUL56, and pUL89 Promotes Terminase Complex Formation. *J Virol.* 2017 Jun 15;91(12):e02384-16.
101. Krosky PM, Underwood MR, Turk SR, Feng KW, Jain RK, Ptak RG, et al. Resistance of human cytomegalovirus to benzimidazole ribonucleosides maps to two open reading frames: UL89 and UL56. *J Virol.* 1998 Jun;72(6):4721–8.
102. Dittmer A, Drach JC, Townsend LB, Fischer A, Bogner E. Interaction of the putative human cytomegalovirus portal protein pUL104 with the large terminase subunit pUL56 and its inhibition by benzimidazole-D-ribonucleosides. *J Virol.* 2005 Dec 1;79(23):14660–7.
103. Scheffczik H, Savva CGW, Holzenburg A, Kolesnikova L, Bogner E. The terminase subunits pUL56 and pUL89 of human cytomegalovirus are DNA-metabolizing proteins with toroidal structure. *Nucleic Acids Res.* 2002 Apr 1;30(7):1695–703.
104. Köppen-Rung P, Dittmer A, Bogner E. Intracellular Distribution of Capsid-Associated pUL77 of Human Cytomegalovirus and Interactions with Packaging Proteins and pUL93. Sandri-Goldin RM, editor. *J Virol.* 2016 Jul 1;90(13):5876–85.
105. DeRussy BM, Tandon R. Human Cytomegalovirus pUL93 Is Required for Viral Genome Cleavage and Packaging. Sandri-Goldin RM, editor. *J Virol.* 2015 Dec 1;89(23):12221–5.
106. DeRussy BM, Boland MT, Tandon R. Human Cytomegalovirus pUL93 Links Nucleocapsid Maturation and Nuclear Egress. Sandri-Goldin RM, editor. *J Virol.* 2016 Aug 15;90(16):7109–17.
107. Tandon R, Mocarski ES, Conway JF. The A, B, Cs of herpesvirus capsids. *Viruses.* 2015 Feb 26;7(3):899–914.

108. Jean Beltran PM, Cristea IM. The life cycle and pathogenesis of human cytomegalovirus infection: lessons from proteomics. *Expert Rev Proteomics*. 2014 Dec 18;11(6):697–711.
109. Michel D, Chevillotte M, Mertens T. Antiviral Therapy, Drug Resistance and Computed Resistance Profiling. In: Reddehase MJ, Lemmermann NA, editors. *Cytomegaloviruses: From Molecular Pathogenesis to Intervention*. Caister Academic Press; 2013. p. 402–23.
110. Matthews T, Boehme R. Antiviral Activity and Mechanism of Action of Ganciclovir. *Clin Infect Dis*. 1988 Jul 1;10(Supplement_3):S490–4.
111. Crumpacker CS. Antiviral Therapy. In: Knipe DM, Howley PM, editors. *Fields Virology*. 4th ed. Philadelphia: Lippincott Williams & Wilkins; 2001. p. 393–433.
112. Jacobson MA. Current Management of Cytomegalovirus Disease in Patients with AIDS. *AIDS Res Hum Retroviruses*. 1994 Aug 16;10(8).
113. Kimberlin DW, Jester PM, Sánchez PJ, Ahmed A, Arav-Boger R, Michaels MG, et al. Valganciclovir for Symptomatic Congenital Cytomegalovirus Disease. *N Engl J Med*. 2015 Mar 5;372(10):933–43.
114. Green ML, Leisenring W, Xie H, Mast TC, Cui Y, Sandmaier BM, et al. Cytomegalovirus viral load and mortality after haemopoietic stem cell transplantation in the era of pre-emptive therapy: a retrospective cohort study. *Lancet Haematol*. 2016 Mar;3(3):e119-27.
115. Littler E, Stuart AD, Chee MS. Human cytomegalovirus UL97 open reading frame encodes a protein that phosphorylates the antiviral nucleoside analogue ganciclovir. *Nature*. 1992 Jul;358(6382):160–2.
116. Gentry BG, Gentry SN, Jackson TL, Zemlicka J, Drach JC. Phosphorylation of antiviral and endogenous nucleotides to di- and triphosphates by guanosine monophosphate kinase. *Biochem Pharmacol*. 2011 Jan 1;81(1):43–9.
117. Biron KK, Stanat SC, Sorrell JB, Fyfe JA, Keller PM, Lambe CU, et al. Metabolic activation of the nucleoside analog 9-[(2-hydroxy-1-(hydroxymethyl)ethoxy)methyl]guanine in human diploid fibroblasts infected with human cytomegalovirus. *Proc Natl Acad Sci U S A*. 1985 Apr 1;82(8):2473–7.
118. Jung D, Dorr A. Single-Dose Pharmacokinetics of Valganciclovir in HIV- and CMV-Seropositive Subjects. *J Clin Pharmacol*. 1999 Aug 1;39(8):800–4.
119. Kimberlin DW, Acosta EP, Sánchez PJ, Sood S, Agrawal V, Homans J, et al. Pharmacokinetic and Pharmacodynamic Assessment of Oral Valganciclovir in the Treatment of Symptomatic Congenital Cytomegalovirus Disease. *J Infect Dis*. 2008 Mar 15;197(6):836–45.
120. Perrottet N, Decosterd LA, Meylan P, Pascual M, Biollaz J, Buclin T. Valganciclovir in Adult Solid Organ Transplant Recipients. *Clin Pharmacokinet*. 2009 Jun;48(6):399–418.
121. Lurain NS, Chou S. Antiviral drug resistance of human cytomegalovirus. Vol. 23, *Clinical Microbiology Reviews*. American Society for Microbiology Journals; 2010. p. 689–712.
122. Chou S. Rapid In Vitro Evolution of Human Cytomegalovirus UL56 Mutations That

- Confer Letermovir Resistance. *Antimicrob Agents Chemother.* 2015 Oct 1;59(10):6588–93.
123. Elion GB, Furman PA, Fyfe JA, de Miranda P, Beauchamp L, Schaeffer HJ. Selectivity of action of an antiherpetic agent, 9-(2-hydroxyethoxymethyl) guanine. *Proc Natl Acad Sci U S A.* 1977 Dec 1;74(12):5716–20.
124. Schaeffer HJ, Beauchamp L, de Miranda P, Elion GB, Bauer DJ, Collins P. 9-(2-Hydroxyethoxymethyl)guanine activity against viruses of the herpes group. *Nature.* 1978 Apr;272(5654):583–5.
125. Talarico CL, Burnette TC, Miller WH, Smith SL, Davis MG, Stanat SC, et al. Acyclovir is phosphorylated by the human cytomegalovirus UL97 protein. *Antimicrob Agents Chemother.* 1999 Aug 1;43(8):1941–6.
126. Lowance D, Neumayer H-H, Legendre CM, Squifflet J-P, Kovarik J, Brennan PJ, et al. Valacyclovir for the Prevention of Cytomegalovirus Disease after Renal Transplantation. *N Engl J Med.* 1999 May 13;340(19):1462–70.
127. Cihlar T, Chen MS. Identification of enzymes catalyzing two-step phosphorylation of cidofovir and the effect of cytomegalovirus infection on their activities in host cells. *Mol Pharmacol.* 1996;50(6).
128. Xiong X, Smith JL, Kim C, Huang E shang, Chen MS. Kinetic analysis of the interaction of cidofovir diphosphate with human cytomegalovirus DNA polymerase. *Biochem Pharmacol.* 1996 Jun 14;51(11):1563–7.
129. Xiong X, Smith JL, Chen MS. Effect of incorporation of cidofovir into DNA by human cytomegalovirus DNA polymerase on DNA elongation. *Antimicrob Agents Chemother.* 1997 Mar 1;41(3):594–9.
130. Chemaly RF, Hill JA, Voigt S, Peggs KS. In vitro comparison of currently available and investigational antiviral agents against pathogenic human double-stranded DNA viruses: A systematic literature review. Vol. 163, *Antiviral Research.* Elsevier; 2019. p. 50–8.
131. Lalezari JP, Stagg RJ, Kuppermann BD, Holland GN, Kramer F, Ives D V., et al. Intravenous cidofovir for peripheral cytomegalovirus retinitis in patients with AIDS: A randomized, controlled trial. *Ann Intern Med.* 1997 Feb 15;126(4):257–63.
132. De Clercq E, Field HJ. Antiviral prodrugs - the development of successful prodrug strategies for antiviral chemotherapy. *Br J Pharmacol.* 2006 Jan 1;147(1):1–11.
133. De Clercq E. Selective Anti-Herpesvirus Agents. *Antivir Chem Chemother.* 2013 Jun 1;23(3):93–101.
134. Hostetler KY, Rybak RJ, Beadle JR, Gardner MF, Aldern KA, Wright KN, et al. *In vitro* and *in vivo* Activity of 1-O-Hexadecylpropane-Diol-3-Phospho-Ganciclovir and 1-O-Hexadecylpropanediol-3-Phospho-Penciclovir in Cytomegalovirus and Herpes Simplex Virus Infections. *Antivir Chem Chemother.* 2001 Feb 22;12(1):61–70.
135. Hostetler KY. Alkoxyalkyl prodrugs of acyclic nucleoside phosphonates enhance oral antiviral activity and reduce toxicity: Current state of the art. *Antiviral Res.* 2009 May 1;82(2):A84–98.
136. Williams-Aziz SL, Hartline CB, Harden EA, Daily SL, Prichard MN, Kushner NL, et al. Comparative activities of lipid esters of cidofovir and cyclic cidofovir against

- replication of herpesviruses in vitro. *Antimicrob Agents Chemother.* 2005 Sep 1;49(9):3724–33.
137. Kern ER, Collins DJ, Wan WB, Beadle JR, Hostetler KY, Quenelle DC. Oral treatment of murine cytomegalovirus infections with ether lipid esters of cidofovir. *Antimicrob Agents Chemother.* 2004 Sep 1;48(9):3516–22.
 138. Bidanset DJ, Beadle JR, Wan WB, Hostetler KY, Kern ER. Oral Activity of Ether Lipid Ester Prodrugs of Cidofovir against Experimental Human Cytomegalovirus Infection. *J Infect Dis.* 2004 Aug 1;190(3):499–503.
 139. James SH, Price NB, Hartline CB, Lanier ER, Prichard MN. Selection and Recombinant Phenotyping of a Novel CMX001 and Cidofovir Resistance Mutation in Human Cytomegalovirus. *Antimicrob Agents Chemother.* 2013 Jul 1;57(7):3321–5.
 140. Marty FM, Winston DJ, Chemaly RF, Boeckh MJ, Mullane KM, Shore TB, et al. Brincidofovir for Prevention of Cytomegalovirus (CMV) after Allogeneic Hematopoietic Cell Transplantation (HCT) in CMV-Seropositive Patients: A Randomized, Double-Blind, Placebo-Controlled, Parallel-Group Phase 3 Trial. *Biol Blood Marrow Transplant.* 2016;22(3):S23.
 141. Marty FM, Winston DJ, Rowley SD, Vance E, Papanicolaou GA, Mullane KM, et al. CMX001 to Prevent Cytomegalovirus Disease in Hematopoietic-Cell Transplantation. *N Engl J Med.* 2013 Sep 26;369(13):1227–36.
 142. Crumpacker CS. Mechanism of action of foscarnet against viral polymerases. *Am J Med.* 1992 Feb;92(2 SUPPL. 1):S3–7.
 143. Walmsley SL, Chew E, Read SE, Vellend H, Salit I, Rachlis A, et al. Treatment of Cytomegalovirus Retinitis with Trisodium Phosphonoformate Hexahydrate (Foscarnet). *J Infect Dis.* 1988 Mar 1;157(3):569–72.
 144. Torres-Madriz G, Boucher HW. Immunocompromised Hosts: Perspectives in the Treatment and Prophylaxis of Cytomegalovirus Disease in Solid-Organ Transplant Recipients. *Clin Infect Dis.* 2008 Sep 1;47(5):702–11.
 145. Chou S, Marousek G, Parenti DM, Gordon SM, LaVoy AG, Ross JG, et al. Mutation in Region III of the DNA Polymerase Gene Conferring Foscarnet Resistance in Cytomegalovirus Isolates from 3 Subjects Receiving Prolonged Antiviral Therapy. *J Infect Dis.* 1998 Aug 1;178(2):526–30.
 146. de Smet MD, Meenken CJ, van den Horn GJ. Fomivirsen - a phosphorothioate oligonucleotide for the treatment of CMV retinitis. *Ocul Immunol Inflamm.* 1999 Dec;7(3–4):189–98.
 147. Azad RF, Driver VB, Tanaka K, Crooke RM, Anderson KP. Antiviral activity of a phosphorothioate oligonucleotide complementary to RNA of the human cytomegalovirus major immediate-early region. *Antimicrob Agents Chemother.* 1993 Sep 1;37(9):1945–54.
 148. Geary RS, Henry SP, Grillone LR. Fomivirsen. *Clin Pharmacokinet.* 2002;41(4):255–60.
 149. Prichard MN, Gao N, Jairath S, Mulamba G, Krosky P, Coen DM, et al. A Recombinant Human Cytomegalovirus with a Large Deletion in UL97 Has a Severe Replication Deficiency. *J Virol.* 1999;73(7).

150. Wolf DG, Courcelle CT, Prichard MN, Mocarski ES. Distinct and separate roles for herpesvirus-conserved UL97 kinase in cytomegalovirus DNA synthesis and encapsidation. *Proc Natl Acad Sci*. 2001 Feb 13;98(4):1895–900.
151. Baek M-C, Krosky PM, Pearson A, Coen DM. Phosphorylation of the RNA polymerase II carboxyl-terminal domain in human cytomegalovirus-infected cells and in vitro by the viral UL97 protein kinase. *Virology*. 2004 Jun 20;324(1):184–93.
152. Iwahori S, Umaña AC, VanDeusen HR, Kalejta RF. Human cytomegalovirus-encoded viral cyclin-dependent kinase (v-CDK) UL97 phosphorylates and inactivates the retinoblastoma protein-related p107 and p130 proteins. *J Biol Chem*. 2017 Apr 21;292(16):6583–99.
153. Milbradt J, Weibel R, Auerochs S, Sticht H, Marschall M. Novel Mode of Phosphorylation-triggered Reorganization of the Nuclear Lamina during Nuclear Egress of Human Cytomegalovirus. *J Biol Chem*. 2010 Apr 30;285(18):13979–89.
154. Biron KK, Harvey RJ, Chamberlain SC, Good SS, Smith AA, Davis MG, et al. Potent and Selective Inhibition of Human Cytomegalovirus Replication by 1263W94, a Benzimidazole L-Riboside with a Unique Mode of Action. *Antimicrob Agents Chemother*. 2002 Aug 1;46(8):2365–72.
155. Koszalka GW, Johnson NW, Good SS, Boyd L, Chamberlain SC, Townsend LB, et al. Preclinical and Toxicology Studies of 1263W94, a Potent and Selective Inhibitor of Human Cytomegalovirus Replication. *Antimicrob Agents Chemother*. 2002 Aug 1;46(8):2373–80.
156. Lalezari JP, Aberg JA, Wang LH, Wire MB, Miner R, Snowden W, et al. Phase I dose escalation trial evaluating the pharmacokinetics, anti-human cytomegalovirus (HCMV) activity, and safety of 1263W94 in human immunodeficiency virus-infected men with asymptomatic HCMV shedding. *Antimicrob Agents Chemother*. 2002 Sep;46(9):2969–76.
157. Ma JD, Nafziger AN, Villano SA, Gaedigk A, Bertino JS. Maribavir pharmacokinetics and the effects of multiple-dose maribavir on cytochrome P450 (CYP) 1A2, CYP 2C9, CYP 2C19, CYP 2D6, CYP 3A, N-acetyltransferase-2, and xanthine oxidase activities in healthy adults. *Antimicrob Agents Chemother*. 2006 Apr 1;50(4):1130–5.
158. Marty FM, Ljungman P, Papanicolaou GA, Winston DJ, Chemaly RF, Strasfeld L, et al. Maribavir prophylaxis for prevention of cytomegalovirus disease in recipients of allogeneic stem-cell transplants: a phase 3, double-blind, placebo-controlled, randomised trial. *Lancet Infect Dis*. 2011 Apr 1;11(4):284–92.
159. Chou S, Marousek GI. Maribavir Antagonizes the Antiviral Action of Ganciclovir on Human Cytomegalovirus. *Antimicrob Agents Chemother*. 2006 Oct 1;50(10):3470–2.
160. Evers DL, Komazin G, Shin D, Hwang DD, Townsend LB, Drach JC. Interactions among antiviral drugs acting late in the replication cycle of human cytomegalovirus. *Antiviral Res*. 2002 Oct 1;56(1):61–72.
161. Chou S, Ercolani RJ, Marousek G, Bowlin TL. Cytomegalovirus UL97 Kinase Catalytic Domain Mutations That Confer Multidrug Resistance. *Antimicrob Agents Chemother*. 2013 Jul;57(7):3375–9.
162. Reitsma JM, Savaryn JP, Faust K, Sato H, Halligan BD, Terhune SS. Antiviral Inhibition Targeting the HCMV Kinase pUL97 Requires pUL27-Dependent

- Degradation of Tip60 Acetyltransferase and Cell-Cycle Arrest. *Cell Host Microbe*. 2011 Feb 17;9(2):103–14.
163. Prichard MN, Quenelle DC, Bidanset DJ, Komazin G, Chou S, Drach JC, et al. Human cytomegalovirus UL27 is not required for viral replication in human tissue implanted in SCID mice. *Virology*. 2006 Mar 29;3(1):18.
 164. Lischka P, Hewlett G, Wunberg T, Baumeister J, Paulsen D, Goldner T, et al. In vitro and in vivo activities of the novel anticytomegalovirus compound AIC246. *Antimicrob Agents Chemother*. 2010 Mar 1;54(3):1290–7.
 165. Lischka P, Hewlett G, Wunberg T, Baumeister J, Paulsen D, Goldner T, et al. In vitro and in vivo activities of the novel anticytomegalovirus compound AIC246. *Antimicrob Agents Chemother*. 2010 Mar 1;54(3):1290–7.
 166. Chemaly RF, Ullmann AJ, Stoelben S, Richard MP, Bornhäuser M, Groth C, et al. Letermovir for Cytomegalovirus Prophylaxis in Hematopoietic-Cell Transplantation. *N Engl J Med*. 2014 May 8;370(19):1781–9.
 167. Goldner T, Hewlett G, Ettischer N, Ruebsamen-Schaeff H, Zimmermann H, Lischka P. The novel anticytomegalovirus compound AIC246 (Letermovir) inhibits human cytomegalovirus replication through a specific antiviral mechanism that involves the viral terminase. *J Virol*. 2011 Oct 15;85(20):10884–93.
 168. Goldner T, Hempel C, Ruebsamen-Schaeff H, Zimmermann H, Lischka P. Geno- and phenotypic characterization of human cytomegalovirus mutants selected in vitro after letermovir (AIC246) exposure. *Antimicrob Agents Chemother*. 2014 Jan 1;58(1):610–3.
 169. Chou S. Comparison of Cytomegalovirus Terminase Gene Mutations Selected after Exposure to Three Distinct Inhibitor Compounds. *Antimicrob Agents Chemother*. 2017 Nov 1;61(11):e01325-17.
 170. Chou S. A third component of the human cytomegalovirus terminase complex is involved in letermovir resistance. *Antiviral Res*. 2017 Dec 1;148:1–4.
 171. Jung S, Michel M, Stamminger T, Michel D. Fast breakthrough of resistant cytomegalovirus during secondary letermovir prophylaxis in a hematopoietic stem cell transplant recipient. *BMC Infect Dis*. 2019 Dec 8;19(1):388.
 172. Komatsu TE, Hodowanec AC, Colberg-Poley AM, Pikis A, Singer ME, O’Rear JJ, et al. In-depth genomic analyses identified novel letermovir resistance-associated substitutions in the cytomegalovirus UL56 and UL89 gene products. *Antiviral Res*. 2019 Sep;169:104549.
 173. Townsend LB, Devivar R V., Turk SR, Nassiri MR, Drach JC. Design, Synthesis, and Antiviral Activity of Certain 2,5,6-Trihalo-1-(β -D-ribofuranosyl)benzimidazoles. *J Med Chem*. 1995 Sep;38(20):4098–105.
 174. Underwood MR, Harvey RJ, Stanat SC, Hemphill ML, Miller T, Drach JC, et al. Inhibition of human cytomegalovirus DNA maturation by a benzimidazole ribonucleoside is mediated through the UL89 gene product. *J Virol*. 1998 Jan;72(1):717–25.
 175. McVoy MA, Nixon DE. Impact of 2-bromo-5,6-dichloro-1- β -D-ribofuranosyl benzimidazole riboside and inhibitors of DNA, RNA, and protein synthesis on human cytomegalovirus genome maturation. *J Virol*. 2005 Sep 1;79(17):11115–27.

176. Lorenzi PL, Landowski CP, Brancale A, Song X, Townsend LB, Drach JC, et al. N-methylpurine DNA glycosylase and 8-oxoguanine dna glycosylase metabolize the antiviral nucleoside 2-bromo-5,6-dichloro-1-(beta-D-ribofuranosyl)benzimidazole. *Drug Metab Dispos*. 2006 Jun 24;34(6):1070–7.
177. Underwood MR, Ferris RG, Sellese DW, Davis MG, Drach JC, Townsend LB, et al. Mechanism of action of the ribopyranoside benzimidazole GW275175X against human cytomegalovirus. *Antimicrob Agents Chemother*. 2004 May 1;48(5):1647–51.
178. Williams SL, Hartline CB, Kushner NL, Harden EA, Bidanset DJ, Drach JC, et al. In vitro activities of benzimidazole D- and L-ribonucleosides against herpesviruses. *Antimicrob Agents Chemother*. 2003 Jul 1;47(7):2186–92.
179. Kern ER, Hartline CB, Rybak RJ, Drach JC, Townsend LB, Biron KK, et al. Activities of benzimidazole D- and L-ribonucleosides in animal models of cytomegalovirus infections. *Antimicrob Agents Chemother*. 2004 May 1;48(5):1749–55.
180. Reefschlaeger J, Bender W, Hallenberger S, Weber O, Eckenberg P, Goldmann S, et al. Novel non-nucleoside inhibitors of cytomegaloviruses (BAY 38-4766): in vitro and in vivo antiviral activity and mechanism of action. *J Antimicrob Chemother*. 2001 Dec 1;48(6):757–67.
181. McSharry JJ, McDonough A, Olson B, Hallenberger S, Reefschlaeger J, Bender W, et al. Susceptibilities of human cytomegalovirus clinical isolates to BAY38-4766, BAY43-9695, and ganciclovir. *Antimicrob Agents Chemother*. 2001 Oct 1;45(10):2925–7.
182. Buerger I, Reefschlaeger J, Bender W, Eckenberg P, Popp A, Weber O, et al. A Novel Nonnucleoside Inhibitor Specifically Targets Cytomegalovirus DNA Maturation via the UL89 and UL56 Gene Products. *J Virol*. 2002 Oct 1;75(19):9077–86.
183. Alam Z, Al-Mahdi Z, Zhu Y, McKee Z, Parris DS, Parikh HI, et al. Anti-cytomegalovirus activity of the anthraquinone atanyl blue PRL. *Antiviral Res*. 2015 Feb;114:86–95.
184. Flamand L, Lautenschlager I, Krueger GRF, Ablashi D V., Pritchett JC, Naesens L, et al. Treating HHV-6 Infections: The Laboratory Efficacy and Clinical Use of Anti-HHV-6 Agents. *Hum Herpesviruses HHV-6A, HHV-6B HHV-7*. 2014 Jan 1;311–31.
185. Krippendorff B-F, Lienau P, Reichel A, Huisinga W. Optimizing Classification of Drug-Drug Interaction Potential for CYP450 Isoenzyme Inhibition Assays in Early Drug Discovery. *J Biomol Screen*. 2007 Feb;12(1):92–9.
186. O'Connor CM, Murphy EA. A myeloid progenitor cell line capable of supporting human cytomegalovirus latency and reactivation, resulting in infectious progeny. *J Virol*. 2012 Sep;86(18):9854–65.
187. Hughes JP, Rees S, Kalindjian SB, Philpott KL. Principles of early drug discovery. *Br J Pharmacol*. 2011 Mar;162(6):1239–49.
188. Timoshenko O, Al-Ali A, Martin BAB, Sweet C. Role of mutations identified in ORFs M56 (terminase), M70 (primase) and M98 (endonuclease) in the temperature-sensitive phenotype of murine cytomegalovirus mutant tsm5. *Virology*. 2009 Sep 15;392(1):114–22.
189. Lipinski CA, Lombardo F, Dominy BW, Feeney PJ. Experimental and computational approaches to estimate solubility and permeability in drug discovery and development

- settings. *Adv Drug Deliv Rev.* 2001 Mar 1;46(1-3):3-26.
190. Phillips SL, Cygnar D, Thomas A, Bresnahan WA. Interaction between the Human Cytomegalovirus Tegument Proteins UL94 and UL99 Is Essential for Virus Replication. *J Virol.* 2012;86(18):9995.
 191. Silva MC, Yu Q-C, Enquist L, Shenk T. Human Cytomegalovirus UL99-Encoded pp28 Is Required for the Cytoplasmic Envelopment of Tegument-Associated Capsids. *J Virol.* 2003 Oct 1;77(19):10594-605.
 192. Banaszynski LA, Chen L chun, Maynard-Smith LA, Ooi AGL, Wandless TJ. A Rapid, Reversible, and Tunable Method to Regulate Protein Function in Living Cells Using Synthetic Small Molecules. *Cell.* 2006 Sep 8;126(5):995-1004.
 193. Adam BL, Jervey TY, Kohler CP, Wright GL, Nelson JA, Stenberg RM. The human cytomegalovirus UL98 gene transcription unit overlaps with the pp28 true late gene (UL99) and encodes a 58-kilodalton early protein. *J Virol.* 1995 Sep 1;69(9):5304-10.
 194. Tischer BK, Smith GA, Osterrieder N. En passant mutagenesis: a two step markerless red recombination system. *Methods Mol Biol.* 2010;634:421-30.
 195. Heckman KL, Pease LR. Gene splicing and mutagenesis by PCR-driven overlap extension. *Nat Protoc.* 2007 Apr 12;2(4):924-32.
 196. Laemmli UK. Cleavage of structural proteins during the assembly of the head of bacteriophage T4. *Nature.* 1970 Aug;227(5259):680-5.
 197. Spearman C. The method of "right and wrong cases" ("constant stimulae") without Gauss's formulae. *Br J Psychol* 1904-1920. 1908 Jan 1;2(3):227-42.
 198. Kärber G. Beitrag zur kollektiven Behandlung pharmakologischer Reihenversuche. *Naunyn Schmiedebergs Arch Exp Pathol Pharmacol.* 1931 Jul;162(4):480-3.

10 Appendix

10.1 Toxicity of chemicals

Substance	GHS Symbol	Hazard statements	Precautionary statements
2- mercaptoethanol		H301 + H331-H310- H315-H317-H318- H373-H410	P261-P280-P301 + P310 + P330-P302 + P352 + P310- P305 +P351 + P338 + P310-P403 +P233
Acetic acid		H226-H314	P280-P305 + P351 + P338- P310
Acid Blue 129 (Atanyl Blue PRL)		H315-H319-H335	P261-P305 + P351 + P338
Acrylamide		H301-H312 + H332- H315-H317-H319- H340-H350-H361f- H372	P201-P280-P301 + P310- P305 + P351 + P338-P308 + P313
Ammonium Persulfate		H272-H302-H315- H317-H319-H334- H335	P220-P261-P280-P305 + P351 +P338-P342 + P311
Bromophenol Blue		H332-H302-H319	P261-P264-P280
Boric Acid		H360FD	P201-P308 + P313
Chloramphenicol		H350	P201-P308 + P313

Crystal Violet solution		H319-H351-H411	P273-P281-P305 + P351 + P338
EDTA		H319	P305 + P351 + P338
Ethanol		H225-H319	P210-P280-P305 + P351 + P338-P337 + P313-P403 + P235
Ethidium Bromide		H302-H330-H341	P201-P260-P264-P280-P304 + P340 + P310-P403 + P233
Hydrochloric acid		H290-H314-H335	P261-P280-P305 + P351 + P338-P310
Imidazole		H302-H314-H360D	P201-P260-P280-P303 + P361 + P353-P305 + P351 + P338-P308 + P313
Isopropanol		H225-H319-H336	P210-P261-P305 + P351 + P338
Kanamycin		H360	P201-P308 + P313
Liquid Nitrogen		H281	P202-P271 + P403-P282
Methanol		H225-H301 + H331-H370	P210-P260-P280-P301 + P310-P311

Nonidet® P40		H302-H318-H411	P280-P301 + P312-P305 + P351 + P338
Pefabloc SC		H314	P280 - P303 + P361 + P353 - P305 + P351 + P338 - P310
Penicillin		H317-H334	P261-P280-P342 + P311
Sodium Dodecyl Sulfate		H315-H318-H335	P280-P304 + P340 + P312-P305 + P351 + P338 + P310
Sodium Hydroxide		H290-H314	P280-P305 + P351 + P338-P310
Staurosporine		H340-H350	P201 - P202 - P280 - P308 + P313 - P405 - P501
Streptomycin		H302-H361	P281
TCEP		H314	P280 - P301 + P330 + P331 - P303 + P361 + P353 - P305 + P351 + P338 - P310
TEMED		H225-H302-H314-H332	P210-P280-P305 + P351 + P338-P310

10.2 Curriculum vitae

Curriculum Vitae not given due to data protection laws.

Lebenslauf aus datenschutzrechtlichen Gründen nicht enthalten.

11 Acknowledgements

I would firstly like to thank my supervisor Prof. Dr. Wolfram Brune for giving me the opportunity to work with this fascinating topic. This work would not be possible without his sound guidance and advice as well as his willingness to give me room to develop my own ideas and lines of inquiry.

I would also like to thank my co-supervisor Prof. Dr. Thomas Dobner for his advice and assistance throughout the completion of this work.

I thank Prof. Dr. Nicole Fischer for agreeing to be the second examiner of this work, and Prof. Dr. Elke Oetjen and Dr. Charlotte Uetrecht for forming my examination committee.

Special thanks must be given to Prof. Dr. Thomas Krey and Luisa Stroeh of the Medizinische Hochschule Hannover for their invaluable help with the ongoing efforts to crystallize the pUL98 protein. Prof. Dr. Thomas Schulz and Jessica Rückert are also owed great thanks for allowing me to screen the Small Compound Library at the Medizinische Hochschule Hannover as well as their essential assistance in carrying out the screen.

For his help in designing the pUL98 expression system as well as his kind gifts of the expression vector and bacteria I humbly thank Dr. Shankar Kumar. I also thank Prof. Dr. Beate Sodeik for gifting samples of HSV-1.

I would like to give special thanks to my colleague Dr. Eleonore Ostermann for being a great source of advice throughout my PhD candidacy and for proofreading this work. I owe her many, many cakes!

Thanks also to my colleagues in the Department of Virus-Host Interaction: Elena, Enrico, Felix, Florian, Giadia, Jiajia, Kerstin, Luis, Martina, Olha, Renke, Sylvia, Tianyu, Xuan, and Yingqi. Working with all of you was great and I wish you all the best in and out of the lab!

I thank my family for their support through all these years, without which this work would not be possible.

Lastly, I would like to give special thanks to my partner, Tom, who has steadfastly supported me and stayed by my side throughout my PhD, and to whom this work is dedicated.

12 Eidesstattliche Versicherung

Hiermit versichere ich, Theodore I. Potgieter geboren am 09.06.1990 in Sasolburg (Südafrika), an Eides statt, die vorliegende Dissertation selbst verfasst und keine anderen als die angegebenen Hilfsmittel benutzt zu haben. Die eingereichte schriftliche Fassung entspricht der auf dem elektronischen Speichermedium. Ich versichere, dass diese Dissertation nicht in einem früheren Promotionsverfahren eingereicht wurde.

Hamburg, September 2019

Theodore I. Potgieter